Doctoral theses at NTNU, 2022:32

Pramod KC

Characterization of the accessory olfactory pathway in the noctuid moth – from the labial pit organ to protocerebral centers

Doctoral thesis

NTNU
Norwegian University of Science and Technology
Thesis for the Degree of
Philosophiae Doctor
Faculty of Social and Educational Sciences
Department of Psychology

NTNU
Norwegian University of
Science and Technology

Pramod KC

Characterization of the accessory olfactory pathway in the noctuid moth – from the labial pit organ to protocerebral centers

Thesis for the Degree of Philosophiae Doctor

Trondheim, March 2022

Norwegian University of Science and Technology
Faculty of Social and Educational Sciences
Department of Psychology

NTNU
Norwegian University of
Science and Technology

NTNU
Norwegian University of Science and Technology

Thesis for the Degree of Philosophiae Doctor

Faculty of Social and Educational Sciences
Department of Psychology

ISBN 978-82-326-6536-5 (printed ver.)
ISBN 978-82-326-6683-6 (electronic ver.)
ISSN 1503-8181 (printed ver.)
ISSN 2703-8084 (online ver.)

Doctoral theses at NTNU, 2022:32

Printed by NTNU Grafisk senter

Preface and Acknowledgements

The work presented here was carried out at the Chemosensory Laboratory, Department of Psychology, Norwegian University of Science and Technology (NTNU). During my PhD period, I have become acquainted with many people inside and outside of the department who assisted for making this thesis possible.

I am very thankful to my supervisor, Professor Bente G. Berg, for providing me a platform to perform this kind of research in an inspiring environment. It was a true privilege to work with you in my master thesis as well. Thank you for believing in me to continue as a PhD student. I have learned and grown in this PhD period with you. Thank you for giving me the opportunity of gaining firsthand experience with writing scientific research articles, attending conferences, and analyzing data. Dear Bente, your thoughtful guidance, constant motivation, and emotional support has helped me immensely. You assisted me to continue in the research field when I was about to fall. I would also like to acknowledge my co-supervisor, Associate Professor Pål Kvello, for his valuable support. Your frequent late-night stays in the lab, guiding me how to make Amira reconstructions and registrations, have expanded my knowledge and improved my confidence. I cannot leave without giving sincere thanks to Dr. Xi Chu, who has guided me in each and every step. Dear Xi, your positive energy for the sake of science has always inspired me. I am lucky to have had the opportunity to collaborate with you and received your valuable advice. I profited from your knowledge during the data collection phases and periods of scientific paper writings as well. Moreover, I thank Dr. Elena Ian, who taught me how to perform calcium imaging experiments. In addition, you showed me how to improve my Amira reconstructions. I also thank Dr. Jonas Hansen Kymre for his academic and nonacademic discussions, and his constructive suggestions.

Besides, I would like to thank all the master students in the group who contributed to the lively atmosphere in Chemosensory lab. It was actually my second home, where I spent a lot of time. Particularly, I would like to thank Ina

Saltvik, whom I served as co-supervisor for during her master project. Furthermore, nothing would have been the way it was in Trondheim without having met people like Liv Rygh, my landlord. I rented an apartment in her house for four years. She was always there to take care of my family when I was out of the town for the conferences and research stays abroad.

Finally, I want to acknowledge the most special person in my life, my adorable wife, Rojina, for her love, support, kindness, and patience. I would not have managed without your encouragement and of course your continuous care for our children, Prisha and Rutvik. I would also like to thank my father, mother, and brother who were always there for me during happy and sad moments. Thank you!

List of content

List of papers

Paper I

KC, P., Chu, X., Kvello, P., Zhao, X.-C., Wang, G.-R., & Berg, B. G. (2020). Revisiting the Labial Pit Organ Pathway in the Noctuid Moth, *Helicoverpa armigera*. *Frontiers in Physiology, 11(202)*. https://doi.org/10.3389/fphys.2020.00202.

Paper II

Chu, X., KC, P., Ian, E., Kvello, P., Liu, Y., Wang, G. R., & Berg, B. G. (2020). Neuronal architecture of the second-order CO_2 pathway in the brain of a noctuid moth. *Scientific Reports, 10(1)*, 19838. https://doi.org/10.1038/s41598-020-76918-1.

Paper III

KC, P., Ian, E., Chu, X., & Berg, B. G. (2021). *Elevated levels of CO_2 affect sex pheromone processing in the moth olfactory system*. Unsubmitted manuscript.

Abbreviations

AL	Antennal lobe
ALT	Antennal lobe tract
AMMC	Antennal-mechanosensory and motor center
AST	Antennal suboesophageal tract
Ca	Calyx
CO_2	Carbon dioxide
Cu	Cumulus
dALT	Dorsal ALT
Dma	Anterior dorsomedial
dmALT	Dorsomedial ALT
Dmp	Posterior dorsomedial
EAG	Electroantennogram
GNG	Gnathal ganlion
GRs	Gustatory receptors
HCO_3^-	Bicarbonate
IR	Ionotropic receptor
lALT	Lateral ALT
LH	Lateral horn
LPO	Labial pit organ
LPOG	Labial pit organ glomerulus
mALT	Medial ALT
MGC	Macroglomerular complex
OG	Ordinary glomerulus
OR	Odor receptor
PN	Projection neuron

ppm	Parts per million
tALT	Transverse ALT
VNC	Ventral nerve cord

Summary

Insects detect external fluctuations in atmospheric carbon dioxide (CO_2) for a variety of different reasons. Herbivorous species, like lepidopterans, can sense small variations in external CO_2 for the purpose of finding a suitable host plant both in relation to feeding and egg laying. Lepidopteran species detect CO_2 via a specialized organ located on the peripheral segment of the labial palps, the labial palp pit organ (LPO). Based on tracing of LPO sensory neurons targeting one distinct antennal-lobe (AL) glomerulus in the sphinx moth, the projections originating from the LPO was described as "*an accessory olfactory pathway in Lepidoptera*" already in the 1980 ties.

Carbon dioxide is a ubiquitous gas abundant in Earth's atmosphere and the concentration of this gas is currently increasing at an unprecedented rate. It is not known how the general rise in CO_2 will influence organisms that use this gas as an environmental cue. Fluctuations in external CO_2 may affect their behaviors in different ways, dependent on the species, ecological niche, and context. It is therefore important to acquire knowledge on the processing of atmospheric CO_2 input and the neural circuits involved in this system.

The noctuid moth, *Helicoverpa armigera,* is a suitable model to unravel neural principles typifying the CO_2 pathway. Both physiological and morphological characterizations of the CO_2 sensory neurons have been performed previously in this species. In this PhD project, the main aim was to obtain new knowledge about the CO_2 pathway in moths, from the periphery to higher brain centers. The first part of the work was accomplished by carrying out focused mass staining experiments labeling the sensory neurons in the labial pit organ (LPO) specifically. The previous studies, which included staining of sensory neurons located both inside and outside the pit organ, reported three main target areas, including the LPO glomerulus (LPOG) in both ALs, the gnathal ganglion, and the ventral nerve cord. By performing selective labeling of the LPO sensory neurons inside the pit and the neurons located outside the pit, we could demonstrate that the

LPO sensory neurons terminate in the LPOG exclusively while the additional sensory neurons target the two other regions, the gnathal ganglion and the ventral nerve cord. We also utilized the single-neuron labeling technique resulting in morphological identification of three main types of LPO sensory neurons; in addition to finding a bilateral and unilateral type, as expected, we also discovered a contralateral type. It is worth noticing that the CO_2 information, being based on one signal molecule and targeting one distinct AL glomerulus, is conveyed along sensory projections forming such a complex and non-uniform pattern.

The second part of this PhD study describes how CO_2 information is relayed by second-order projection neurons (PNs) originating from the LPOG and terminating in higher brain centers. We investigated the morphologies of individual LPOG-PNs by means of the single-neuron labeling technique. Here, we discovered that the LPOG PNs differ significantly from the typical uniglomerular PNs originating in the ordinary glomeruli. The CO_2 information is relayed to wide areas of the protocerebrum, but via other antennal lobe tracts (ALT) than the classical medial ALT. Many of the individually stained LPOG-PNs followed the relatively thin fiber bundle classified as the transverse ALT. Another unique property of the LPOG-PNs was that they often bypassed the calyces before terminating in the lateral horn (LH). Interestingly, we found that their terminal projections in the LH overlapped with projections of PNs connected with the ordinary glomeruli, possibly indicating that this is a site for integrating inputs from the plant odors and CO_2.

Since we found overlapping terminals of LPOG PNs and OG PNs in the LH, suggesting a crosstalk between these two sub-systems, we asked ourselves whether there might be a putative interaction between the CO_2 and pheromone sub-system at the lower synaptic level, i.e., the AL. Having access to the behaviorally relevant stimuli connected with the male-specific glomeruli in this species, we were able carry out calcium-imaging experiments to test whether CO_2 might affect pheromone-elicited responses. By staining the uniglomerular medial-tract PNs with a calcium-sensitive dye we could measure the odor-evoked response in the

macroglomerular complex (MGC) during stimulation with the pheromone alone and in combination with CO_2. The results showed decreased pheromone responses when the CO_2 was added to the pheromone stimuli. When we resected the LPO, the suppression effect was eliminated for the lower concentrations of CO_2, indicating the involvement of inhibitory local interneurons innervating both the LPOG and the MGC. The maintenance of the suppression for the high-concentration CO_2, indicated an alternative input channel. Additional experiments including measurement of summated potentials from the antenna, indicated that high concentrations of CO_2 may suppress the response of the antennal sensory neurons directly.

Altogether, the results presented here expand our knowledge on how CO_2 information is transmitted from the periphery to the higher brain areas.

Introduction

In the year 1752, a curious and meticulous young medical student named Joseph Black (1728-1799) performed a series of experiments in the chemistry lab with *magnesia alba* - a magnesium carbonate compound that loses weight when heated. Bemused with this finding, he speculated that different forms of air were integrated within the magnesium carbonate and that some of this air was released when heated. This air was therefore named 'fixed air'. The fixed air was later identified as carbon dioxide (CO_2; Black, 1756). The discovery of CO_2 marked the beginning of a rapid advancement in exploring the functions of this gas, including its vital role in the photosynthesis of plants (Shevela et al., 2019) and cell respiration of animals (Cummins et al., 2014; West, 2014). Besides, carbon dioxide was reported to be connected with global warming already at the end of the eighteenth century (Anderson et al., 2016; Arrhenius, 1897), and its role as an anesthetic agent was discovered in the 1930s (Waters, 1933). Generally, living organisms have CO_2-sensitive pathways serving a variety of distinct functions (reviewed by Cummins et al., 2014). Insects, for example, can detect small variations in external CO_2 fluctuations for a variety of different reasons. Whereas mosquitos are attracted by increasing CO_2 concentrations and thereby find humans and other animals (Gillies, 1980; Wolff & Riffell, 2018), flying fruit flies utilize this gas for detecting rotten fruit (Faucher et al., 2013; Wasserman et al., 2013). Herbivorous insects, on the other hand, like moths, utilize the CO_2 emitted by plants for finding nutritious hosts (Guerenstein et al., 2004b; Hättenschwiler & Schafellner, 2004; Rasch & Rembold, 1994). In addition to the general importance of understanding the neural systems underlying the insect-specific abilities of detecting fluctuations in the external CO_2-concentrations, the topic is especially relevant in our time because of the global climate change and the alarming increase in atmospheric CO_2 level. Since the plant-feeding insects are crucial for plant pollination, the current rise in CO_2 concentration may interfere with their natural behavior in ways that can in fact severely impact the world food production. The need to understand how

information about CO_2 is processed by the insect nervous system is therefore important both for basic and applied research.

Carbon dioxide: The gas of life

Carbon dioxide, a miracle molecule, makes life on earth possible. It was present in the atmosphere prior to the genesis of life. The level of CO_2 in the atmosphere has fluctuated over various geological periods from around 7000 parts per million (ppm) during the Cambrian period (~ 500 million years ago) to around 600 ppm during the Cretaceous period (~ 100 million years ago; Hetherington & Raven, 2005). The current level, just recently reported, is around 410 ppm (Blunden & Arndt, 2020). Life would not exist without CO_2; this gas made it possible for organisms on land, in rivers, and even in the ocean to grow and prosper. Carbon dioxide is a ubiquitous odor molecule, and biological systems for detecting it exist in phylogenetically diverse organisms like plants, bacteria, insects, nematodes, and other animals (reviewed by Cummins et al., 2014). The gas is unique among odorants because of its small size, extreme volatility, and relative solubility in both water and lipids. Carbon dioxide is also environmentally ubiquitous at a relatively high concentration (0.04%) as compared to other typical odor molecules. A small change in the environmental CO_2 may influence the activity of omnipresent insects. The global rise of atmospheric CO_2 poses a putative threat to insects and the ecosystems they depend on (Burrows et al., 2011). The increase may facilitate several negative effects such as decreasing oviposition, disturbing pheromone detection (Guerenstein & Hildebrand, 2008; Robinson et al., 2012), and shifting the species' distribution (Chen et al., 2011), possibly causing extinctions (Dirzo et al., 2014). It is therefore utterly important to acquire knowledge on processing of atmospheric CO_2 input and the neural circuits involved in this system.

Behavioral responses to CO_2 – examples from different insect species

Insects detect external CO_2 fluctuations for a variety of different reasons. Concerning social insects, knowledge about their behavioral responses to external CO_2 levels are obtained from studies performed in open environment as well as inside their nests. Social bees, for example, begin to fan their wings when the CO_2 level inside a beehive becomes too high (5,000 ppm), indicating poor ventilation and increased temperature (Seeley, 1974). Wingless ants, on the other hand, open or close the nest entrance to optimize ventilation (Kleineidam & Roces, 2000). In addition, ants use information about increasing CO_2 concentration to locate their hive (Buehlmann et al., 2012).

Solitary insects living in an open environment detect external CO_2 for other purposes. Finding relevant food is one drive, even when they are several meters away from the source (Stange & Stowe, 1999). A fruit fly, for instance, feeds on fermented food sources that produce CO_2. Therefore, we might expect that the fruit fly is always attracted to high concentrations of this gas. However, findings from experiments investigating walking versus flying behavior showed different results (Wasserman et al., 2013). A walking fruit fly always avoids high concentration of CO_2 whereas a flying one is attracted to such a stimulus. Concerning walking flies, the avoidance response to CO_2 might indicate that the insect is faced with a predator or another threat. In fact, stressed flies emit a particular CO_2 like compound that may serve as a social signal to mediate conspecific avoidance behavior (Suh et al., 2004).

Herbivorous insects, like lepidopterans, detect small variations in external CO_2 for the purpose of finding a suitable host plant both in relation to feeding and egg laying (Guerenstein & Hildebrand, 2008). For instance, the female cactus moth, *Cactoblastis cactorum*, is reported to assess whether a particular individual of the host plant, *Opuntia stricta,* is suitable for oviposition by measuring its metabolic activity in the form of nightly CO_2 assimilation (Stange, 1997; Stange et

al., 1995). Another example, related to feeding behavior, is the sphinx moth, *Manduca sexta*, and its ability of estimating, via measuring the CO_2 level, the general health of the relevant host plant, *Datura wrightii*, including its abundance of nectar, and/or a flower not recently fed on (Guerenstein et al., 2004b; Thom et al., 2004).

Helicoverpa armigera is a suitable model for studying the system devoted to CO_2

One of several good reasons for utilizing the noctuid moth, *Helicoverpa armigera,* as an object for studying neural principles devoted to CO_2 processing is the knowledge on peripheral mechanisms already obtained in this species, including mapping of the peripheral part of the CO_2 pathway (Zhao et al., 2013), physiological characterization of CO_2 sensory neurons (Stange, 1992), and even the identification of CO_2 receptors (Ning et al., 2016; Xu & Anderson, 2015).

The natural habitats of this heliothine moth are widespread across all continents, except Antarctica. It is believed that the lepidopteran species arose at the same time as the flowering plants, in the late Cretaceous period (Kawahara et al., 2019) when the concentration of CO_2 was around 600 ppm (Barral et al., 2017). Generally, these anthophilous adult insects feed on nectar and thereby pollinate their host plants. The noctuid moths are most active at the dusk, about one hour after sunset. Thereafter, the flight activity gradually decreases throughout the night (Riley et al., 1992). Generally, the activities of these herbivorous species are correlated with those of night blooming plants relying heavily on the insects for pollination. Here, moths benefit from the plants' refreshing nectar (Guerenstein et al., 2004b; Thom et al., 2004) and from suitable sites for egg laying. The night blooming flowers open at dusk and release concentrations of CO_2 up to 200 ppm above the ambient concentration (Guerenstein et al., 2004b), thereby indicating the abundance of fresh and high-quality nectar. Whereas adult moths serve an important role as pollinators, some of the larvae cause serious damage on crops,

however. The larvae of *H. armigera* is one of the most serious pests causing substantial damage on agriculture worldwide by injuring almost 200 food plants (Cunningham & Zalucki, 2014; Zalucki et al., 1986; Zalucki et al., 1994). Field experiments have shown that the larvae attack mostly young leaves, flowers, and the developing fruits (Hardwick, 1965). These parts of the plant have the highest metabolic activities and they therefore release higher amount of CO_2 into the air. Also, fast-growing plant organs usually have a high respiration rate. Notably, CO_2 alone has been shown to be attractive for the larvae (Rasch & Rembold, 1994). Taken together, both the larvae and adults use the naturally occurring CO_2 gradient surrounding relevant host plants or parts of host plants as an attractive stimulus. In both cases, the behaviors are important in an ecological context.

The CO_2-detecting organ is separated from the main olfactory organ in moths

As in other lepidopteran species, there are two distinct olfactory sensory organs in *H. armigera*. Whereas the main organ, the antenna, is responsible for detecting volatile organic compounds including plant odors and pheromones, a special organ situated at the mouthparts is devoted to recognizing the inorganic CO_2. This secondary olfactory organ, called the labial pit organ (LPO) is localized in the terminal segment of the labial palp (Fig. 1). The LPO organ is one of the synapomorphies of all lepidopteran species (Kristensen et al., 2007). The labial palp consists of three segments, of which the distal one has a pit-like structure that houses a densely packed array of sensilla. The numbers and morphologies of LPO sensilla vary across different lepidoptera species (Fig. 2). In the moths, *H. armigera*, *Mythimna separata,* and *Grapholita molesta,* for example, the pit houses two main types of sensilla – one hair- and one club-like type distributed in distal and proximal areas of the LPO, respectively (Dong et al., 2014; Song et al., 2016; Zhao et al., 2013). In other moths, the pit is reported to house mainly club-shaped sensilla (reviewed by Guerenstein & Hildebrand, 2008; Stange & Stowe, 1999). The purpose of the morphologically different sensilla types is unknown. The

hair-shaped sensillum type houses only one sensory neuron while the club-shaped type houses either one or two sensory neurons (Zhao et al., 2013).

The LPO sensilla have multiple pores and thereby resemble the typical olfactory sensilla located on the antennae. However, the CO_2 sensory neurons have a unique dendritic architecture, with considerably more branches than other chemosensory neurons (Guerenstein & Hildebrand, 2008; Shanbhag et al., 1999). The CO_2 sensory neurons resemble in many ways the sensory neuron types responding to temperature and humidity. Firstly, all these neuron types respond to ambient changes (reviewed by Guerenstein & Hildebrand, 2008), secondly, all neuron types respond bidirectionally to gradient changes, and thirdly, the dendritic branching patterns of these neuron types are similar (Stange & Stowe, 1999).

The name of the organ, 'labial pit organ' (LPO), was given by John Hildebrand and his collaborators (Kent et al., 1986). They traced the sensory neurons housed inside the labial pit in a group of sphinx moths, including *Manduca sexta,* and the silk moth, *Bombyx mori*. Since they demonstrated that the LPO sensory axons project directly into the antennal lobe (AL), the primary olfactory center of the insect brain, they also classified these projections as '*an accessory olfactory pathway in Lepidoptera*' (Kent et al., 1986).

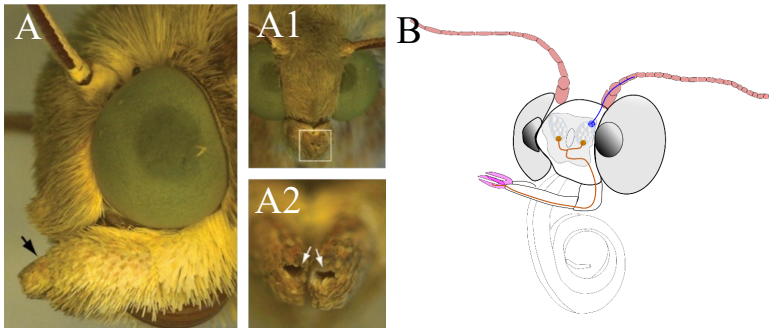

Fig. 1: Position of the labial pit organ (LPO). **(A**) Lateral view of the moth head with the labial palp (black arrow). **(A1)** Frontal image showing the peripheral part of the labial palps, indicated by the white square box. **(A2)** Magnified image of the square box in **(A1)** showing the opening (white arrows) of the LPOs (picture source: Zhao et al., 2013). **(B)** Schematic diagram showing central projections of sensory neurons from the LPO and the antenna, respectively. Central projections of the sensory neurons housed inside the LPO are indicated by *brown* and those projecting from the antennae are indicated by *blue*.

Peripheral detection of the CO_2 cues - sensory neuron properties

Sensory neurons housed inside the LPO respond to changes in CO_2 concentration. This was demonstrated for the first time by means of extracellular recordings from LPO sensory neurons in *Rhodogastria* moths (Bogner et al., 1986). A few years later, similar responses were recorded from LPO neurons in *H. armigera* (Stange, 1992). In this study, Stange concluded that the sensory organ can detect fluctuations in CO_2-density of 0.14%, or 0.5 ppm, which relate to the variations occurring in natural environments.

Generally, electrophysiological recordings from many insect species within different orders have shown that the CO_2 sensory neurons display phasic-tonic response profiles. This neuron type responds quickly with a phasic burst of action potentials as soon as it encounters the changes in CO_2 concentration, clearly marking the onset of the stimulus. Reports about small variations in the onset of the phasic response may be due to differences in the experimental procedure and/or location of the CO_2 sensory neurons (Bogner et al., 1986; Faucher et al., 2013; Grant & O'Connell, 2007; Ning et al., 2016). When the stimulus is prolonged, the phasic response plateau is transformed into a sustained firing frequency, constituting a tonic phase. The tonic phase is non-adapting (except for in *Cactoblastis cactorum*; Stange, 1997), differing from the typical odor responses, which adapt (Kaissling et al., 1987). In fact, recordings from ant CO_2 sensory neurons showed no evidence of fatigue or adaptation during a stimulation period lasting more than an hour (Kleineidam et al., 2000). The non-adapting, phasic-tonic response allows continuous tracking of a filamentous plume of CO_2, such as performed by, for example, mosquitoes (Grant et al., 1995). Whereas the CO_2 sensory neurons in higher insect orders usually display excitatory responses to fluctuations in concentration of the gas (Guerenstein et al., 2004a; Ziesmann, 1996), some lower insect orders display inhibitory responses to CO_2, such as damselflies (Piersanti et al., 2016), termites (Ziesmann, 1996), ticks (Steullet &

Guerin, 1992), and centipedes (Yamana et al., 1986).

Do the CO_2 sensory neurons respond to the CO_2 stimulus only? Early studies assumed that these neurons were narrowly tuned, responding to CO_2 specifically. However, when testing other odor stimuli on fruit flies, it was shown that the CO_2-tuned neurons actually responded more broadly (MacWilliam et al., 2018). It was also demonstrated inhibitory responses in these sensory neurons during stimulation with amines. In damselflies, on the other hand, amines activate the CO_2 sensory neurons via excitation (Piersanti et al., 2016).

Surprisingly, the gaseous CO_2 cue is detected by a type of gustatory receptor (GR), not an olfactory receptor. The co-located carbon dioxide receptors, GR21a and GR63a, were discovered in the fruit fly (Jones et al., 2007; Kwon et al., 2007). These two GRs form a heterodimeric receptor shown to be necessary and sufficient for detection of CO_2. The identification and characterization of these gustatory receptors led to the finding of similar receptors across different species (Robertson & Kent, 2009). The number of distinct GR types detecting CO_2 varies slightly, ranging from three in moths and mosquitoes, to two in fruit flies, and none in honeybees (Robertson & Kent, 2009) (Fig.2).

The CO_2 gustatory receptors in moth were in fact identified in *H. armigera* (Xu & Anderson, 2015). The three receptors, named HarmGR 1, HarmGR 2, and HarmGR 3, are all expressed in the labial palps. Among these, the two co-expressed receptors, HarmGR 1 and Harm GR 3, are required for detection of CO_2 whereas the remaining receptor, HarmGR 2, may act as a modulator (Ning et al., 2016). Orthologs of HarmGR 1, HarmGR 2, and HarmGR 3 have been identified in mosquitoes, i.e. CquiGR 1, CquiGR 2, and CquiGR 3 (Xu et al., 2020). Interestingly, also here, two co-expressed receptors, CquiGR 2 and CquiGR 3, were found to display robust responses to CO_2 (Xu et al., 2020), whereas co-expression of receptors CquiGR 1 and CquiGR 2 did not induce any response to CO_2.

The signal transduction cascade transforming the external CO_2 signals into trains of neuronal action potentials in the sensory neurons is not yet uncovered. One possible transduction mechanism involves G-proteins (Yao & Carlson, 2010), similar to the transduction proposed for the standard odor receptors (ORs; Wicher et al., 2008). However, the idea implying that GRs may function as ligand-gated ion channels cannot be excluded. In addition, there has been uncertainty about whether it is the CO_2 *per se* or a metabolic biproduct of CO_2, such as bicarbonate or protons, that constitute the essential signal. Recent investigations from insects showed, however that the relevant signal binding to the gustatory receptor is the CO_2 molecule itself, not the bicarbonate (Xu et al., 2020). Though, the exact binding site of the CO_2 in the receptor molecule is not discovered.

Generally, GRs are considered to be the most ancient of the chemosensory receptor proteins in arthropods (Eyun et al., 2017). The GRs are comparable with insects' ORs and possess an internal N-terminus and an external C-terminus (Zhang et al., 2011). Gustatory receptors are mainly involved in gustation. In addition to their involvement in sensing carbon dioxide, there are a few cases reporting about gustatory receptors being involved in pheromone detection (Bray & Amrein, 2003).

Different from the common air-borne odorants, like hydrophobic pheromones and plant odorants, which need odorant binding proteins (OBPs) for reaching to their respective receptors, the CO_2 is moderately soluble in the sensillum lymph and may not require the binding proteins. Yet, one OBP (OBP5) was identified in the labial palp of *H. armigera* (Guo et al., 2018). At this point, however, it is not known whether OBP5 is selectively expressed in sensilla housing CO_2 sensory neurons or in sensilla possibly housing other olfactory sensory neurons (Guo et al., 2018).

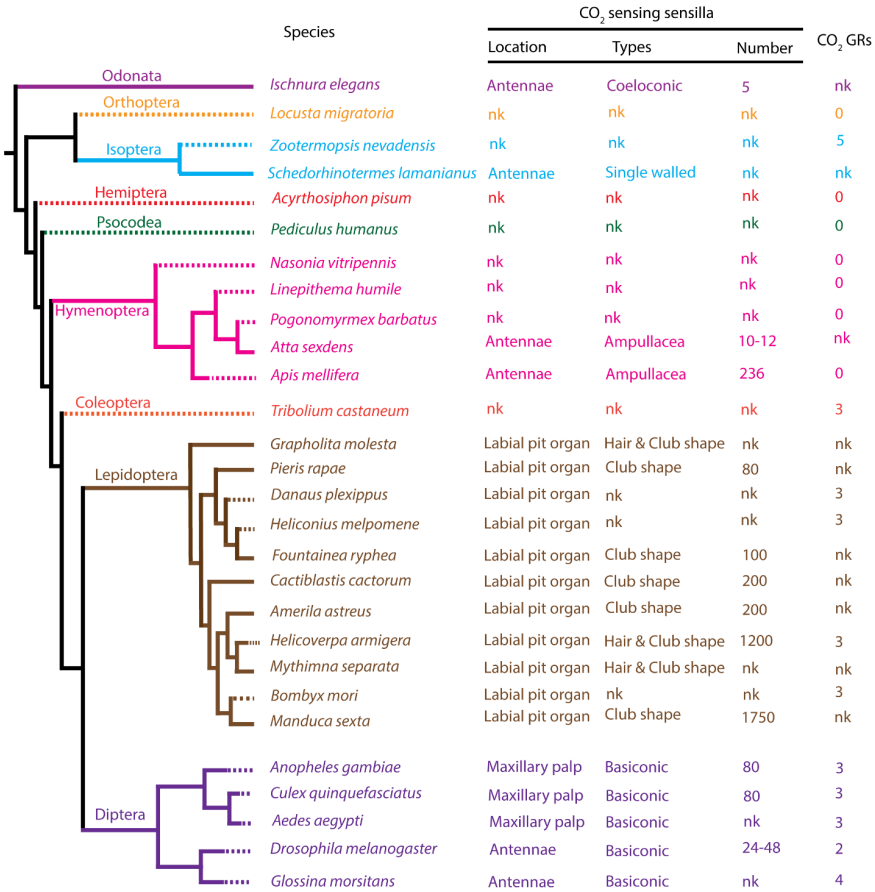

Fig. 2: Phylogeny of various insect species including their CO_2 sensory organ and number of CO_2 gustatory receptors (GRs, indicated by dotted lines). *I. elegans* (Piersanti et al., 2016; Piersanti et al., 2010); *L. migratoria* (Wang et al., 2014); *Z. nevadensis* (Terrapon et al., 2014); *S. lamanianus* (Ziesmann, 1996); *A. pisum* (Robertson & Kent, 2009); *P. humanus* (Robertson & Kent, 2009); *N. vitripennis* (Robertson & Kent, 2009); *L. humile* (Robertson & Kent, 2009; Smith et al., 2011a); *P. barbatus* (Robertson & Kent, 2009; Smith et al., 2011b); *A. sexdens* (Kleineidam et al., 2000); *A. mellifera* (Robertson & Kent, 2009; Stange & Stowe, 1999); *T. castaneum* (Robertson & Kent, 2009); *G. molesta* (Song et al., 2016); *P. rapae* (Lee et al., 1985); *D. plexippus* (Zhan et al., 2011); *H. melpomene* (Briscoe et al., 2013); *F. ryphea* (Lastra-Valdés et al., 2020); *C. cactorum* (Stange et al., 1995); *A. astreus* (Bogner et al., 1986); *H. armigera* (Zhao et al., 2013); *M. separata* (Dong et al., 2014); *B. mori* (Wanner & Robertson, 2008); *M. sexta* (Kent et al., 1986); *A. gambiae* (Lu et al., 2007; Robertson & Kent, 2009); *C. quinquefasciatus* (Robertson & Kent, 2009; Syed & Leal, 2007); *A. aegypti* (Bohbot et al., 2014; Erdelyan et al., 2012); *D. melanogaster* (Jones et al., 2007; Riesgo-Escovar et al., 1997); *G. morsitans* (Obiero et al., 2014; Soni et al., 2019); nk, not known

Projections of the LPO sensory neurons target the primary olfactory center

The axons of the CO_2-responding sensory neurons in the LPO target a single glomerulus in the primary olfactory center, the antennal lobe (AL). Tracing studies from different lepidopteran species have reported a common projection pattern including stained axons confined to the labial nerve and bilateral innervations in the labial pit organ glomerulus (LPOG; Bogner et al., 1986; Kent et al., 1986; Ma et al., 2017; Zhao et al., 2013). The postero-ventrally located LPOG is one of the largest glomeruli in the moth AL (Zhao et al., 2016). In *H. armigera*, it is estimated that around 1200 LPO sensory neurons terminate in this glomerulus (Zhao et al., 2013). Notably, the LPOG, being located postero-ventrally in the AL, is not innervated by any of the antennal sensory axons. The olfactory sensory neurons on the antenna, which project along the antennal nerve, terminate in all AL glomeruli except for the LPOG.

Generally, the insect AL corresponds to the olfactory bulb (OB) in vertebrates (reviewed by Hildebrand & Shepherd, 1997). Both structures are composed of spherical structures called glomeruli which receive information from peripherally located olfactory neurons. Thus, they are the first relay station in the network of neurons processing olfactory information (Hansson & Christensen, 1999). In the moth AL, the glomeruli are organized into three main groups: 1) the male-specific macroglomerular complex (MGC) which processes information about pheromones, 2) the ordinary glomeruli (OGs) which process information about plant odorants, and 3) the LPOG, devoted to encoding CO_2 input (Zhao et al., 2016). The AL of *H. armigera*, totally contains a total of 79 glomeruli, including three MGC units: the cumulus (Cu), the posterior dorsomedial unit (dmp), and anterior dorsomedial units (dma). The Cu and dmp receive input from sensory neurons detecting the primary and secondary pheromone components, *cis*-11-hexadecenal (Z11-16:Al) and *cis*-9-hexadecenal (Z9-16:Al), respectively, whereas, the dma receives input from sensory neurons tuned to an interspecific

signal acting as a behavioral antagonist, *cis*-9-tetradecenal (Z9-14:Al; Wu et al., 2015). Notably, all antennal axons project into the ipsilateral AL exclusively, whereas the LPO axons send bilateral projections, terminating in the LPOG of both ALs – however, with somewhat denser innervation of the ipsi- than the contralateral side (Kent et al., 1986). Whereas antennal sensory neurons tuned to humidity and temperature are reported to project to the AL, taste and mechanosensory neurons bypass the AL and target regions in the tritocerebrum and antennal-mechanosensory and motor center (AMMC), respectively (Homberg et al., 1989; Jorgensen et al., 2006). Besides, sensory neurons in other appendages, such as the proboscis, terminate outside the AL as well (Kvello et al., 2006).

Second-order signaling along parallel antennal-lobe tracts

From the LPOG in the AL, the CO_2 information is conveyed to higher brain centers via second-order projection neurons (PNs) passing along one of several parallel AL tracts (ALTs). Generally, the projections of the LPOG PNs in moths have been poorly described. So far, only one main study on this system has been carried out. This previous investigation, which was based on the intracellular recording and staining technique, reported morphological and physiological properties of six CO_2-responding output neurons originating from the LPOG in *M. sexta* (Guerenstein et al., 2004a). The identified neurons responded to increased CO_2 concentrations applied to the LPO and not to the plant odors tested. The uniglomerular PNs, having dendritic arborizations in the LPOG only and a cell body located in the lateral cluster, were reported to project in the most prominent of the ALTs, the medial ALT (mALT), which targets two main protocerebral regions, i.e., the calyces of the mushroom bodies and the lateral horn (LH; Guerenstein et al., 2004a). A recent study on *H. armigera* reported a multiglomerular PN having dendritic arborizations both in the LPOG and other glomeruli (Kymre et al., 2021a). This neuron passed along another tract, the mediolateral ALT (mlALT), which is considerably thinner than the medial tract and projects directly to the lateral protocerebrum, including the LH, without

innervating the calyces (Homberg et al., 1988; Kymre et al., 2021a).

In addition to the above-mentioned tracts, the mALT and the mlALT, there are four more tracts in moths, i.e., the lateral-, transverse-, dorsomedial- and dorsal ALT (lALT, tALT, dmALT, and dALT, respectively; Homberg et al., 1988;Ian et al., 2016b; Kymre et al., 2021a). Altogether the medial-, mediolateral-, and lateral ALT are classified as the main tracts, seemingly being connected with most of the AL glomeruli. Thus, both pheromone-information from the three MGC-units and plant-odor information from the numerous OGs are carried along each of the three main tracts in H. armigera (Chu et al., 2020; Kymre et al., 2021b). The transverse- and dorsomedial ALT, on the other hand, are reported to convey signal information from distinct groups of AL glomeruli (Kymre et al., 2021a). Notably, these groups include glomeruli in the region housing the LPOG. In addition to the above-mentioned tracts, the antenno-suboesophageal tract (AST) connects the AL with ventrally located regions including the gnathal ganglion (GNG; Homberg et al., 1988).

Higher brain centers processing chemosensory information

As mentioned above, information from the two main olfactory sub-systems of male moths, devoted to pheromones and plant odors, are conveyed along all the main ALTs. In the protocerebral target areas, however, the most prominent tract, the medial, separates these two signal categories into spatially distinct regions. Both previous and recent studies have clearly demonstrated that the MGC-PNs terminate in the superior lateral protocerebrum (SLP) whereas PNs from OGs target the LH, which is located more laterally and ventrally (Chu et al., 2020; Homberg et al., 1988; Kanzaki et al., 2003; Zhao et al., 2014). This kind of signal segregation includes the medial-tract axon terminals within the calyces as well (Chu et al., 2020; Homberg et al., 1988). In fact, the only protocerebral region displaying substantial overlap of these signal categories is the column, a pillar-shaped structure within the superior intermediate protocerebrum (SIP) being innervated by lateral-tract PNs both from the MGC and the ordinary glomeruli (Chu et al., 2020).

In addition to the pheromone- and the plant odor sub-systems, the CO_2 arrangement constitutes a third olfactory sub-system in the male moth. Each of these sub-systems relates to three non-overlapping regions in the AL, formed by the MGC, the OGs, and the LPOG, respectively. Based on previous and recent data on the projection patterns of the two first-mentioned sub-systems, an interesting question is how the odor information from the third sub-system, tuned to CO_2, is represented in the higher brain centers.

Aims of the thesis

Principal aim: In this thesis, the main aim was to explore the neural pathway devoted to processing external CO_2 signals in the noctuid moth, *H. armigera* - from the labial pit organ, through the primary olfactory processing center, and to the higher brain areas. By combining different experimental approaches, including mass staining experiments, sharp intracellular labeling of first- and second order neurons, confocal microscopy, three-dimensional reconstructions, and calcium imaging, we intend to characterize anatomical properties of single neurons and neuron populations and to explore how this arrangement may influence on other chemosensory sub-systems, such as the male-specific pheromone system.

Specific aims

i. To map the central projections of the LPO-sensory neurons specifically and to characterize the morphological structure of individual LPO-neurons.

ii. To identify the morphologies of individual second-order PNs originating from the LPOG including which ALTs these neurons are confined to and which protocerebral areas they target.

iii. To clarify whether the target areas of the LPOG-PNs overlap with terminal areas of PNs of the other two sub-systems, devoted to pheromones and plant odors, respectively.

iv. To clarify whether external CO_2 signals influence the activity in MGC medial-tract PNs.

Synopses of the individual papers

Paper I

KC, P., Chu, X., Kvello, P., Zhao, X.-C., Wang, G.-R., & Berg, B. G. (2020). Revisiting the Labial Pit Organ Pathway in the Noctuid Moth, *Helicoverpa armigera*. *Frontiers in Physiology*, *11*(202). https://doi.org/10.3389/fphys.2020.00202.

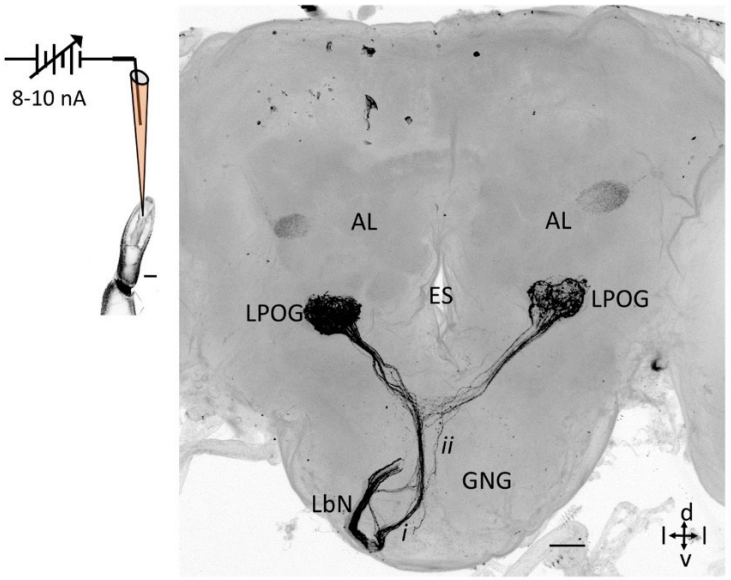

In this study we performed a thorough morphological characterization of the sensory neurons housed inside the labial pit organ (LPO), including neurons encapsulated by the hair-shaped and club-shaped sensilla. As indicated by the title of the article, we revisited the LPO pathway in the noctuid moth. In the previous reports (Kent et al., 1986; Zhao et al., 2013), which were based on mass staining experiments including not only LPO sensory neurons but also other sensory neurons originating from the external part of the labial palp, the massive labeling visualized in the data covered stained projections targeting three main areas of the

central nervous system: 1) the LPO glomerulus (LPOG) in both antennal lobes (ALs), 2) the gnathal ganglion (GNG) and adjacent regions, and 3) the ventral nerve cord (VNC). By utilizing a more focused mass staining technique labeling neurons only inside the LPO, we were able to show that the LPO sensory neurons project to the LPOG exclusively. Additional staining experiments including dye application onto the sensory neurons localized outside the LPO, demonstrated that these neurons target the GNG and the VNC. The focused mass staining could not resolve the morphologies of individual LPO sensory neurons types, however. Therefore, we performed additional iontophoretic staining experiments of single LPO sensory neurons (both inside the LPO and the LPOG). The results from this part of the study showed three morphological types of LPO neurons: one bilateral neuron type targeting both LPOGs; one unilateral neuron type targeting the ipsilateral LPOG only, and one contralateral neuron type targeting the LPOG in the contralateral AL. In addition to these findings, we also performed selective mass labeling of neurons housed by the two sensillum types, i.e. club-shaped versus hair-shaped. Both staining experiments showed stronger innervation of the ipsilateral LPOG than the contralateral LPOG.

Paper II

Chu, X., KC, P., Ian, E., Kvello, P., Liu, Y., Wang, G. R., & Berg, B. G. (2020). Neuronal architecture of the second-order CO_2 pathway in the brain of a noctuid moth. Scientific Reports, 10(1), 19838. https://doi.org/10.1038/s41598-020-76918-1.

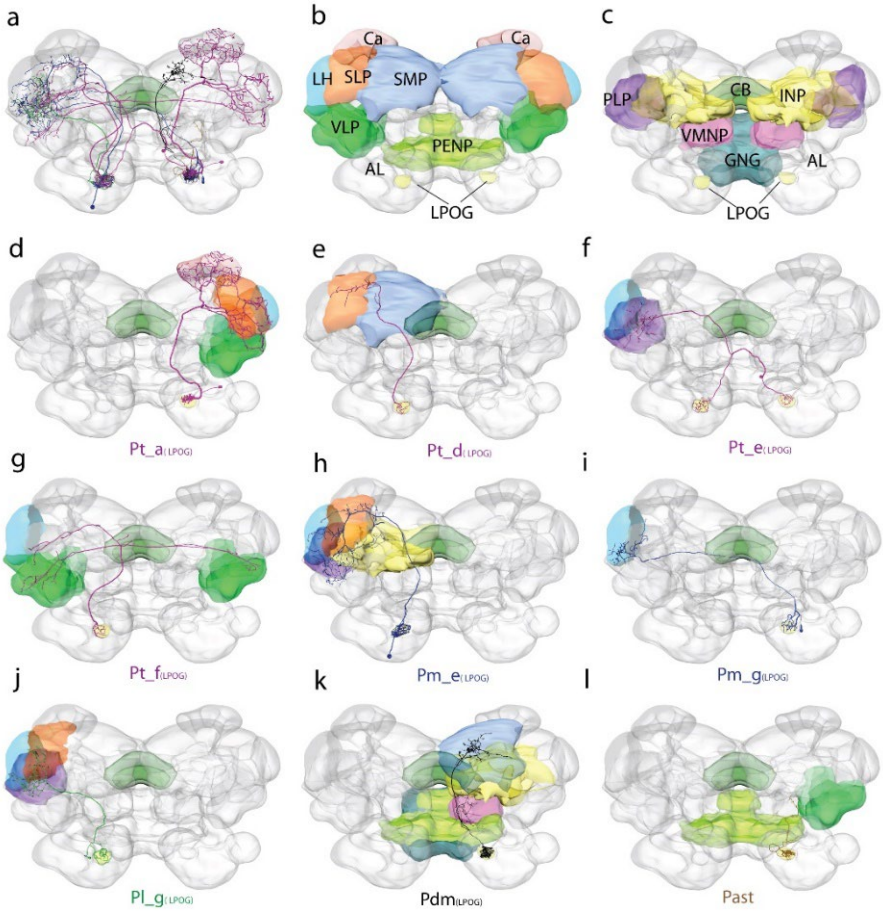

To obtain more information about the second-order level of the CO_2-pathway, we carried out staining experiments from the projection neurons (PNs) conveying the signals from the labial pit organ glomerulus (LPOG) to higher protocerebral

regions. In this paper, we report the morphologies of individual LPOG PNs by utilizing the intracellular labeling technique in combination with confocal microscopy and digital reconstructions by means of the AMIRA visualization software. In addition, we performed focused mass staining experiments from several simultaneously stained LPOG PNs. Our data comprised totally 15 individual LPOG PNs forming nine neuron subtypes. Each PN followed one of five antennal lobe tracts (ALTs): 1) the transverse ALT, 2) the medial ALT, 3) the lateral ALT, 4) the dorsomedial ALT, and 5) the antennal suboesophageal tract. Many of the PN types described here are novel – notably, 10 of the 15 PNs identified were confined to the relatively thin and, so far, poorly described transverse ALT. Generally, the population of uniglomerular LPOG PNs sent their branches to widespread protocerebral areas. An interesting finding was that the LPOG PNs innervated the mushroom body calyces modestly, whereas the lateral horn (LH) was substantially innervated. Many of the terminal branches overlapped in the LH. This result was corroborated by mass staining experiments as well. The LH is a previously well-described target area of plant-odor PNs originating from the numerous ordinary antennal-lobe glomeruli. We assume that the projection pattern indicates the importance of integrating the CO_2 input with plant odor information in the higher brain center.

Paper III

KC, P., Ian, E., Chu X., & Berg, B. G. (2021). *Elevated levels of CO_2 affect sex pheromone processing in the moth olfactory system*. Unsubmitted manuscript.

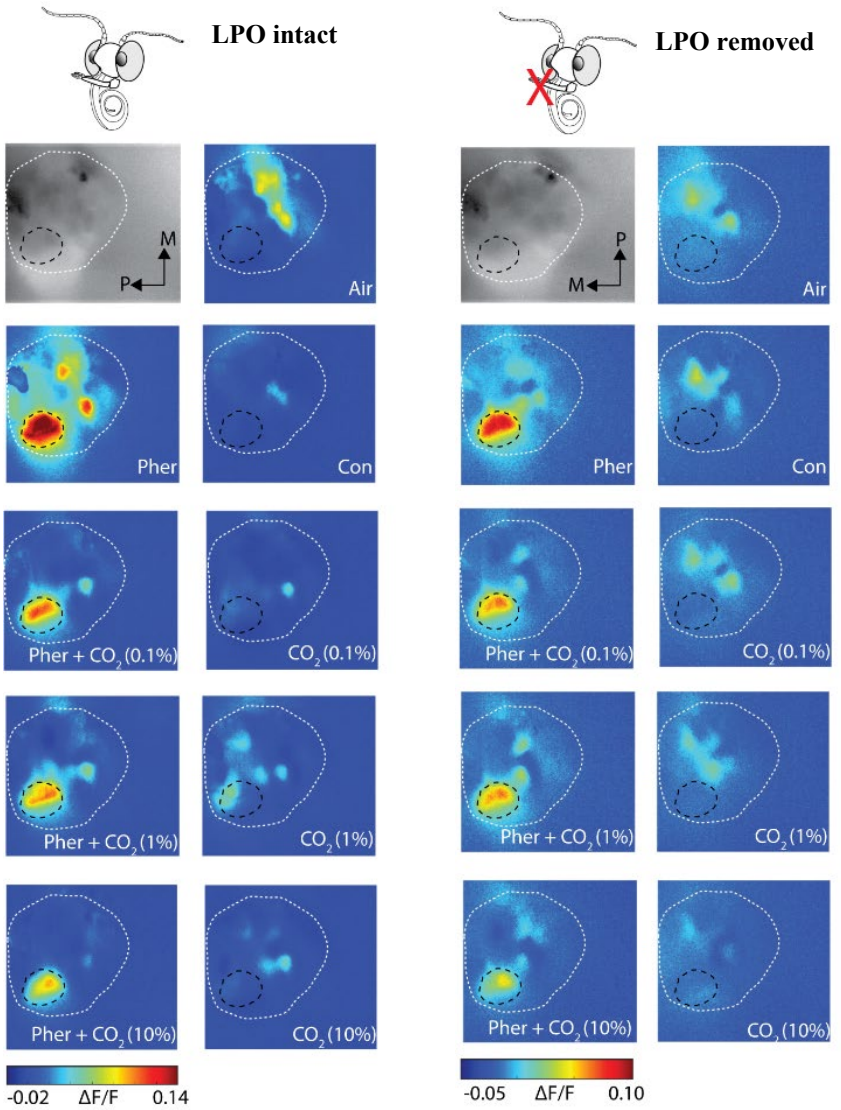

Based on the new anatomical findings in paper II on the overlapping lateral-horn (LH) terminals of projection neurons (PNs) originating from the labial pit organ glomerulus (LPOG) and the ordinary glomeruli (OGs), respectively, we decided to investigate whether there might be a putative interaction of the CO_2 system with the other olfactory sub-system, i.e, the male-specific system for pheromone processing, at the lower synaptic level, the antennal-lobe (AL) level. Paper III is an unpublished work containing data mainly from calcium imaging experiments including measurements of pheromone-evoked responses in the AL during exposure of different CO_2 concentrations. Here, we applied a calcium-sensitive dye, Fura 2, into the calyces thereby labeling the medial-tract PNs selectively. Then, we perform calcium imaging measurements from the dendrites of the retrogradely labeled PNs in the male-specific region of the AL, the macroglomerular complex (MGC). As we intend to include the data obtained here into a more comprehensive study, we present the results as an unpublished manuscript.

By testing the pheromone blend alone and together with different concentrations of CO_2, we discovered that elevated levels of CO_2 suppress the pheromone responses in the MGC. This could be due to activation of inhibitory local interneurons (LNs) innervating both the MGC and the LPOG. To investigate this issue, we performed new calcium imaging measurements in insects with removed LPOs. Interestingly, while no suppression was observed during application of low CO_2 concentrations, the high concentration still induced a lowering of the pheromone response. To investigate whether the maintained suppression might originate from another putative CO_2 channel, such as the antenna, we then performed electroantennogram (EAG) experiments. Here, we found a suppression effect of the pheromone-evoked EAG-responses during application of CO_2 at the high concentration.

Altogether, the results obtained indicate that CO_2 suppresses pheromone-responses of male-specific medial-tract PNs. This effect appears to originate from two different sources. At low CO_2 concentration, the PNs receive inhibitory input

from AL LNs being activated by the LPO neurons, and at high concentration, the PNs are suppressed by the male-specific sensory input being directly influenced by CO_2-signals in the antenna.

Discussion

We employed *Helicoverpa armigera* as a model organism to investigate the CO_2 pathways, from the periphery to the higher brain centers. Initially, we updated the knowledge on the peripheral part of the signal pathway, including precise morphological identification of the LPO sensory neurons which were shown to project to the LPOGs exclusively. In addition to the previously reported bilateral LPO sensory neurons, our single-cell labeling experiments resulted in identification of two additional categories, i.e., one ipsilateral- and one contralateral. Furthermore, the relatively challenging task of mapping the second-order PNs originating in the LPOG and tracing their paths to the higher protocerebral brain centers was successfully achieved. The results obtained explored an assembly of morphologically diverse LPOG PNs including nine distinct types, all differing markedly from the 'typical' uniglomerular output neuron originating from the ordinary AL glomeruli. In line with the previous indication of the peripheral CO_2 projections in lepidoptera as *an accessory olfactory pathway* (Kent et al., 1986), our data indicated the relevance of integrating the CO_2 input with the other classes of odor information in the brain – firstly, by the substantial overlap of plant odor and CO_2 signals in the previously well-described higher-order olfactory center, the LH, and secondly, by the suppression effect induced by CO_2 on pheromone responses at the lower synaptic levels. Shortly summarized, the three papers included in this thesis, provide new findings on the first- and second-order neurons of the CO_2 pathway of the noctuid moth.

Morphological properties typifying the LPO sensory neurons

The LPO sensory neurons in moths are morphologically heterogenous

The designation of the peripheral CO_2 pathway in lepidoptera as an '*accessory olfactory pathway*', utilized for the first time by researchers in John Hildebrand's group, was based on mass staining experiments including application of dye onto the truncated part of the peripheral labial-palp segment. which demonstrated fibers

projecting to the LPOG, gnathal ganglion, and the ventral nerve cord (Kent et al., 1986). It was, however, not clear whether all three projection areas originated from the LPO sensory neurons. Notably, one of the main findings published in paper I, is that the sensory neurons housed within the LPO project to the AL exclusively. This fact was clarified by implementing *focused* mass staining from the neurons housed inside the pit organ. We also managed to perform single-cell staining experiments demonstrating, for the first time, three morphologically distinct types of LPO sensory neurons. As expected, we found both bilateral and ipsilateral neurons. This coincides with both present and previous findings showing a somewhat stronger staining in the ipsilateral LPOG than the contralateral (Kent et al., 1986; Ma et al., 2017; Zhao et al., 2013). However, the discovery of contralaterally projecting LPO neurons was in fact not expected. Generally, both the LPO sensory neurons and the olfactory sensory neurons (OSNs) on the antenna are bipolar neurons with two branches extending from the cell body – one dendritic part housed inside the sensillum and one axon projecting directly into the primary olfactory center of the brain. An essential difference, however, is that the antennal OSNs project their axons unilaterally while a substantial proportion of the LPO neurons project bilateral. The reason for this morphological difference is not yet clarified. Regarding the unilateral OSNs, this is a feature characterizing olfactory sensory neurons in almost all organisms, including both vertebrates and invertebrates (reviewed by Hildebrand & Shepherd, 1997). One relevant question is therefore why a significant number of LPO sensory neurons in moths are bilateral. One possible reason could be that the bilateral CO_2 neurons contribute to increasing the signal-to-noise ratio (Louis et al., 2008). Actually, in fruit flies, which do possess bilateral olfactory sensory, these neurons possess a lower detection threshold and also have the ability to make concentration measurements with a resolution almost 1.5 times better than unilateral sensory neurons (Louis et al., 2008). However, the next question would then be why this is more necessary for CO_2 input than for common odor signals. An alternative explanation might be that the LPO neurons are directly involved in fine graded spatial orientation on the host plant based on

distinct concentration gradients of CO_2. Detection of optimal oviposition sites is essential for the success of the offspring, and it is well known that such spots include metabolically active parts of the plant releasing high levels of CO_2. Thus, as compared with the ipsilateral projections from the main olfactory organ – which are reported not to detect chemical gradients (Kennedy, 1983; Kennedy & Marsh, 1974; Mafra-Neto & Cardé, 1994) - the arrangement of the accessory organ, including bilateral projections makes sense because it may directly monitor fine fluctuations of the chemosensory signal locally within different parts of the plant.

As mentioned above, the successful labeling of individual LPO neurons, included not only a bilateral and an ipsilateral type, as expected - but also a newly discovered contralateral type (Fig.3). As shown in Fig. 2C and D, Paper I, there are even two morphological sub-categories of these contralateral neurons – one following the main fiber bundle in the direction of the esophagus before crossing the midline, dorsally of the gnathal ganglion (GNG), and the other crossing the brain midline ventrally, already at the level of the GNG, and projecting contralaterally up to the AL. Interestingly, this contralateral course overlaps with that of the main fiber bundle of LPO projections originating from the other labial palp (see the figure below, which is reproduced from the Fig. S1 in the Supplementary Material of Paper I). The precise function of this pattern consisting of both parallel and overlapping projections is difficult to interpret. However, it is obvious that the LPO of the noctuid moth houses a morphologically multifaceted assembly of sensory neurons conveying signals about presumably one and the same stimulus, CO_2. This arrangement may serve as an ideal model for future investigations of how the neural system encodes sensory input.

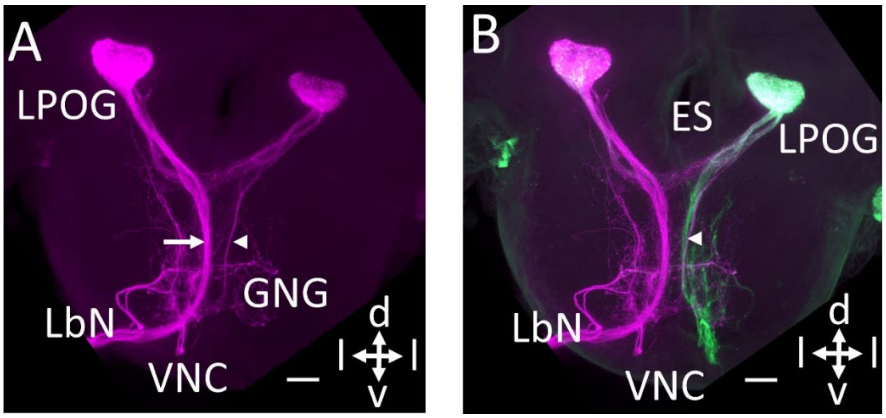

Fig. 3. Double-labeled preparation showing the staining pattern of sensory neurons originating from the terminal segment of the right (magenta) and left (green) labial palp respectively. **(A)** Confocal image (maximum intensity projection) showing sensory axons from the right palp, stained by Micro-Ruby. A thick sub-branch projects ipsilaterally (arrow) whereas a thin sub-branch projects contralaterally (arrowhead). **(B)** Double-labeling showing an overlay of the Micro-Ruby staining from the right palp (magenta) and Alexa-488 staining from the left palp (green). The thick fiber bundle from the left palp merges with the thin sub-bundle from the right palp (arrowhead). The non-focused mass staining including application of dye in the truncated part of the terminal labial palp resulted in labeled projections not only in the labial pit organ glomerulus (LPOG), but in the gnathal ganglion (GNG) and ventral nerve cord (VNC) as well. ES, esophagus; LbN, labial nerve; d, dorsal; v, ventral; l, lateral. Scale bars: 50 µm.

Comparison of sensory neurons tuned to CO_2 across different species

Interestingly, a comparison across different insect orders, such as Lepidoptera and Diptera, demonstrates some similarities but also marked differences as concerns morphological characteristics of the sensory neurons tuned to CO_2. The CO_2 sensory neurons in fruit flies and mosquitoes are housed on the antennae and the maxillary palp, respectively (Stocker et al., 1983). Like in lepidopterans, their axons project into one single glomerulus in the AL. Different from lepidopterans, however, fruit flies and most mosquitoes have ipsilateral CO_2 projections (Anton et al., 2003; Suh et al., 2004). Another distinction between the two insect orders is the amount of sensory neurons tuned to CO_2. In dipterans, the number of the CO_2 sensory neurons is quite small, that is 24-48 in fruit flies (Riesgo-Escovar et al., 1997) and 80 in mosquitoes (Lu et al., 2007; Syed & Leal, 2007), whereas the lepidopteran species studied here, *H. armigera*, has approximately 1200 CO_2

sensory neurons (Zhao et al., 2013). Regarding the lepidopteran species, diurnal butterflies and nocturnal moths have a similar system for detecting CO_2. As demonstrated in figure 4, the nocturnal *H. armigera* and diurnal *Aglais urticae* possess comparable LPO projections, except for a weaker innervation of the contralateral LPOG in the butterfly (Fig 4). Whether this is due to methodological conditions or a real difference in the omposition of bilateral, unilateral, and contralateral neurons is not clarified.

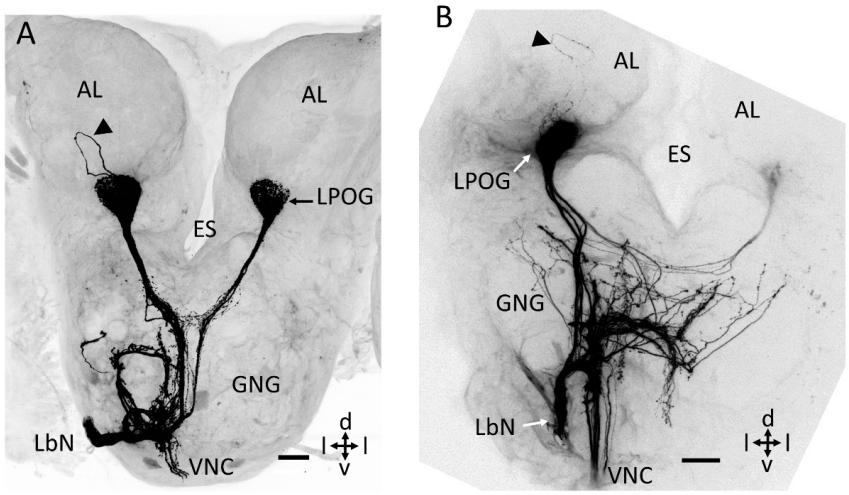

Fig. 4. Confocal images showing the central projection patterns of sensory neurons originating from the terminal segment of the labial palp in *H. armigera* and *Aglais urticae*. (A, B). In addition to the main projections inside the labial pit organ glomerulus (LPOG), a few branches ramifying outside the ipsilateral LPOG can be seen in both species (arrowheads); Figure a is adopted from paper I, and Figure b was kindly provided by Xi Chu; AL, antennal lobe; ES, esophagus; GNG, gnathal ganglion; LbN, labial nerve; VNC, ventral nerve cord. d, dorsal; v, ventral; l, lateral. Scale bars: 50 µm.

Several studies have reported about physiological properties of LPO sensory neurons in moth species and their specific tuning to CO_2 (Bogner et al., 1986; Guerenstein et al., 2004a; Stange, 1992). These sensory neurons are highly sensitive to small fluctuations in CO_2 concentration. The LPO sensory neurons in H. armigera, for example, can detect an increase in the gas as low as 0.5 ppm over the ambient level (Stange, 1992).

Morphological properties of LPOG output neurons

Second-order neurons from the LPOG project along uncommon AL tracts

To explore how CO_2 information is processed in the subsequent signal pathway, we performed a combination of single-cell labeling and mass labeling of the second-order PNs originating in the LPOG (paper II). One interesting topic that appeared from this part of our study is that the LPOG PNs are special by projecting to a large extent along other tracts than the classical medial tract, mALT. In fact, a majority of the stained LPOG output neurons, approximately 65%, were confined to the so far relatively poorly described transverse tract, tALT. As mentioned above, a recent article on AL neurons in heliothine moths reported that this relatively thin fiber bundle, identified as a separate tract in these species only five years ago, seems to be linked not to all glomeruli but to an assembly located ventro-posteriorly in the AL termed the VPGs, of which the LPOG is one of the units (Kymre et al., 2021a). Notably, the previous article by Kymre et al. mentioned another tract that appeared to originate exclusively from this VPG cluster – the dorsomedial tract, dmALT (Kymre et al., 2021a). This is in full agreement with the findings presented here, in paper II, including an LPOG PN passing along the dmALT. In contrast to the previously reported dorsomedial-tract PNs that were bilateral, the one presented here, in paper II, was unilateral, however – again indicating the uniqueness of the CO_2 pathway. It is worth noting that the dmALT is the thinnest of all tracts; in *M. sexta*, it is reported to include only three axons (Homberg et al., 1988). Concerning the mapping of AL tracts conveying CO_2 signals, it should be mentioned that our finding of only two medial-tract LPOG PNs, as reported in paper II, appears to contradict somehow with the previous report from *M. sexta*, including a majority of LPOG PNs passing along the mALT (Guerenstein et al., 2004a). However, at that time all transverse-tract PNs were classified as medial-tract neurons. The term transverse tract was introduced in the fruit fly in 2012 (Tanaka et al., 2012) and in the moth in 2016 (Ian et al., 2016a). In the study performed by Hildebrand and his colleagues, the

neuron named ‘PN-2’, for example, is obviously confined to the transverse tract (see Fig. 6a in Guerenstein et al., 2004a).

The second-order CO_2 pathway bypasses to a significant degree the calyces

Altogether, the LPOG PNs identified here were morphologically diverse, evidenced by 15 individual neurons forming as many as nine subtypes. Yet, most of them shared a morphological similarity in terms of not innervating the calyces. None of the medial-tract LPOG PNs identified here and only one-third of the transverse-tract LPOG PNs terminated in the calyces. Weak innervation in the calyces is also reported for second-order PNs conveying CO_2 signals in fruit flies (Lin et al., 2013). Generally, the calyces are a well-known olfactory center for sensory integration and memory formation (Heisenberg et al., 1985). The modest terminal projections of the LPOG PNs in the calyces indicate that the CO_2 input is negligibly involved in classic learning principles typifying this neuropil region. That is in fact not surprising since CO_2 is a ubiquitous cue and as such is expected to have a minimal effect on experience-based olfactory learning mechanisms. Interestingly, PNs processing input about other ubiquitous cues, such as temperature and humidity, have also been reported to display little or no connection with the calyces in fruit flies and cockroaches (Marin et al., 2020; Nishino et al., 2003).

Different from the majority of LPOG PNs stained here, the above-mentioned LPOG PNs in *M. sexta* were reported to target the calyces on their route to the LH (Guerenstein et al., 2004a). Whether these differences are due to methodological issues or imply real interspecific distinctions are not clarified.

Terminal projections of LPOG PNs and ordinary medial-tract PNs overlap in the LH

Interestingly, as shown in paper II, the majority of stained LPOG PNs had overlapping projection terminals in the second higher-order olfactory center, the LH, which is assumed to play a role in innate behavior (Schultzhaus et al., 2017). It is well known that this area also receives axon terminals of numerous medial-tract PNs originating in the ordinary glomeruli (Homberg et al., 1988; Ian et al., 2016b; Kymre et al., 2021a). These glomeruli, in turn, receive input from the plant odor responding sensory neurons on the antennae of both males and females. A purely male-specific higher-order region, receiving input from the MGC glomeruli, is located more dorso-medially in the protocerebrum (Chu et al., 2020; Kymre et al., 2021b). We found an overlap of terminal projections originating from LPOG PNs and PNs from ordinary glomeruli in the LH (Fig. 5), indicating the importance of that brain region for integration of sensory input about the CO_2 and plant odors. This kind of incorporation corresponds well with the previously reported data from behavioral studies of these herbivorous species demonstrating the importance of detecting CO_2 signals emitted by relevant host plants (Thom et al., 2004). Whether the second-order PNs of the two sub-systems make synaptic contact with the same third-order neurons is not known, however.

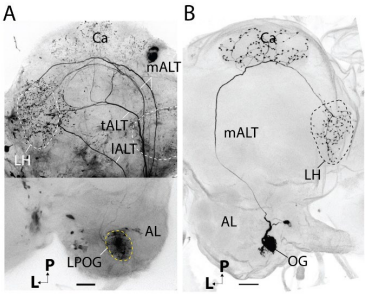

Fig. 5. Projection patterns of an assembly of LPOG PNs and one typical medial-tract PN originating from an ordinary glomerulus. **(A)** Confocal image (maximum intensity projection) of LPOG-neurons obtained via anterograde labeling from the LPOG including PNs confined to the transverse, medial, and lateral antennal-lobe tract (ALT; tALT, mALT, and lALT). Overlapping projection terminals occur in the lateral horn (LH) whereas the calyces (Ca) is weakly innervated. **(B)** Confocal image (maximum intensity projection) of a typical uniglomerular PN following the mALT and innervating the Ca and LH. Figures are adopted from paper II; L, lateral; P, posterior; Scale bars: 50 µm.

Comparison of the second-order CO_2 pathway across different species

Projection neurons tuned to CO_2 have previously been identified in the fruit fly, *D. melanogaster* (Lin et al., 2013), the hawk moth, *M. sexta* (Guerenstein et al., 2004a), and cotton bollworm, *H. armigera* (Paper II). A comparison of the morphological characteristics of the second-order PNs across these insect species demonstrates substantial similarities but also marked differences between the lepidopteran and the dipteran species. Even though the CO_2 system in fruit flies serves a completely different role than that of moths, their CO_2-PNs share many commonalities. Firstly, these PNs have minimal innervations in the calyces. In both insect groups, the axons of uniglomerular PNs innervating the calyces are confined either to the lALT or the tALT. (Lin et al., 2013; Paper II). Secondly, the PNs signaling input about CO_2 generally have diverse branching patterns in the protocerebrum and innervate mostly the LH. Thirdly, no medial-tract CO_2-PNs neither in fruit flies nor in moths seem to innervate the calyces. The most prominent morphological difference between the neuron populations of the two insect groups is that most CO_2-specific PNs in fruit flies are multiglomerular whereas those in moths are uniglomerular. In conclusion, the second-order pathways for CO_2 signaling in the two orders are comparable.

A putative link between the subsystems devoted to CO_2 and pheromones

Paper II indicated that CO_2 signals are essentially integrated with plant odor input at the second synaptic level and equivalently separated from pheromone information. However, since all three sub-systems are spatially represented in the AL in form of three non-overlapping glomerular arrangements – 1) LPOG, 2) MGC, and 3) ordinary glomeruli – that are interconnected via numerous multiglomerular local interneurons (LNs; Kymre et al., 2021a), we decided to investigate whether there are putative cross-talks between the pheromone and CO_2 system at the AL level. The relation between these two sub-systems of male moths

has not been investigated at any neuronal level previously. Even though all LPOG PNs identified in this study were uniglomerular neurons, the glomerulus itself, the LPOG, is not completely isolated but rather connected to other glomeruli by the large number of multiglomerular LNs in *H. armigera*. There are even a few multiglomerular PNs passing along the mediolateral tract, mlALT, that might be involved in this kind of crosstalk (Kymre et al., 2021a).

By performing retrograde labeling of all medial-tract output neurons with a calcium-sensitive dye (via dye application into the calyces), we could measure odor-evoked responses within distinct AL glomeruli (paper III). Here, we measured pheromone-induced responses in the easily identifiable MGC units. The stimulation with pheromone alone versus pheromone paired with CO_2, showed a decrease of the 'pure' pheromone-response when the gas was added to the odor stimulus. Our initial assumption implying that this suppression effect was mediated solely via the multiglomerular LNs, however, was not supported by a follow-up experiment including removal of the LPO. The suppression effect was gone for the low concentration of CO_2 but still present for the high concentration. Additional experiments including measurements of summated responses from the sensory neurons on the antennae (electroantennogram, EAG), indicated that the high-concentration suppression effect might be mediated via peripheral input from the antennae. This suppression effect could be due to several conditions. One could be a conformation change of the pheromone binding protein in the sensillum lymph due to CO_2-induced acidity (Mohanty et al., 2004). Another alternative reason could be that such an increase in acids activates ionotropic receptors (IRs) on the dendritic membrane of the OSNs. Studies in fruit flies have shown that carbonic acid, one of the metabolic products of hydration of CO_2, binds to IRs expressed in OSNs (Ai et al., 2010). Here, the co-expressed IR64a and IR8a, being present in coeloconic sensilla, detect acids. It is unknown at this stage, however, whether similar types of IRs are expressed in pheromone-specific sensilla of male moths or in other types of olfactory sensilla of moths. However, recently the homologous of the IR64a gene was found on the antennae of *H. armigera* (Liu et al., 2018),

indicating that the neuron expressing this receptor protein could detect acidosis produced by increased CO_2 concentrations. Whether an acid-sensing IR is, in fact, involved in suppressing the pheromone response is unknown. Future experiments utilizing genetically modified individuals lacking the relevant IRs might contribute to explaining the underlying mechanism.

But what is the meaning of an LPO in male moths that is similar to the LPO in females - a significant function of which is to provide suitable sites for egg-laying? It is generally accepted that CO_2 signals emitted from night-blooming plants, which are often 200 ppm above ambient CO_2 concentration (Guerenstein et al., 2004b), are important both for male and female moths since they guide the insects to relevant food sources. Generally, the CO_2 sensing system seems to play an important role for nectar foraging. One exception, however, is the cactus moth where only females possess an LPO (Stange et al., 1995). Single sensillum recordings have revealed that the LPO sensory neurons can follow short, intermittent increases in CO_2 level for stimuli delivered at a frequency as high as 10 Hz, indicating that the moth is able to track a plume of CO_2 and locate the source from relatively long distances (Guerenstein et al., 2004a; Stange, 1992). Another possible argument for the presence of a CO_2 detecting system in male moths is that it might facilitate the detection of a calling female sitting on the host plant. However, the meaning of a CO_2-induced *suppression* effect on the pheromone responses in the male moth is still an unanswered issue. Among sensible speculations, one might be that we see an effect similar to the previously reported interaction between pheromone and plant odor signaling including a mutual inhibition between two sub-systems (Deisig et al., 2012; Pregitzer et al., 2012).

In the experimental design, we performed two sets of calcium imaging measurements for each moth - one with intact and one with removed labial palps. During removal of the labial palp, the insect was taken out of the setup. This could have resulted in slight displacement of the focal plane during measurements in the second stimulation set. Besides, the physical intervention of taking away an

external organ may have influenced the total physiological condition of the insect. In future experiments, the surface of the palps should rather be covered, and with the insect positioned within the setup. Generally, the kind of calcium imaging experiments carried out here, would be optimally suited for genetically modified insects, especially distinct CO_2 GR knock-out mutants.

Methodological considerations

The examination of the CO_2 neural circuitry was enabled by the use of mainly three different experimental techniques: 1) anterograde and retrograde mass labeling, 2) intracellular single neuron staining, and 3) calcium imaging. Each of these methods allowed us to explore distinct aspects of A) the central projection pattern of the LPO sensory neurons, B) morphological characteristics of individual neurons at the two initial levels of the CO_2 pathway, and C) the effect of paired pheromone and CO_2 stimulation onto the odor-evoked responses in secondary medial-tract PNs. These methodological methods complemented each other by providing high- and low-resolution morphological data and combining them with physiological data. The results obtained from these approaches contribute to acquiring a relatively precise overview of the initial two levels of the CO_2-processing pathway in the noctuid moth. Future studies should include further exploration of the physiological properties characterizing the various neuron types, both at the first and second level of the signaling pathway. Here, it is relevant to compare with the electrophysiological results previously obtained from LPO sensory neurons in *H. armigera* and LPOG PNs in *M. sexta* (Guerenstein et al., 2004a; Stange, 1992). In addition, it is absolutely relevant and feasible to test, at the AL level, whether CO_2 influences on plant-odor-responses in the large population medial-tract PNs connected with the numerous ordinary glomeruli.

Conclusions

1. The sensory neurons in the LPO project exclusively to the LPOG. Individual LPO sensory neurons are morphologically diverse including both bilaterally, ipsilaterally, and contralaterally projecting neurons.
2. Sensory axons confined to the labial nerve and terminating in areas of the central nervous system, such as the GNG and the VNC, originate from sensory neurons located outside the LPO.
3. Uniglomerular PNs from the LPOG display a projection pattern differing markedly from that of the typical AL PNs by passing their axons mainly along the transverse tract. The morphologically different LPOG PNs project along at least four additional antennal lobe tracts, i.e. the mALT, lALT, dmALT, and the AST.
4. Generally, the LPOG PNs innervate the calyces weakly suggesting a modest role of this neuron population in associative memory formation. Notably, none of the medial-tract neurons originating in the LPOG had projection terminals in the Ca.
5. Most of the labeled LPOG PNs terminated in the LH, in a region seemingly overlapping with the target area of PNs linked to the ordinary glomeruli, indicating that inputs about CO_2 and plant odors are integrated in this region.
6. While pheromones and CO_2 are represented in spatially distinct protocerebral areas indicating a lack of signal exchange at the second synaptic level, inputs from the two types of chemosensory stimuli are linked at lower levels – indicated by suppression effects on the pheromone responses of second-order PNs from AL LNs as well as from male-specific antennal sensory neurons when CO_2 is added to the relevant blend.
7. Future studies should include a methodologically improved design to investigate more precisely how signals from CO_2 and pheromones interact at the level of the antennal lobe and antenna, respectively.

References

Ai, M., Min, S., Grosjean, Y., Leblanc, C., Bell, R., Benton, R., & Suh, G. S. (2010). Acid sensing by the Drosophila olfactory system. *Nature*, *468*(7324), 691-695. https://doi.org/10.1038/nature09537.

Anderson, T. R., Hawkins, E., & Jones, P. D. (2016). CO_2, the greenhouse effect and global warming: from the pioneering work of Arrhenius and Callendar to today's Earth System Models. *Endeavour*, *40*(3), 178-187. https://doi.org/https://doi.org/10.1016/j.endeavour.2016.07.002.

Anton, S., van Loon, J. J. A., Meijerink, J., Smid, H. M., Takken, W., & Rospars, J.-P. (2003). Central projections of olfactory receptor neurons from single antennal and palpal sensilla in mosquitoes. *Arthropod Structure & Development*, *32*(4), 319-327. https://doi.org/https://doi.org/10.1016/j.asd.2003.09.002.

Arrhenius, S. (1897). On the Influence of Carbonic Acid in the Air upon the Temperature of the Earth. *Publications of the Astronomical Society of the Pacific*, *9*, 14. https://doi.org/10.1086/121158.

Barral, A., Gomez, B., Fourel, F., Daviero-Gomez, V., & Lécuyer, C. (2017). CO_2 and temperature decoupling at the million-year scale during the Cretaceous Greenhouse. *Scientific Reports*, *7*(1), 8310. https://doi.org/10.1038/s41598-017-08234-0.

Black, J. (1756). Experiments upon magnesia alba, quicklime, and some other alcaline substances. *Essays and Observations: Physical and Literary*, *2*, 157–225.

Blunden, J., & Arndt, D. S. (Eds.). (2020). *State of the Climate in 2019* (Vol. 101). American Meteorological Society, S1-S429. https://doi.org/10.1175/2020BAMSStateoftheClimate.1.

Bogner, F., Boppre, M., Ernst, K. D., & Boeckh, J. (1986). CO_2 sensitive receptors on labial palps of Rhodogastria moths (Lepidoptera: Arctiidae): physiology, fine structure and central projection. *Journal of Comparative Physiology A*, *158*(6), 741-749.

Bohbot, J. D., Sparks, J. T., & Dickens, J. C. (2014). The maxillary palp of *Aedes aegypti*, a model of multisensory integration. *Insect Biochemistry and Molecular Biology*, *48*, 29-39. https://doi.org/https://doi.org/10.1016/j.ibmb.2014.02.007.

Bray, S., & Amrein, H. (2003). A putative Drosophila pheromone receptor expressed in male-specific taste neurons is required for efficient courtship. *Neuron*, *39*(6), 1019-1029. https://doi.org/10.1016/s0896-6273(03)00542-7.

Briscoe, A. D., Macias-Muñoz, A., Kozak, K. M., Walters, J. R., Yuan, F., Jamie, G. A., Martin, S. H., ….. Jiggins, C. D. (2013). Female behaviour drives expression and evolution of gustatory receptors in butterflies. *PLoS genetics*, *9*(7), e1003620-e1003620. https://doi.org/10.1371/journal.pgen.1003620.

Buehlmann, C., Hansson, B. S., & Knaden, M. (2012). Path integration controls nest-plume following in desert ants. *Current Biology*, *22*(7), 645-649. https://doi.org/10.1016/j.cub.2012.02.029.

Burrows, M. T., Schoeman, D. S., Buckley, L. B., Moore, P., Poloczanska, E. S., Brander, K. M., Brown, C., ….. Richardson, A. J. (2011). The Pace of Shifting Climate in Marine and Terrestrial Ecosystems. *Science*, *334*(6056), 652-655. https://doi.org/10.1126/science.1210288.

Chen, I.-C., Hill, J. K., Ohlemüller, R., Roy, D. B., & Thomas, C. D. (2011). Rapid Range Shifts of Species Associated with High Levels of Climate Warming. *Science*, *333*(6045), 1024-1026. https://doi.org/10.1126/science.1206432.

Chu, X., Heinze, S., Ian, E., & Berg, B. G. (2020). A Novel Major Output Target for Pheromone-Sensitive Projection Neurons in Male Moths. *Frontiers in cellular Neuroscience*, *14*(147). https://doi.org/10.3389/fncel.2020.00147.

Cummins, E. P., Selfridge, A. C., Sporn, P. H., Sznajder, J. I., & Taylor, C. T. (2014). Carbon dioxide-sensing in organisms and its implications for human disease. *Cellular and Molecular Life Sciences*, *71*(5), 831-845. https://doi.org/10.1007/s00018-013-1470-6.

Cunningham, J. P., & Zalucki, M. P. (2014). Understanding heliothine (Lepidoptera: Heliothinae) pests: what is a host plant? *Journal of Economic Entomology*, *107*(3), 881-896. https://doi.org/10.1603/ec14036.

Deisig, N., Kropf, J., Vitecek, S., Pevergne, D., Rouyar, A., Sandoz, J.-C., Lucas, P., Gadenne, C., Anton, S., & Barrozo, R. (2012). Differential Interactions of Sex Pheromone and Plant Odour in the Olfactory Pathway of a Male Moth. *PLoS One*, *7*(3), e33159. https://doi.org/10.1371/journal.pone.0033159.

Dirzo, R., Young, H. S., Galetti, M., Ceballos, G., Isaac, N. J. B., & Collen, B. (2014). Defaunation in the Anthropocene. *Science*, *345*(6195), 401-406. https://doi.org/10.1126/science.1251817.

Dong, J., Liu, H., Tang, Q., Liu, Y., Zhao, X., & Wang, G. (2014). Morphology, type and distribution of the labial-palp pit organ and its sensilla in the oriental armyworm, *Mythimna separata* (Lepidoptera: Noctuidae). *Acta Entomologica Sinica*, *57*(6), 681-687.

Erdelyan, C. N. G., Mahood, T. H., Bader, T. S. Y., & Whyard, S. (2012). Functional validation of the carbon dioxide receptor genes in *Aedes aegypti* mosquitoes using RNA interference. *Insect Molecular Biology*, *21*(1), 119-127. https://doi.org/https://doi.org/10.1111/j.1365-2583.2011.01120.x.

Eyun, S.-i., Soh, H. Y., Posavi, M., Munro, J. B., Hughes, D. S. T., Murali, S. C., Qu, J., … Lee, C. E. (2017). Evolutionary History of Chemosensory-Related Gene Families across the Arthropoda. *Molecular Biology and Evolution*, *34*(8), 1838-1862. https://doi.org/10.1093/molbev/msx147.

Faucher, C. P., Hilker, M., & de Bruyne, M. (2013). Interactions of Carbon Dioxide and Food Odours in Drosophila: Olfactory Hedonics and Sensory Neuron Properties. *PLoS One*, *8*(2), e56361. https://doi.org/10.1371/journal.pone.0056361.

Gillies, M. T. (1980). The role of carbon dioxide in host-finding by mosquitoes (Diptera: Culicidae): a review. *Bulletin of Entomological Research*, *70*(4), 525-532. https://doi.org/10.1017/S0007485300007811.

Grant, A. J., Aghajanian, J. G., O'Connell, R. J., & Wigton, B. E. (1995). Electrophysiological responses of receptor neurons in mosquito maxillary palp sensilla to carbon dioxide. *Journal of Comparative Physiology A*, *177*(4), 389-396. https://doi.org/10.1007/BF00187475.

Grant, A. J., & O'Connell, R. J. (2007). Electrophysiological Responses from Receptor Neurons in Mosquito Maxillary Palp Sensilla. In G. R. Bock & G. Cardew (Eds.), *Ciba Foundation Symposium 200 - Olfaction in Mosquito-Host Interactions* (pp. 233-253). https://doi.org/10.1002/9780470514948.ch17.

Guerenstein, P. G., Christensen, T. A., & Hildebrand, J. G. (2004a). Sensory processing of ambient CO_2 information in the brain of the moth *Manduca sexta*. *Journal of Comparative Physiology A*, *190*(9), 707-725. https://doi.org/10.1007/s00359-004-0529-0.

Guerenstein, P. G., E, A. Y., Van Haren, J., Williams, D. G., & Hildebrand, J. G. (2004b). Floral CO_2 emission may indicate food abundance to nectar-feeding moths. *Naturwissenschaften*, *91*(7), 329-333. https://doi.org/10.1007/s00114-004-0532-x.

Guerenstein, P. G., & Hildebrand, J. G. (2008). Roles and effects of environmental carbon dioxide in insect life. *Annual Review of Entomology*, *53*, 161-178. https://doi.org/10.1146/annurev.ento.53.103106.093402.

Guo, M., Chen, Q., Liu, Y., Wang, G., & Han, Z. (2018). Chemoreception of Mouthparts: Sensilla Morphology and Discovery of Chemosensory Genes in Proboscis and Labial Palps of Adult *Helicoverpa armigera* (Lepidoptera: Noctuidae). *Frontiers in physiology*, *9*, 970-970. https://doi.org/10.3389/fphys.2018.00970.

Hansson, B. S., & Christensen, T. A. (1999). Functional Characteristics of the Antennal Lobe. In B. S. Hansson (Ed.), *Insect Olfaction* (pp. 125-161). Springer Berlin Heidelberg. https://doi.org/10.1007/978-3-662-07911-9_6.

Hardwick, D. F. (1965). The Corn Earworm Complex. *Memoirs of the Entomological Society of Canada*, *97*(S40), 5-247. https://doi.org/10.4039/entm9740fv.

Heisenberg, M., Borst, A., Wagner, S., & Byers, D. (1985). Drosophila mushroom body mutants are deficient in olfactory learning. *Journal of Neurogenetics*, *2*(1), 1-30. https://doi.org/10.3109/01677068509100140.

Hetherington, A. M., & Raven, J. A. (2005). The biology of carbon dioxide. *Current Biology*, *15*(11), R406-410. https://doi.org/10.1016/j.cub.2005.05.042.

Hildebrand, J. G., & Shepherd, G. M. (1997). MECHANISMS OF OLFACTORY DISCRIMINATION: Converging Evidence for Common Principles Across Phyla. *Annual Review of Neuroscience*, *20*(1), 595-631. https://doi.org/10.1146/annurev.neuro.20.1.595.

Homberg, U., Christensen, T. A., & Hildebrand, J. G. (1989). Structure and function of the deutocerebrum in insects. *Annual Review of Entomology*, *34*, 477-501. https://doi.org/10.1146/annurev.en.34.010189.002401.

Homberg, U., Montague, R. A., & Hildebrand, J. G. (1988). Anatomy of antenno-cerebral pathways in the brain of the sphinx moth *Manduca sexta*. *Cell and Tissue Research*, *254*(2), 255-281.

Hättenschwiler, S., & Schafellner, C. (2004). Gypsy moth feeding in the canopy of a CO_2-enriched mature forest. *Global Change Biology*, *10*(11), 1899-1908. https://doi.org/https://doi.org/10.1111/j.1365-2486.2004.00856.x.

Ian, E., Berg, A., Lillevoll, S. C., & Berg, B. G. (2016a). Antennal-lobe tracts in the noctuid moth, *Heliothis virescens*: new anatomical findings. *Cell and Tissue Research*, *366*(1), 23-35. https://doi.org/10.1007/s00441-016-2448-0

Ian, E., Zhao, X. C., Lande, A., & Berg, B. G. (2016b). Individual Neurons Confined to Distinct Antennal-Lobe Tracts in the Heliothine Moth: Morphological Characteristics and Global Projection Patterns. *Frontiers in Neuroanatomy*, *10*, 101. https://doi.org/10.3389/fnana.2016.00101

Jones, W. D., Cayirlioglu, P., Kadow, I. G., & Vosshall, L. B. (2007). Two chemosensory receptors together mediate carbon dioxide detection in Drosophila. *Nature*, *445*(7123), 86-90. https://doi.org/10.1038/nature05466.

Jorgensen, K., Kvello, P., Almaas, T. J., & Mustaparta, H. (2006). Two closely located areas in the suboesophageal ganglion and the tritocerebrum receive projections of gustatory receptor neurons located on the antennae and the proboscis in the moth *Heliothis virescens*. *Journal of Comparative Neurology*, *496*(1), 121-134. https://doi.org/10.1002/cne.20908.

Kaissling, K. E., Strausfeld, C. Z., & Rumbo, E. R. (1987). Adaptation Processes in Insect Olfactory Receptors. *Annals of the New York Academy of Sciences*, *510*(1), 104-112. https://doi.org/https://doi.org/10.1111/j.1749-6632.1987.tb43475.x.

Kanzaki, R., Soo, K., Seki, Y., & Wada, S. (2003). Projections to Higher Olfactory Centers from Subdivisions of the Antennal Lobe Macroglomerular Complex of the Male Silkmoth. *Chemical Senses*, *28*(2), 113-130. https://doi.org/10.1093/chemse/28.2.113.

Kawahara, A. Y., Plotkin, D., Espeland, M., Meusemann, K., Toussaint, E. F. A., Donath, A., Gimnich, F., ….. Breinholt, J. W. (2019). Phylogenomics reveals the evolutionary timing and pattern of butterflies and moths. *Proceedings of the National Academy of Sciences*, *116*(45), 22657-22663. https://doi.org/10.1073/pnas.1907847116.

Kennedy, J. S. (1983). Zigzagging and casting as a programmed response to wind-borne odour: a review. *Physiological Entomology*, *8*(2), 109-120. https://doi.org/https://doi.org/10.1111/j.1365-3032.1983.tb00340.x.

Kennedy, J. S., & Marsh, D. (1974). Pheromone-regulated anemotaxis in flying moths. *Science*, *184*(4140), 999-1001. https://doi.org/10.1126/science.184.4140.999.

Kent, K. S., Harrow, I. D., Quartararo, P., & Hildebrand, J. G. (1986). An accessory olfactory pathway in Lepidoptera: the labial pit organ and its central projections in *Manduca sexta* and certain other sphinx moths and silk moths. *Cell and Tissue Research*, *245*(2), 237-245. https://doi.org/10.1007/bf00213927.

Kleineidam, C., & Roces, F. (2000). Carbon dioxide concentrations and nest ventilation in nests of the leaf-cutting ant *Atta vollenweideri*. *Insectes Sociaux*, *47*(3), 241-248. https://doi.org/10.1007/PL00001710.

Kleineidam, C., Romani, R., Tautz, J., & Isidoro, N. (2000). Ultrastructure and physiology of the CO_2 sensitive sensillum ampullaceum in the leaf-cutting ant *Atta sexdens*. *Arthropod Structure & Development*, *29*(1), 43-55. https://www.ncbi.nlm.nih.gov/pubmed/18088913.

Kristensen, N. P., Scoble, M., & Karsholt, O. (2007). Lepidoptera phylogeny and systematics: the state of inventorying moth and butterfly diversity. *Zootaxa*, *1668*, 699-747.

Kvello, P., Almaas, T. J., & Mustaparta, H. (2006). A confined taste area in a lepidopteran brain. *Arthropod Structure & Development*, *35*(1), 35-45. https://doi.org/10.1016/j.asd.2005.10.003.

Kwon, J. Y., Dahanukar, A., Weiss, L. A., & Carlson, J. R. (2007). The molecular basis of CO_2 reception in Drosophila. *Proceedings of the National Academy of Sciences*, *104*(9), 3574-3578. https://doi.org/10.1073/pnas.0700079104.

Kymre, J. H., Berge, C. N., Chu, X., Ian, E., & Berg, B. G. (2021a). Antennal-lobe neurons in the moth *Helicoverpa armigera*: Morphological features of projection neurons, local interneurons, and centrifugal neurons. *Journal of Comparative Neurology*, *529*(7). https://doi.org/https://doi.org/10.1002/cne.25034

Kymre, J. H., Liu, X., Ian, E., Berge, C. N., Wang, G., Berg, B. G., Zhao, X., & Chu, X. (2021b). Distinct protocerebral neuropils associated with attractive and aversive female-produced odorants in the male moth brain. *eLife*, *10*, e65683. https://doi.org/10.7554/eLife.65683.

Lastra-Valdés, J., Silva, J. R. M. C. d., & Duarte, M. (2020). Morphology and histology of vom Rath's organ in brush-footed butterflies (Lepidoptera: Nymphalidae). *PLoS One*, *15*(4), e0231486. https://doi.org/10.1371/journal.pone.0231486.

Lee, J.-K., Selzer, R., & Altner, H. (1985). Lamellated outer dendritic segments of a chemoreceptor within wall-pore sensilla in the labial palp-pit organ of the butterfly, *Pieris rapae* L. (Insecta, Lepidoptera). *Cell and Tissue Research*, *240*(2), 333-342. https://doi.org/10.1007/bf00222343.

Lin, H. H., Chu, L. A., Fu, T. F., Dickson, B. J., & Chiang, A. S. (2013). Parallel neural pathways mediate CO_2 avoidance responses in Drosophila. *Science.*, *340*(6138), 1338-1341. https://doi.org/10.1126/science.1236693.

Liu, N.-Y., Xu, W., Dong, S.-L., Zhu, J.-Y., Xu, Y.-X., & Anderson, A. (2018). Genome-wide analysis of ionotropic receptor gene repertoire in Lepidoptera with an emphasis on its functions of *Helicoverpa armigera*. *Insect Biochemistry and Molecular Biology*, *99*, 37-53. https://doi.org/https://doi.org/10.1016/j.ibmb.2018.05.005.

Louis, M., Huber, T., Benton, R., Sakmar, T. P., & Vosshall, L. B. (2008). Bilateral olfactory sensory input enhances chemotaxis behavior. *Nature Neuroscience*, *11*(2), 187-199. https://doi.org/10.1038/nn2031.

Lu, T., Qiu, Y. T., Wang, G., Kwon, J. Y., Rutzler, M., Kwon, H. W., Pitts, R. J., ….. Zwiebel, L. J. (2007). Odor coding in the maxillary palp of the malaria vector mosquito *Anopheles gambiae*. *Current Biology*, *17*(18), 1533-1544. https://doi.org/10.1016/j.cub.2007.07.062.

Ma, B. W., Zhao, X. C., Berg, B. G., Xie, G. Y., Tang, Q. B., & Wang, G. R. (2017). Central Projections of Antennal and Labial Palp Sensory Neurons in the Migratory Armyworm *Mythimna separata*. *Frontiers in cellular Neuroscience*, *11*, 370. https://doi.org/10.3389/fncel.2017.00370.

MacWilliam, D., Kowalewski, J., Kumar, A., Pontrello, C., & Ray, A. (2018). Signaling Mode of the Broad-Spectrum Conserved CO(2) Receptor Is One of the Important Determinants of Odor Valence in Drosophila. *Neuron*, *97*(5), 1153-1167.e1154. https://doi.org/10.1016/j.neuron.2018.01.028.

Mafra-Neto, A., & Cardé, R. T. (1994). Fine-scale structure of pheromone plumes modulates upwind orientation of flying moths. *Nature*, *369*(6476), 142-144. https://doi.org/10.1038/369142a0.

Marin, E. C., Büld, L., Theiss, M., Sarkissian, T., Roberts, R. J. V., Turnbull, R., ……Jefferis, G. S. X. E. (2020). Connectomics Analysis Reveals First-, Second-, and Third-Order Thermosensory and Hygrosensory Neurons in the Adult Drosophila Brain. *Current Biology*, *30*(16), 3167-3182.e3164. https://doi.org/10.1016/j.cub.2020.06.028.

Mohanty, S., Zubkov, S., & Gronenborn, A. M. (2004). The solution NMR structure of Antheraea polyphemus PBP provides new insight into pheromone recognition by pheromone-binding proteins. *Journal of molecular biology*, *337*(2), 443-451. https://doi.org/10.1016/j.jmb.2004.01.009.

Ning, C., Yang, K., Xu, M., Huang, L. Q., & Wang, C. Z. (2016). Functional validation of the carbon dioxide receptor in labial palps of *Helicoverpa armigera* moths. *Insect. Biochem. Mol. Biol.*, *73*, 12-19. https://doi.org/10.1016/j.ibmb.2016.04.002.

Nishino, H., Yamashita, S., Yamazaki, Y., Nishikawa, M., Yokohari, F., & Mizunami, M. (2003). Projection neurons originating from thermo- and hygrosensory glomeruli in the antennal lobe of the cockroach. *Journal of Comparative Neurology*, *455*(1), 40-55. https://doi.org/10.1002/cne.10450.

Obiero, G. F. O., Mireji, P. O., Nyanjom, S. R. G., Christoffels, A., Robertson, H. M., & Masiga, D. K. (2014). Odorant and Gustatory Receptors in the Tsetse Fly *Glossina morsitans*. *PLOS Neglected Tropical Diseases*, *8*(4), e2663. https://doi.org/10.1371/journal.pntd.0002663.

Piersanti, S., Frati, F., Rebora, M., & Salerno, G. (2016). Carbon dioxide detection in adult Odonata. *Zoology*, *119*(2), 137-142. https://doi.org/https://doi.org/10.1016/j.zool.2016.01.003.

Piersanti, S., Rebora, M., & Gaino, E. (2010). A scanning electron microscope study of the antennal sensilla in adult zygoptera. *Odonatologica*, *39*, 235-241.

Pregitzer, P., Schubert, M., Breer, H., Hansson, B., Sachse, S., & Krieger, J. (2012). Plant odorants interfere with detection of sex pheromone signals by male *Heliothis virescens*. *Frontiers in cellular neuroscience*, *6*(42). https://doi.org/10.3389/fncel.2012.00042.

Rasch, C., & Rembold, H. (1994). Carbon-dioxide — highly attractive signal for larvae of *Helicoverpa armigera*. *Naturwissenschaften*, *81*(5), 228-229. https://doi.org/10.1007/BF01138549.

Riesgo-Escovar, J. R., Piekos, W. B., & Carlson, J. R. (1997). The Drosophila antenna: ultrastructural and physiological studies in wild-type and lozenge mutants. *Journal of Comparative Physiology A*, *180*(2), 151-160. https://doi.org/10.1007/s003590050036.

Riley, J. R., Armes, N. J., Reynolds, D. R., & Smith, A. D. (1992). Nocturnal observations on the emergence and flight behaviour of *Helicoverpa armigera* (Lepidoptera: Noctuidae) in the post-rainy season in central India. *Bulletin of Entomological Research*, *82*(2), 243-256. https://doi.org/10.1017/S0007485300051798.

Robertson, H. M., & Kent, L. B. (2009). Evolution of the gene lineage encoding the carbon dioxide receptor in insects. *Journal of Insect Science*, *9*, 19. https://doi.org/10.1673/031.009.1901.

Robinson, E. A., Ryan, G. D., & Newman, J. A. (2012). A meta-analytical review of the effects of elevated CO_2 on plant-arthropod interactions highlights the importance of interacting environmental and biological variables. *New Phytologist*, *194*(2), 321-336. https://doi.org/10.1111/j.1469-8137.2012.04074.x.

Schultzhaus, J. N., Saleem, S., Iftikhar, H., & Carney, G. E. (2017). The role of the Drosophila lateral horn in olfactory information processing and behavioral response. *Journal of Insect Physiology*, *98*, 29-37. https://doi.org/https://doi.org/10.1016/j.jinsphys.2016.11.007.

Seeley, T. D. (1974). Atmospheric carbon dioxide regulation in honey-bee (*Apis mellifera*) colonies. *Journal of Insect Physiology*, *20*(11), 2301-2305. https://www.ncbi.nlm.nih.gov/pubmed/4424243.

Shanbhag, S. R., Muller, B., & Steinbrecht, R. A. (1999). Atlas of olfactory organs of *Drosophila melanogaster* - 1. Types, external organization, innervation and distribution of olfactory sensilla. *International Journal of Insect Morphology & Embryology*, *28*(4), 377-397. https://doi.org/Doi 10.1016/S0020-7322(99)00039-2.

Shevela, D., Björn, L., & Govindjee, G. (2019). *Photosynthesis: Solar Energy for Life*. https://doi.org/10.1142/10522.

Smith, C. D., Zimin, A., Holt, C., Abouheif, E., Benton, R., Cash, E., Croset, V., ….. Tsutsui, N. D. (2011a). Draft genome of the globally widespread and invasive Argentine ant (*Linepithema humile*). *Proceedings of the National Academy of Sciences*, *108*(14), 5673. https://doi.org/10.1073/pnas.1008617108.

Smith, C. R., Smith, C. D., Robertson, H. M., Helmkampf, M., Zimin, A., Yandell, M., Holt, C., ….. Gadau, J. (2011b). Draft genome of the red harvester ant *Pogonomyrmex barbatus*. *Proceedings of the National Academy of Sciences*, *108*(14), 5667-5672. https://doi.org/10.1073/pnas.1007901108.

Song, Y. Q., Sun, H. Z., & Wu, J. X. (2016). Ultrastructural characteristics of the proboscis and the labial palp pit organ in the oriental fruit moth, *Grapholita molesta*. *Bulletin of Insectology*, *69*(1), 59-66.

Soni, N., Chahda, J. S., & Carlson, J. R. (2019). Odor coding in the antenna of the tsetse fly *Glossina morsitans*. *Proceedings of the National Academy of Sciences*, *116*(28), 14300. https://doi.org/10.1073/pnas.1907075116.

Stange, G. (1992). High resolution measurement of atmospheric carbon dioxide concentration changes by the labial palp organ of the moth *Heliothis armigera* (Lepidoptera: Noctuidae). *Journal of Comparative Physiology A*, *171*(3), 317-324. https://doi.org/10.1007/bf00223962.

Stange, G. (1997). Effects of changes in atmospheric carbon dioxide on the location of hosts by the moth, *Cactoblastis cactorum*. *Oecologia.*, *110*(4), 539-545. https://doi.org/10.1007/s004420050192.

Stange, G., Monro, J., Stowe, S., & Osmond, C. B. (1995). The CO_2 sense of the moth *Cactoblastis cactorum* and its probable role in the biological control of the CAM plant *Opuntia stricta*. *Oecologia*, *102*(3), 341-352. https://doi.org/10.1007/BF00329801.

Stange, G., & Stowe, S. (1999). Carbon dioxide sensing structures in terrestrial arthropods. *Microscopy Research and Technique*, *47*(6), 416-427. https://doi.org/10.1002/(SICI)1097-0029(19991215)47:6 416::AID-JEMT5 3.0.CO;2-X

Steullet, P., & Guerin, P. M. (1992). Perception of breath components by the tropical bont tick, *Amblyomma variegatum Fabricius* (Ixodidae). *Journal of Comparative Physiology A*, *170*(6), 665-676. https://doi.org/10.1007/BF00198976.

Stocker, R. F., Singh, R. N., Schorderet, M., & Siddiqi, O. (1983). Projection patterns of different types of antennal sensilla in the antennal glomeruli of *Drosophila melanogaster*. *Cell and Tissue Research*, *232*(2), 237-248. https://doi.org/10.1007/bf00213783.

Suh, G. S., Wong, A. M., Hergarden, A. C., Wang, J. W., Simon, A. F., Benzer, S., Axel, R., & Anderson, D. J. (2004). A single population of olfactory sensory neurons mediates an innate avoidance behaviour in Drosophila. *Nature*, *431*(7010), 854-859. https://doi.org/10.1038/nature02980.

Syed, Z., & Leal, W. S. (2007). Maxillary Palps Are Broad Spectrum Odorant Detectors in *Culex quinquefasciatus*. *Chemical Senses*, *32*(8), 727-738. https://doi.org/10.1093/chemse/bjm040.

Tanaka, N. K., Suzuki, E., Dye, L., Ejima, A., & Stopfer, M. (2012). Dye fills reveal additional olfactory tracts in the protocerebrum of wild-type Drosophila. *Journal of Comparative Neurology*, *520*(18), 4131-4140. https://doi.org/10.1002/cne.23149.

Terrapon, N., Li, C., Robertson, H. M., Ji, L., Meng, X., Booth, W., Chen, Z., Childers, C. P., ….. Liebig, J. (2014). Molecular traces of alternative social organization in a termite genome. *Nature Communications*, *5*(1), 3636. https://doi.org/10.1038/ncomms4636.

Thom, C., Guerenstein, P. G., Mechaber, W. L., & Hildebrand, J. G. (2004). Floral CO_2 reveals flower profitability to moths. *Journal of Chemical Ecology*, *30*(6), 1285-1288. https://doi.org/10.1023/B:JOEC.0000030298.77377.7d.

Wang, X., Fang, X., Yang, P., Jiang, X., Jiang, F., Zhao, D., Li, B., ….. Kang, L. (2014). The locust genome provides insight into swarm formation and long-distance flight. *Nature Communications*, *5*(1), 2957. https://doi.org/10.1038/ncomms3957.

Wanner, K. W., & Robertson, H. M. (2008). The gustatory receptor family in the silkworm moth *Bombyx mori* is characterized by a large expansion of a single lineage of putative bitter receptors. *Insect Molecular Biology*, *17*(6), 621-629. https://doi.org/https://doi.org/10.1111/j.1365-2583.2008.00836.x

Wasserman, S., Salomon, A., & Frye, Mark A. (2013). Drosophila Tracks Carbon Dioxide in Flight. *Current Biology*, *23*(4), 301-306. https://doi.org/https://doi.org/10.1016/j.cub.2012.12.038.

Waters, R. M. (1933). USE OF CARBON DIOXIDE IN ANESTHESIA. *Journal of the American Medical Association*, *100*(16), 1275-1276. https://doi.org/10.1001/jama.1933.02740160059028

West, J. B. (2014). Joseph Black, carbon dioxide, latent heat, and the beginnings of the discovery of the respiratory gases. *American Journal of Physiology-Lung Cellular and Molecular Physiology*, *306*(12), L1057-1063. https://doi.org/10.1152/ajplung.00020.2014.

Wicher, D., Schafer, R., Bauernfeind, R., Stensmyr, M. C., Heller, R., Heinemann, S. H., & Hansson, B. S. (2008). Drosophila odorant receptors are both ligand-gated and cyclic-nucleotide-activated cation channels. *Nature*, *452*(7190), 1007-1011. https://doi.org/10.1038/nature06861.

Wolff, G. H., & Riffell, J. A. (2018). Olfaction, experience and neural mechanisms underlying mosquito host preference. *Journal of Experimental Biology*, *221*(Pt 4), jeb157131. https://doi.org/10.1242/jeb.157131.

Wu, H., Xu, M., Hou, C., Huang, L.-Q., Dong, J.-F., & Wang, C.-Z. (2015). Specific olfactory neurons and glomeruli are associated to differences in behavioral responses to pheromone components between two Helicoverpa species. *Frontiers in Behavioral Neuroscience*, *9*(206). https://doi.org/10.3389/fnbeh.2015.00206.

Xu, P., Wen, X., & Leal, W. S. (2020). CO_2 per se activates carbon dioxide receptors. *Insect Biochemistry and Molecular Biology*, *117*, 103284-103284. https://doi.org/10.1016/j.ibmb.2019.103284.

Xu, W., & Anderson, A. (2015). Carbon dioxide receptor genes in cotton bollworm *Helicoverpa armigera*. *Naturwissenschaften*, *102*(3-4), 11. https://doi.org/10.1007/s00114-015-1260-0.

Yamana, K., Toh, Y., & Tateda, H. (1986). Electrophysiological Studies on the Temporal Organ of the Japanese House Centipede, *Thereuonema hilgendorfi*. *Journal of Experimental Biology*, *126*(1), 297. http://jeb.biologists.org/content/126/1/297

Yao, C. A., & Carlson, J. R. (2010). Role of G-Proteins in Odor-Sensing and CO_2-Sensing Neurons in Drosophila. *The Journal of Neuroscience*, *30*(13), 4562-4572. https://doi.org/10.1523/jneurosci.6357-09.2010.

Zalucki, M., Daglish, G., Firempong, S., & Twine, P. (1986). The Biology and Ecology of *Heliothis armigera* (Hubner) and *Heliothis punctigera Wallengren* (Lepidoptera, Noctuidae) in Australia - What Do We Know. *Australian Journal of Zoology*, *34*(6), 779-814. https://doi.org/https://doi.org/10.1071/ZO9860779.

Zalucki, M., Murray, D., Gregg, P., Fitt, G., Twine, P., & Jones, C. (1994). Ecology of *Helicoverpa armigera* (Hubner) and *Heliothis punctigera* (Wallengren) in the Inland of Australia - Larval Sampling and Host-Plant Relationships During Winter and Spring. *Australian Journal of Zoology*, *42*(3), 329-346. https://doi.org/https://doi.org/10.1071/ZO9940329.

Zhan, S., Merlin, C., Boore, Jeffrey L., & Reppert, Steven M. (2011). The Monarch Butterfly Genome Yields Insights into Long-Distance Migration. *Cell*, *147*(5), 1171-1185. https://doi.org/https://doi.org/10.1016/j.cell.2011.09.052.

Zhang, H. J., Anderson, A. R., Trowell, S. C., Luo, A. R., Xiang, Z. H., & Xia, Q. Y. (2011). Topological and functional characterization of an insect gustatory receptor. *PLoS One*, *6*(8), e24111. https://doi.org/10.1371/journal.pone.0024111.

Zhao, X.-C., Chen, Q.-Y., Guo, P., Xie, G.-Y., Tang, Q.-B., Guo, X.-R., & Berg, B. G. (2016). Glomerular identification in the antennal lobe of the male moth *Helicoverpa armigera*, *Journal of Comparative Neurology*, *524*(15), 2993-3013. https://doi.org/doi:10.1002/cne.24003.

Zhao, X.-C., Kvello, P., Løfaldli, B. B., Lillevoll, S. C., Mustaparta, H., & Berg, B. G. (2014). Representation of pheromones, interspecific signals, and plant odors in higher olfactory centers; mapping physiologically identified antennal-lobe projection neurons in the male heliothine moth. *Frontiers in system Neuroscience*, *8*, 186-186. https://doi.org/10.3389/fnsys.2014.00186.

Zhao, X. C., Tang, Q. B., Berg, B. G., Liu, Y., Wang, Y. R., Yan, F. M., & Wang, G. R. (2013). Fine structure and primary sensory projections of sensilla located in the labial-palp pit organ of *Helicoverpa armigera* (Insecta). *Cell and Tissue Research*, *353*(3), 399-408. https://doi.org/10.1007/s00441-013-1657-z.

Ziesmann, J. (1996). The physiology of an olfactory sensillum of the termite *Schedorhinotermes lamanianus*: carbon dioxide as a modulator of olfactory sensitivity. *Journal of Comparative Physiology A*, *179*(1), 123-133. https://doi.org/10.1007/BF00193440.

Individual papers

Paper I

frontiers in Physiology

ORIGINAL RESEARCH
published: 17 March 2020
doi: 10.3389/fphys.2020.00202

Revisiting the Labial Pit Organ Pathway in the Noctuid Moth, *Helicoverpa armigera*

*Pramod KC[1], Xi Chu[1], Pål Kvello[2], Xin-Cheng Zhao[3], Gui-Rong Wang[4] and Bente Gunnveig Berg[1]**

[1] Chemosensory Laboratory, Department of Psychology, Norwegian University of Science and Technology (NTNU), Trondheim, Norway, [2] Department of Teacher Education, Norwegian University of Science and Technology (NTNU), Trondheim, Norway, [3] Department of Entomology, College of Plant Protection, Henan Agricultural University, Zhengzhou, China, [4] State Key Laboratory for Biology of Plant Disease and Insect Pests, Institute of Plant Protection, Chinese Academy of Agricultural Sciences, Beijing, China

Lepidopteran species detect CO_2 via a specialized organ located on the peripheral segment of the labial palps, the labial palp pit organ (LPO). Based on tracing of LPO sensory neurons targeting one distinct antennal-lobe glomerulus, Kent and her colleagues described the projections originating from the LPO in the sphinx moth as "*an accessory olfactory pathway in Lepidoptera*" already in the 1980 ties. In spite of similar reports from studies of other lepidopteran species, however, it has been an unresolved issue whether additional termination areas of the labial nerve, such as the gnathal ganglion (GNG) and the ventral nerve cord, are actually output sites of LPO neurons. Since the previous studies have interpreted slightly differently about the projection pattern occurring from the classical mass staining, we performed selective mass staining from the inside of the pit and from the outer surface of the peripheral palp. The results demonstrated that the LPO sensory neurons project exclusively to the LPO glomerulus (LPOG), whereas the non-LPO sensory neurons target the GNG and the ventral nerve cord. Additional iontophoretic staining of individual LPO sensory neurons, performed from the LPO and the LPOG, showed three morphological neuron types: one bilateral targeting the LPOG in both antennal lobes, one unilateral targeting the ipsilateral LPOG only, and one contralateral targeting the LPOG in the other antennal lobe. Finally, to explore putative differences in the projection pattern of neurons housed by two previously reported sensillum types in the pit, i.e., hair-shaped sensilla located distally and club-shaped sensilla located proximally, we performed mass staining from two different levels of the peripheral palp. We found a projection pattern implying stronger innervation of the ipsi- than the contralateral LPOG in both staining experiments.

Keywords: LPO sensory pathway, LPOG, antennal lobe, individual sensory neurons, iontophoretic staining

OPEN ACCESS

Edited by:
Shigehiro Namiki,
The University of Tokyo, Japan

Reviewed by:
Peter Bräunig,
RWTH Aachen University, Germany
Xue Jun Sun,
University of Alberta, Canada

****Correspondence:***
Bente Gunnveig Berg
bente.berg@ntnu.no

Specialty section:
This article was submitted to Invertebrate Physiology, a section of the journal Frontiers in Physiology

Received: *06 December 2019*
Accepted: *21 February 2020*
Published: *17 March 2020*

Citation:
KC P, Chu X, Kvello P, Zhao X-C, Wang G-R and Berg BG (2020) Revisiting the Labial Pit Organ Pathway in the Noctuid Moth, Helicoverpa armigera. Front. Physiol. 11:202. doi: 10.3389/fphys.2020.00202

INTRODUCTION

Many insect species possess the ability to detect even small fluctuations in the atmospheric carbon dioxide (CO_2) concentration. When it comes to herbivorous insects, this gas is known to serve multiple roles in their interactions with host plants. The sphinx moth, *Manduca sexta,* for instance, is attracted to CO_2 emitted by freshly opened *Datura wrightii* flowers, which contain large amounts of nectar (Thom et al., 2004; Goyret et al., 2008). Generally, Lepidopteran species sense CO_2 via a

specialized structure called the labial pit organ (LPO; Lee et al., 1985; Kent et al., 1986). It is located on the distal segment of the labial palps where it forms a bottle-shaped cave by being narrow at the tip and wider at the base. Inside there are numerous sensilla containing the sensory neurons detecting CO_2 (Bogner et al., 1986; Stange, 1992).

Based on staining experiments demonstrating massive innervation in one ventrally located glomerulus in both antennal lobes of several sphinx moths and silk moths, Kent and colleagues described the projections originating from the LPO as "*an accessory olfactory pathway in Lepidoptera*" (1986). The innervated glomerulus was named the LPO glomerulus (LPOG). Notably, all other antennal-lobe glomeruli receive ipsilateral input from olfactory sensory neurons located on the antennae [reviewed by Homberg et al. (1989)]. An unresolved issue, however, is whether sensory axons from the LPO also have projections in central areas other than the antennal lobes. In the classical paper about the "accessory olfactory pathway," (Kent et al., 1986) found additional innervations in the gnathal ganglion (GNG), and consecutive studies of other moths have reported additional terminal branches in the ventral nerve cord (Lee and Altner, 1986; Zhao et al., 2013; Ma et al., 2017). In all these studies, dye was applied to the truncated part of the peripheral labial-palp segment. Whereas the two last-mentioned reports insisted that all labeled axons were CO_2-sensitive neurons projecting from the LPO (Zhao et al., 2013; Ma et al., 2017), the original paper suggested that the stained processes in the GNG arose from other sensory neurons on the labial palp (Kent et al., 1986). Thus, even though all previous studies have reported about LPO projections passing bilaterally to the LPOG in each antennal lobe, the total staining pattern including additional axon terminals in other central regions has been interpreted in various ways by the different investigations. Another relevant issue concerns the projection pattern of individual neurons. Although several studies have characterized the LPO sensory neurons, both structurally and functionally (Kent et al., 1986; Stange, 1992, 1997; Stange et al., 1995; Sage, 2002; Guerenstein et al., 2004; Zhao et al., 2013; Ma et al., 2017), we still know little about projection patterns of single axons and how the sampled CO_2 input is integrated in the central nervous system.

Interestingly, two morphological types of LPO sensilla were recently identified in the heliothine moth, *Helicoverpa armigera* (Zhao et al., 2013). Among the total number of approximately 1200 sensilla, ca. 700 were found to be hair-shaped with a smooth cuticle whereas the remaining 500 were club-shaped with a more grooved surface. The hair-shaped sensilla were found to be located distally in the pit and the club-shaped proximally. Similar sensillum types were reported in the migratory armymoth, *Mythimna separata* (Dong et al., 2014). The distinct projection patterns from the neurons housed inside these sensillum categories are not known, however.

In the present study, we performed staining experiments enabling tracing of the LPO-specific pathway in *H. armigera*. The findings demonstrate that the LPOGs are targeted by axons originating from the pit while the GNG and the ventral nerve cord are innervated by sensory neurons located on the outer surface of the peripheral palp segment. Furthermore, in order to explore putative differences in the projection patterns of neurons housed by the two morphological types of LPO sensilla identified in this species, we carried out anterograde mass staining of sensory axons originating in the pit by applying dye not only to its proximal part but also to the intermediate and distal part. In addition, we performed staining of individual sensory neurons by carrying out iontophoretic labeling from the LPOG as well as the LPO. This gave us the opportunity to trace projection patterns of individual LPO neurons.

MATERIALS AND METHODS

Insects and Preparation

Male *H. armigera* pupae (Lepidoptera; Noctuidae, Heliothinae), purchased from China (Henan Jiyuan Baiyun Industry Co., Ltd), were kept in climate chambers (Refritherm 200 and 6E, Struers-Kebo lab, Albertsund, Denmark, or Binder KBF 720, Tuttlingen, Germany) at 24°C and 70% air humidity on a reversed night-day cycle (14 h light and 10 h dark). The moths were supplied 10% sucrose solution. Experiments were conducted 1–3 days after the emergence. According to Norwegian law of animal welfare there are no restrictions regarding experimental use of Lepidoptera.

Anterograde Mass Staining of Sensory Neurons Originating From the Third Segment of the Labial Palp

In all experiments, the insect was placed inside a 1 ml plastic pipette (VWR chemicals, France) with the head exposed and then immobilized with dental wax (Kerr Corporation, Romulus, MI, United States). The outer scales of the third labial-palp segment were carefully removed. In order to determine the LPO specific projections, three types of mass staining experiment were performed. To label the projections of the LPO sensory neurons exclusively, the outer wall of the third segment of the labial palp was first sealed with Vaseline. After that, we applied a localized injection by inserting a blunt glass electrode filled with 4% Micro-Ruby (biotinylated dextran-conjugated tetramethyl rhodamine, Molecular Probes) in 0.2 M potassium acetate (KAc) solution into the LPO, with depolarizing current pulses of 7–8 nA at 1 Hz for 2 min. The presence of non-LPO sensory neurons on the labial palp was determined by applying crystals of fluorescent dye on two distinct sites on the outer surface of the third labial-palp segment: (i) a small longitudinal cutting site carefully made on the cuticle of the outer wall and (ii) a transverse cutting site at the very tip of the labial palp.

For investigating the projection pattern of sensory cells housed in the hair-shaped (distal part) and the club-shaped (basal part) sensilla, two kinds of anterograde mass-staining experiments were conducted by cutting at different sites of the labial-palp segment. We first obtained an overview of all the sensory neurons in both sensillar types of the LPO by applying crystals of Micro-Ruby to the transverse cutting plane at its basal part. To label the sensory cells housed in the hair-shaped sensilla exclusively, crystals of the fluorescent dye were applied at the transverse cutting plane made on the intermediate part of the

LPO. After staining, the insects were kept for three days in dark to allow anterograde axonal transportation of the dye. A dissecting microscope (Leica M60) equipped with a CCD camera (Leica DMC 4500) was used to determine the location of the transverse cuts made for dye application.

In addition, double-labeling experiments including application of two fluorescent dyes were carried out. One dye was allocated to the intermediate part of the LPO and one to the basal. First, the LPO was sectioned at the intermediate part and then exposed to crystals of Alexa 488. After 24 h at 4°C in a humid chamber, the LPO was sectioned at the base and exposed to Micro-Ruby. The insects were then kept for two more days in dark before the brains were dissected.

All brains were dissected out in Ringer's solution [in mM: 150 NaCl, 3 $CaCl_2$, 3 KCl, 25 Sucrose, and 10 N-tris (hydroxymethyl)-methyl-2-amino-ethane sulfonic acid, pH 6.9] before being fixed in a paraformaldehyde solution (4% PFA in 0.1 M phosphate buffer, pH 6.9) for 2 h at room temperature or overnight at 4°C. After fixation, the brains were dehydrated in an ascending ethanol series (50, 70, 90, 96, and 2 × 100%; 10 min each), and finally cleared in methyl salicylate (Sigma-Aldrich, Germany). Preparations were then mounted in permount (Chemi-Teknik As, Oslo).

Iontophoretic Staining of Individual Sensory Neurons

In order to investigate the projection pattern of individual LPO sensory neurons, we first performed iontophoretic staining experiments from the LPO. The insect was immobilized in a plastic pipette as described above. A sharp quartz electrode pulled by a laser-based horizontal puller (P – 2000; Sutter instruments, CA, United States) was used for dye injection. This capillary which contained a fluorescent dye solution (4% Micro-Ruby in 0.2 M potassium acetate solution) was backfilled with 0.2 M KAc and inserted into the LPO via a micromanipulator (Leica microsystems, Wetzlar, Germany). The recording electrode had a resistance of 100–200 MΩ. In addition to anterograde labeling, we performed retrograde labeling by accessing individual sensory neurons projecting to the LPOG. The head cuticle between the eyes was then removed by using a sharp razor-blade knife. The brain was exposed by taking away muscles and tracheas. Likewise, a quartz electrode with dye was inserted into one of the LPOGs. In both types of iontophoretic staining experiments, a chloridized silver wire placed in the eye served as a reference electrode. When the neuron contact was stable, injection of the fluorescent dye was induced via 200 ms pulse depolarizing currents of 8–10 nA for 15 min. After staining, the preparation was kept one to three days at 4°C and then dissected, fixed, dehydrated, cleared, and mounted in methyl salicylate.

Confocal Microscopy

All successfully stained neurons were imaged by using a confocal laser-scanning microscope (LSM 800 Airyscan, LSM 800 GaAsp -Pmt-1, Zeiss, Jena, Germany) equipped with a C-Apochromat 10×/0.45 water objective, Plan-Neofluar 20x/0.5 air objective, and LD LC1 Plan – Apochromat 25×/0.8 imm Korr DIC M 27. The Micro-Ruby (Ex_{max} 555 nm/Em_{max} 580 nm) labeling was excited by the 543-nm line of a HeNe laser, and Alexa 488 (Ex_{max} 495 nm/Em_{max} 519 nm) staining by the 488-nm line of an argon laser. For the samples stained with Micro-Ruby, we used two channels: one for exciting the Micro-Ruby and the other, the 488-nm line of an argon laser, for detecting brain neuropils, made visible via autofluorescence from the sample. We used two detectors: airyscan detecting Micro-Ruby and GaAsP for detecting the autofluorescence. These detectors were used for the double-labeled preparations as well. High-resolution confocal images with 1,024 × 1,024 pixels, at distances of 2 to 6 μm in the z-direction were obtained. The pinhole size was 1 airy unit and the pinhole diameter 36 μm. Images were collected and saved as 8-bit. czi files. In order to quantify the fluorescence intensities in the two LPOGs during dye application to the intermediate and basal segment of the LPO, the 10X water immersion objective with 0.45 NA was used. The image pixel size was set to 0.209 μm and the zoom to 0.8. The images were scanned at 0.55 μs pixel dwelling time. The detector gain was set to 530–630 V, the digital offset to 0, and the digital gain to 1. The axial distance (z thickness) was chosen according to the optimal slicing, i.e., 4.98 μm (having at least 50% overlap of two successive optical sections).

Image Intensity Processing and Statistical Analysis

All the confocal images were processed in the Zen 2.3 software (Blue edition, Carl Zeiss Microscopy GmbH, Jena, Germany). To estimate the density of sensory projections in the ipsilateral and contralateral LPOG, the fluorescence intensity of each LPOG was quantified by using Image J[1]. Furthermore, in order to compare the staining patterns formed by the two types of sensory neurons housed by hair-shaped and club-shaped sensilla, eight preparations labeled from the base of the pit and six from the intermediate part were included in the analysis. First, we selected the relevant part of the confocal stack, i.e., the images containing the LPOGs. The fluorescence intensities of the LPOGs were then registered through measuring the fluorescence in the glomerular region within the stack. The background fluorescence, i.e., the autofluorescence, was quantified in a corresponding manner from the region between the two LPOGs of the same stack. The LPOG fluorescence intensity per square micrometer was then normalized by subtracting the background fluorescence: mean fluorescence intensity within the LPOG area (μm^2) minus mean fluorescence intensity within the randomly selected background area (μm^2). Since the data were not normally distributed, the non-parametric Wilcoxon signed-rank test was performed to analyze the data within subjects. All probabilities given were two-tailed. For analyzes of data linked to the two cutting levels, obtained from different individuals, the Mann-Whitney *U* test was utilized. Effect size (*r*) was calculated by dividing the standardized test statistics by the square root of the sample size (Pallant, 2007). The Statistical

[1]http://imagej.net

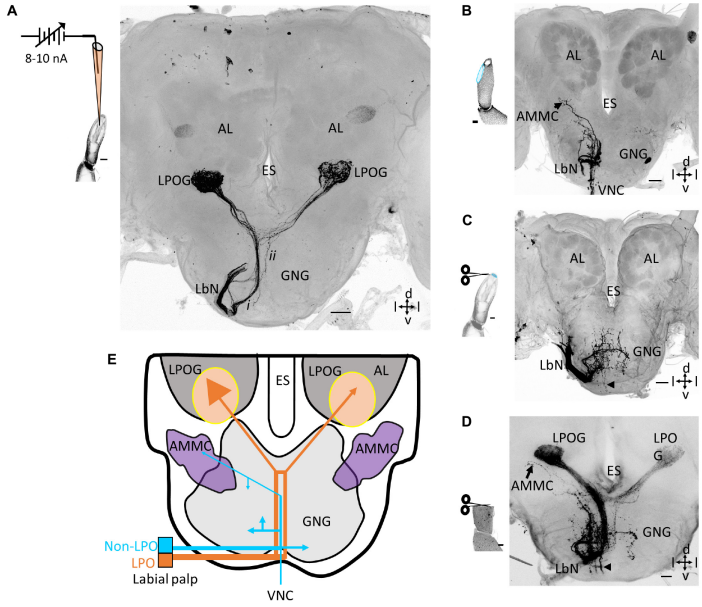

FIGURE 1 | Central projections of neurons in the labial pit organ (LPO) versus non-LPO neurons. **(A)** Confocal image (maximum intensity projection) showing a focused mass staining of sensory neurons housed inside the LPO. As demonstrated, the labeled axons target only the LPOG in both antennal lobes. The labial nerve (LbN) splits into two sub-branches after entering the ipsilateral gnathal ganglion (GNG): one thick main branch (i) and one thin sub-branch (ii). The schematic drawing demonstrates the focused mass staining inside the LPO. The weakly labeled glomerulus located more dorsally in each antennal lobe (AL) is likely visualized due to autofluorescence. **(B)** Projection pattern of sensory neurons from the outer cuticular wall of the labial palp. The axons targeted the GNG and the antennal mechanosensory and motor center (AMMC) on the ipsilateral side. In addition, some fibers projected to the ventral nerve cord (VNC). The schematic drawing indicates the staining site, in *light blue*. **(C)** Projection pattern of sensory neurons originating from the tip of the palp. The axon terminals were bilaterally scattered in the GNG. A few ipsilateral axons projected to the VNC (arrowhead). The schematic drawing indicates the staining site, in *light blue*. **(D)** Projection pattern from a classic mass staining of all sensory neurons including those from the LPO and the outer palp cuticle. The terminal axons targeted the LPOGs in both AL, the GNG, and the VNC (arrowhead). **(E)** Schematic diagram showing the projection pattern of the sensory neurons housed inside and outside the LPO, respectively. The LPO projection pattern in *orange* and the non-LPO in *blue*. The number of endings in the LPOGs represents the intensity of innervations. ES, esophagus; d, dorsal; v, ventral; l, lateral. Scale bars **(A–D)**: 50 μm.

package for the social sciences (SPSS), version 25, was used for statistical analysis.

RESULTS

LPO-Specific Sensory Neurons Terminate in the LPOGs Exclusively

Iontophoretic staining experiments performed by inserting a blunt glass electrode into the pit showed that neurons originating from sensilla located inside the LPO project exclusively to the antennal lobes. Here they target the ventrally located LPOG. As shown in one of totally five successfully labeled preparations, an axon bundle projecting via the labial nerve can be seen (**Figure 1A**). After entering the ipsilateral part of the GNG, it passed on dorsally, close to the midline ipsilaterally in the GNG. About 70 μm ventrally of the esophagus, it divided into two branches, each targeting the LPOG in one antennal lobe. In addition to this main axon bundle projecting ipsilaterally in the GNG, another thin sub-bundle crossed the midline about 170 μm ventrally of the esophagus and projected dorsally on the contralateral side (**Figure 1A**). Confocal images of preparations stained from both sides, showed that this thin sub-branch merged with the main fiber bundle from the other LPO (**Supplementary Figure S1**). None of the fiber bundles extended terminal branches in the GNG. The four remaining preparations successfully stained by the same technique showed a similar projection pattern including a denser innervation in the

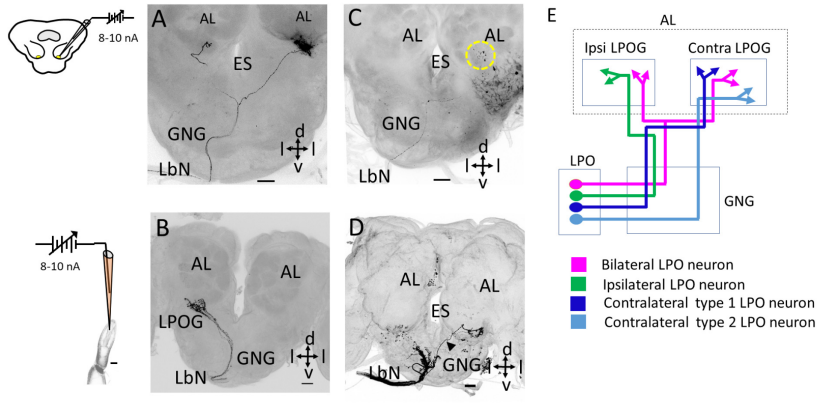

FIGURE 2 | Morphology of individual labial pit organ (LPO) sensory neurons. **(A)** Confocal image (maximum intensity projection) of one bilateral LPO neuron. **(B)** Confocal image (maximum intensity projection) of several co-stained neurons, all projecting to the ipsilateral LPO glomerulus (LPOG). **(C,D)** Confocal images showing projections of two sub-types of contralateral LPO neurons. The neuron in **C**, projects along the main fiber bundle on the ipsilateral side of the gnathal ganglion (GNG) before crossing the midline and targeting the contralateral LPOG. The dotted yellow circle represents the LPOG in the antennal lobe (AL). In **(D)**, one fiber (arrowhead) projecting along the thin axon-bundle on the contralateral side terminates in the contralateral LPOG. The additional fibers in the ipsilateral GNG were assumingly originating from sensilla on the outer palp surface. **(E)** Schematic diagram showing the morphological types of LPO neurons. ES, esophagus; d, dorsal; v, ventral; l, lateral. The neurons in **A,C** were obtained by retrograde staining from the LPOG whereas the neurons in **B,D** were obtained by anterograde staining from LPO. Scale bars **(A–D)** 50 μm.

ipsilateral LPOG than in the contralateral one (**Figure 2B** and **Supplementary Figure S2**).

To determine the projection patterns of sensory neurons located outside the LPO, we first conducted focused mass staining by applying dye to a longitudinal section carefully made on the outer wall of the third labial-palp segment (**Figures 1B,E**). Five successfully labeled preparations showed stained fibers entering the GNG via the labial nerve, but unlike the projection pattern of sensory neurons originating inside the pit, no projections targeted the LPOGs. As shown in **Figure 1B**, the main portion of projections from the outer wall terminated in the ipsilateral GNG. In addition to these innervations, a bundle of fibers projected to the ventral nerve cord and a few axons targeted the ipsilateral antennal mechanosensory and motor center (AMMC). The four remaining preparations stained in the same manner showed similar projection patterns (**Supplementary Figure S3**). In one preparation, a very weak staining can be observed in the LPOGs – possibly due to dye leakage from the outer cuticle (**Supplementary Figure S3E**). An additional series of mass staining experiments from the palp surface were carried out by applying dye onto the distal cross section of the third segment ($n = 5$; **Figure 1C**). Again, a bundle of stained axons confined to the labial palp nerve innervated the GNG. However, unlike the targets of axons originating from the longitudinal section of the palp surface, these fibers terminated not only in the ipsilateral GNG but also the contralateral. Besides, there were only a few axons projecting to the ventral nerve cord and no innervation of the AMMC (**Figures 1C,E** and **Supplementary Figure S4**). Noticeably, combining the three projection patterns obtained by applying dye into the LPO and to the two different regions of the palp surface, gives a total pattern very similar to that obtained when applying dye to the transverse section of the peripheral labial-palp, at the proximal level (**Figure 1D**).

Morphological Characterization of Individual LPO Neurons

We performed iontophoretic staining with a sharp glass electrode both from the LPO and the LPOG, providing morphological identification of individual LPO neurons via anterograde and retrograde labeling, respectively. The assembly of successfully stained neurons comprised three morphological types – all entering the GNG via the labial nerve and then projecting to the LPOG in the antennal lobe (**Figures 2A–E**). The first type comprised bilateral neurons projecting to the LPOG in both antennal lobes (**Figure 2A**). The second type was unilateral, targeting the LPOG in the ipsilateral antennal lobe exclusively (**Figure 2B**). The axons of these two neuron types followed the main fiber bundle ipsilaterally in the GNG. The third neuron type had an axon crossing the midline of the GNG and targeting the LPOG in the contralateral antennal lobe only (**Figures 2C,D**). This contralateral neuron type included two sub-types. One sub-type followed the main axon bundle on the ipsilateral side of the GNG before crossing the midline and terminating in the

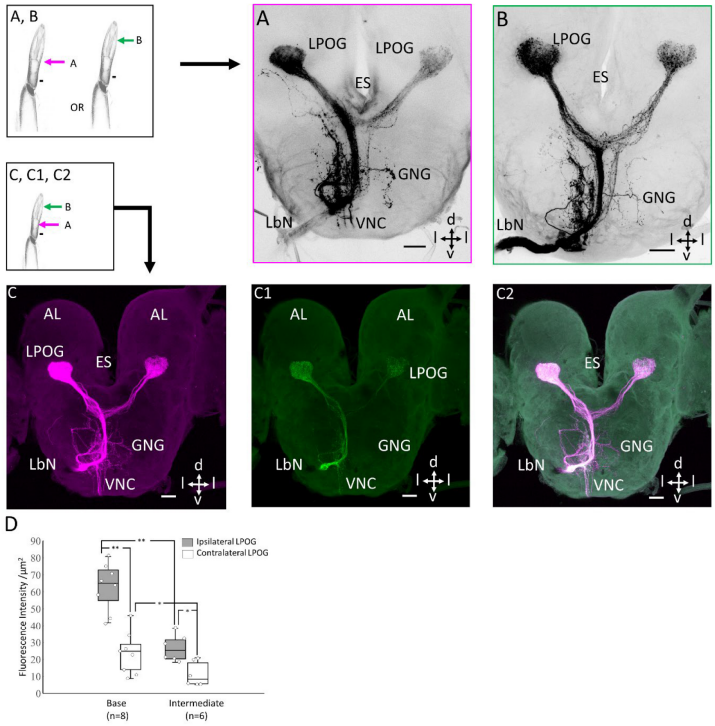

FIGURE 3 | Staining patterns of sensory neurons originating from different segments of the peripheral labial palp. Left upper: Demonstration of application of dye in base or intermediate part of labial palp. Left lower: Schematic diagram showing double-labeling of the labial palp. **(A)** Confocal image of a classic mass staining performed from the transverse cut, at the level of the base of the pit. **(B)** Confocal image of a classic mass staining performed from the transverse cut, at the intermediate level of the pit. **(C–C2)** Double-labeling of the staining experiments performed in **A** and **B** in the same preparation. A difference in fluorescence intensity between the two LPOGs is shown in **C** and **C1**. **(D)** Box plots of quantitative measurements of mean fluorescence intensity in the ipsilateral (*light gray*) and contralateral LPOG (*white*) when the preparation is stained from the base and intermediate part of the labial palp. Wilcoxon signed-rank test $^{*}p < 0.05$; $^{**}p < 0.01$. ES, esophagus; GNG, gnathal ganglion; d, dorsal; v, ventral; l, lateral. Scale bars **(A–C)**: 50 µm.

contralateral LPOG (**Figure 2C**) whereas the other sub-type targeted this glomerulus via the thin bundle on the contralateral side of the GNG (**Figure 2D**, $n = 2$). No other areas of the central nervous system were innervated by the individual neurons.

Projection Patterns of Sensory Neurons Originating From the Intermedial and Basal Part of the Third Labial-Palp Segment

To investigate whether the two morphological types of LPO sensilla (hair-shaped sensilla located distally and club-shaped located basally) house sensory neurons having different projection patterns, mass staining was made from two different sites of the peripheral palp. Fluorescent dye was applied to the transverse cut made at the intermedial and basal part of the third segment, respectively (**Figure 3**). This classic mass staining labeled both the LPO-specific sensory neurons housed inside the pit and non-LPO sensory neurons located on the outer cuticle and tip of the labial palp. Tracing of the LPO sensory neurons from the basal and intermediate part of the palp demonstrated similar projection patterns in the form of stronger fluorescence intensity in the ipsi- than the contra-lateral LPOG (**Figures 3A–C**). In the preparations

stained from the base (n = 8), including both sensillum categories, the mean fluorescence strength was significantly higher within the ipsilateral LPOG (Mdn = 65.071) than in the contralateral (Mdn = 24.76, z = 2.52, p = 0.012, r = 0.89; **Figure 3D**). (ii) Likewise, the samples stained at the intermediate part (n = 6), including hair-shaped sensilla only, showed a significantly stronger fluorescence intensity in the ipsilateral LPOG (Mdn = 25.34) than in the contralateral (Mdn = 8.27, z = 2.20, p = 0.03, r = 0.89; **Figure 3D**). In addition, the mean intensity in the ipsilateral LPOG in the preparations stained from the base was significantly different from the corresponding fluorescence intensity in the preparations stained from the intermediate level (Mann-Whitney U test, U = 48, z = 3.098, $p < 0.01$, r = 0.59; **Figure 3D**). Likewise, the mean intensity in contralateral LPOG in the preparations stained from the base and the intermediate part of the LPO was significantly different (U = 41, z = 2.91, $p < 0.05$, r = 0.82; **Figure 3D**).

Exceptional Staining Pattern in the Antennal Lobe

Two of the preparations that were stained from the base of the third segment of the labial palp demonstrated antennal-lobe projections having a few branches ramifying outside the LPOG. One preparation showed a short axon projecting to an ordinary glomerulus located postero-medially of the LPOG in the ipsilateral antennal lobe (square box in **Figure 4A**). The other preparation included a sensory neuron forming an axonal loop dorsally of the LPOG in the ipsilateral antennal lobe, but without targeting any other glomerulus (**Figure 4B**).

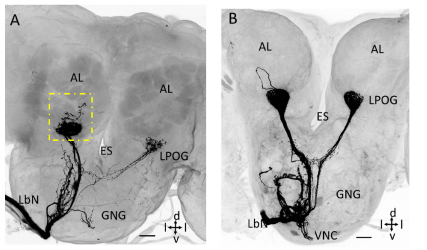

FIGURE 4 | Confocal images showing untypical staining patterns of LPO neurons in the antennal lobe (AL). **(A)** Maximum intensity projection showing, in addition to terminals in the LPO glomerulus (LPOG), a few branches ramifying outside the glomerulus (dotted square box). **(B)** Confocal image showing an axon forming a loop dorsally of LPOG. ES, esophagus; GNG, gnathal ganglion; LbN, Labial nerve; d, dorsal; v, ventral; l, lateral. Scale bars: 50 μm.

DISCUSSION

In this study, we traced the central projections of LPO sensory neurons in the moth brain. By performing focused mass staining from the inner pit and the palp surface, respectively, we found that the LPO sensory neurons project to the antennal lobes exclusively. Neurons located on the outer surface of the palp, on the other hand, target the GNG and the ventral nerve cord. Morphological characterization of individual LPO neurons, obtained both by retrograde and anterograde labeling, revealed three sensory neuron types – one ipsilateral, one bilateral, and one contralateral. In addition, mass-staining experiments including selective labeling of hair-shaped and club-shaped LPO sensilla indicated that the sensory neurons housed inside the different sensillum categories innervate the two LPOGs in slightly different manners.

LPO Sensory Neurons Target the Antennal Lobes Exclusively

Selective staining of sensilla housed inside the pit, carried out for the first time, demonstrated that the LPO sensory neurons of *H. armigera* target the antennal lobes exclusively. This refines the previous findings on central projections of LPO neurons in the current species, reporting about two target areas in addition to the antennal lobes, i.e., the GNG and the ventral nerve cord (Zhao et al., 2013). In the former study, however, a more unspecific staining technique including dye application to the transverse cut surface of the peripheral palp was utilized. Distinct staining of sensilla located on the outer palp surface, as performed here, revealed that the projections originating from this site terminate in the two additional areas – the GNG and the ventral nerve cord. "Merging" the staining patterns obtained from the two labeling techniques utilized in the present study (**Figures 1B,C**), forms a pattern that is very similar to that previously reported by several researchers using the classic mass staining technique (**Figure 1D**; Kent et al., 1986; Lee and Altner, 1986; Zhao et al., 2013; Ma et al., 2017). This confirms the suggestion made by Kent et al. (1986) that the axon projections to the LPOGs originated from sensory neurons housed inside the pit and that the branches seen in the GNG were parts of other sensory neuron types. Interestingly, a short peg sensillum type responding to humidity was recently identified on the labial palp of the Asian longhorned beetle, *Anoplophora glabripennis* (Hall et al., 2019).

Projection Patterns of CO_2 Sensitive Neurons Across Different Insect Species

The fact that the LPO sensory neurons target the LPOG in each antennal lobe, and no other areas of the central nervous system, means that the projection pattern of CO_2 sensitive neurons in the moth is quite similar to that found in other insects, including flies and mosquitoes. For example, in the fruit fly, *D. melanogaster*, the CO_2 sensitive neurons project to a ventrally located antennal-lobe glomerulus, called the V glomerulus (Stocker et al., 1983; Suh et al., 2004), and in the mosquito, *Aedes aegypti*, the corresponding neuron type targets one dorsomedial glomerulus in the antennal lobe (Distler and Boeckh, 1997; Anton et al., 2003; Anton and Rospars, 2004). These two species have ipsilateral projections innervating only one antennal lobe, whereas the moth has a substantial portion of bilateral projections targeting the LPOG in both antennal lobes. Remarkably, yet another well-known mosquito species,

Anopheles gambiae, has bilateral innervation – like the moth (Anton et al., 2003; Anton and Rospars, 2004).

Notably, there seem to be obvious differences in the peripheral arrangement of the CO_2 pathway across the various species. Moths have sensilla dedicated to CO_2 sensory neurons alone (Zhao et al., 2013). Fruit flies and mosquitoes, on the other hand, have their CO_2 sensitive neurons co-located with olfactory sensory neurons inside olfactory sensilla on the antenna and the maxillary palp, respectively (Riesgo-Escovar et al., 1997; Grant and O'Connell, 2007; Lu et al., 2007).

Morphology of Individual LPO Neurons

Previous and present mass staining experiments on lepidoptera, including *M. sexta, Pieris rapae*, and *H. armigera*, have demonstrated that both LPOGs receive input from sensory neurons located within each LPO (Kent et al., 1986; Lee and Altner, 1986). Since only a few individual sensory neurons were previously stained (Guerenstein et al., 2004), knowledge about these neurons' morphologies has been lacking. The three sub-bundles which originate from the labial nerve and project to the LPOGs, as shown in **Figures 1A,D**, already indicate the three morphological types of LPO sensory neurons identified here: one bilateral, one unilateral, and one contralateral type. To our knowledge, no contralateral CO_2 sensory neuron has been reported in any other insect order. Since contralateral projections from olfactory or gustatory sensory neurons have never been reported in any insect species, the LPO projections targeting the contralateral LPOG in the moth brain seem to be unique.

A High Degree of Convergence in the LPOG

Considering the large number LPO sensory neurons, which are housed inside each pit (ca. 1200 sensilla) in *H. armigera* (Zhao et al., 2013), the signal-to-noise ratio in the single target glomerulus is particularly high. The fact that there is a substantial proportion of bilateral projections makes this value even higher. Such an input arrangement might be optimally designed for detecting minor CO_2 fluctuations (Stange, 1992; Guerenstein et al., 2004). Previous reports have shown that the honey bee and the fruit fly perform simultaneous comparison of the odor concentrations detected by the two antennae in order to trace the source (osmotropotaxis; Martin, 1965; Borst and Heisenberg, 1982; Stocker et al., 1990). Due to the very strong convergence in the CO_2 system of the moth, we assume a similar mechanism even though the two palps are very closely located.

DATA AVAILABILITY STATEMENT

All datasets generated for this study are included in the article/**Supplementary Material**.

AUTHOR CONTRIBUTIONS

PKC, XC, PK, and BB contributed to the study concept and design, analysis, and interpretation of data. PKC and XC contributed to the acquisition of data. PKC, XC, PK, X-CZ, and BB contributed to the drafting of the manuscript. PKC, XC, PK, X-CZ, G-RW, and BB contributed to the final manuscript. G-RW and BB contributed to obtaining the funding.

FUNDING

This work was funded by the Norwegian Research Council, project number 287052, to BB, and the National Natural Science Foundation of China, project number 31861133019, to G-RW. The funders had no role in the study design, data collection and analysis, decision to publish, or preparation of the manuscript.

ACKNOWLEDGMENTS

We are grateful to Mari Reitstøen Arnesen for help with data collection and Jonas Hansen Kymre for assistance with the statistical analyses.

SUPPLEMENTARY MATERIAL

The Supplementary Material for this article can be found online at: https://www.frontiersin.org/articles/10.3389/fphys.2020.00202/full#supplementary-material

REFERENCES

Anton, S., and Rospars, J. P. (2004). Quantitative analysis of olfactory receptor neuron projections in the antennal lobe of the malaria mosquito. *Anopheles gambiae. J. Comp. Neurol.* 475, 315–326. doi: 10.1002/cne.20174

Anton, S., Van Loon, J. J. A., Meijerink, J., Smid, H. M., Takken, W., and Rospars, J.-P. (2003). Central projections of olfactory receptor neurons from single antennal and palpal sensilla in mosquitoes. *Arthropod Struct. Dev.* 32, 319–327. doi: 10.1016/j.asd.2003.09.002

Bogner, F., Boppre, M., Ernst, K. D., and Boeckh, J. (1986). Co2 sensitive receptors on labial palps of Rhodogastria moths (*Lepidoptera*: *Arctiidae*): physiology, fine structure and central projection. *J. Comp. Physiol. A* 158, 741–749. doi: 10.1007/bf01324818

Borst, A., and Heisenberg, M. (1982). Osmotropotaxis in *Drosophila melanogaster*. *J. Comp. Physiol.* 147, 479–484. doi: 10.1007/bf00612013

Distler, P., and Boeckh, J. (1997). Central projections of the maxillary and antennal nerves in the mosquito *Aedes aegypti*. *J. Exp. Biol.* 200, 1873–1879.

Dong, J., Liu, H., Tang, Q., Liu, Y., Zhao, X., and Wang, G. (2014). Morphology, type and distribution of the labial-palp pit organ and its sensilla in the oriental armyworm. *Mythimna separata* (*Lepidoptera*: *Noctuidae*). *Acta Entomol. Sin.* 57, 681–687.

Goyret, J., Markwell, P. M., and Raguso, R. A. (2008). Context- and scale-dependent effects of floral Co_2 on nectar foraging by *Manduca sexta*. *Proc. Natl.Acad. Sci. U.S.A.*105, 4565–4570. doi: 10.1073/pnas.0708629105

Grant, A. J., and O'Connell, R. J. (2007). "Electrophysiological Responses from Receptor Neurons in Mosquito Maxillary Palp Sensilla," in *Ciba Foundation Symposium 200 — Olfaction in Mosquito—Host Interactions*, eds G. R. Bock and G. Cardew (Hoboken, NJ: Wiley).

Guerenstein, P. G., Christensen, T. A., and Hildebrand, J. G. (2004). Sensory processing of ambient Co2 information in the brain of the moth *Manduca sexta*. *J. Comp. Physiol. A Neuroethol. Sens. Neural. Behav. Physiol.* 190, 707–725.

Hall, L. P., Graves, F., Myrick, A., Hoover, K., and Baker, T. C. (2019). Labial and maxillary palp recordings of the Asian longhorned beetle, *Anoplophora*

glabripennis, reveal olfactory and hygroreceptive capabilities. *J. Insect Physiol.* 117, 103905. doi: 10.1016/j.jinsphys.2019.103905

Homberg, U., Christensen, T. A., and Hildebrand, J. G. (1989). Structure and function of the deutocerebrum in insects. *Annu. Rev. Entomol.* 34, 477–501. doi: 10.1146/annurev.en.34.010189.002401

Kent, K. S., Harrow, I. D., Quartararo, P., and Hildebrand, J. G. (1986). An accessory olfactory pathway in Lepidoptera: the labial pit organ and its central projections in Manduca sexta and certain other sphinx moths and silk moths. *Cell Tissue Res.* 245, 237–245.

Lee, J.-K., and Altner, H. (1986). Primary sensory projections of the labial palp-pit organ of pieris rapae l. *(Lepidoptera : Pieridae). Int. J. Insect Morphol. Embryol.* 15, 439–448. doi: 10.1016/0020-7322(86)90036-x

Lee, J.-K., Selzer, R., and Altner, H. (1985). Lamellated outer dendritic segments of a chemoreceptor within wall-pore sensilla in the labial palp-pit organ of the butterfly. *Pieris rapae* L. (*Insecta*, *Lepidoptera*). *Cell Tissue Res.* 240, 333–342.

Lu, T., Qiu, Y. T., Wang, G., Kwon, J. Y., Rutzler, M., Kwon, H. W., et al. (2007). Odor coding in the maxillary palp of the malaria vector mosquito *Anopheles gambiae*. *Curr Biol.* 17, 1533–1544. doi: 10.1016/j.cub.2007.07.062

Ma, B. W., Zhao, X. C., Berg, B. G., Xie, G. Y., Tang, Q. B., and Wang, G. R. (2017). Central projections of antennal and labial palp sensory neurons in the migratory armyworm mythimna separata. *Front. Cell Neurosci.* 11:370. doi: 10.3389/fncel.2017.00370

Martin, H. (1965). Osmotropotaxis in the Honey-Bee. *Nature* 208, 59–63. doi: 10.1038/208059a0

Pallant, J. (2007). *Spss Survival Manual*, 3rd Edn. New York, NY: McGraw Hill Open University Press.

Riesgo-Escovar, J. R., Piekos, W. B., and Carlson, J. R. (1997). The *Drosophila antenna*: ultrastructural and physiological studies in wild-type and lozenge mutants. *J. Comp. Physiol. A* 180, 151–160. doi: 10.1007/s003590050036

Sage, R. F. (2002). How terrestrial organisms sense, signal, and respond to carbon dioxide. *Integr. Comp. Biol.* 42, 469–480. doi: 10.1093/icb/42.3.469

Stange, G. (1992). High resolution measurement of atmospheric carbon dioxide concentration changes by the labial palp organ of the moth Heliothis armigera (*Lepidoptera*: *Noctuidae*). *J. Comp. Physiol. A* 171, 317–324.

Stange, G. (1997). Effects of changes in atmospheric carbon dioxide on the location of hosts by the moth, *Cactoblastis cactorum*. *Oecologia* 110, 539–545. doi: 10.1007/s004420050192

Stange, G., Monro, J., Stowe, S., and Osmond, C. B. (1995). The Co2 sense of the moth Cactoblastis cactorum and its probable role in the biological control of the Cam plant Opuntia stricta. *Oecologia* 102, 341–352. doi: 10.1007/BF00329801

Stocker, R. F., Lienhard, M. C., Borst, A., and Fischbach, K. F. (1990). Neuronal architecture of the antennal lobe in Drosophila melanogaster. *Cell Tissue Res.* 262, 9–34. doi: 10.1007/bf00327741

Stocker, R. F., Singh, R. N., Schorderet, M., and Siddiqi, O. (1983). Projection patterns of different types of antennal sensilla in the antennal glomeruli of *Drosophila melanogaster*. *Cell Tissue Res.* 232, 237–248. doi: 10.1007/bf00213783

Suh, G. S., Wong, A. M., Hergarden, A. C., Wang, J. W., Simon, A. F., Benzer, S., et al. (2004). A single population of olfactory sensory neurons mediates an innate avoidance behaviour in Drosophila. *Nature* 431, 854–859. doi: 10.1038/nature02980

Thom, C., Guerenstein, P. G., Mechaber, W. L., and Hildebrand, J. G. (2004). Floral Co2 Reveals Flower Profitability to Moths. *J. Chem. Ecol.* 30, 1285–1288. doi: 10.1023/b:joec.0000030298.77377.7d

Zhao, X. C., Tang, Q. B., Berg, B. G., Liu, Y., Wang, Y. R., Yan, F. M., et al. (2013). Fine structure and primary sensory projections of sensilla located in the labial-palp pit organ of Helicoverpa armigera (Insecta). *Cell Tissue Res.* 353, 399–408. doi: 10.1007/s00441-013-1657-z

Conflict of Interest: The authors declare that the research was conducted in the absence of any commercial or financial relationships that could be construed as a potential conflict of interest.

Supplementary Material

1 Supplementary Figures

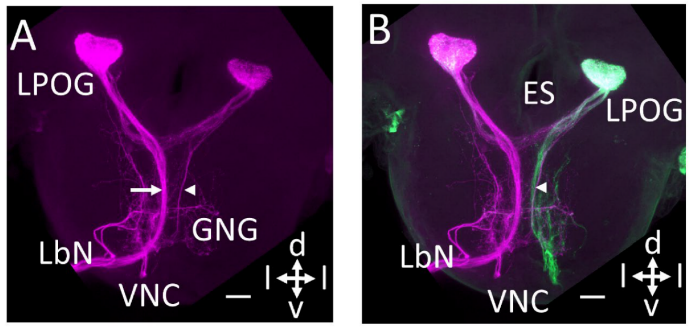

Fig. S1 Double-labeled preparation showing the staining pattern of sensory neurons originating from the terminal segment of the right (*magenta*) and left (*green*) labial palp, respectively. **A**: Confocal image (maximum intensity projection) showing sensory axons from the right palp, stained by Micro-Ruby. A thick sub-branch projects ipsilaterally (arrow) whereas a thin sub-branch projects contralaterally (arrowhead). **B:** Double-labeling showing an overlay of the Micro-Ruby staining from the right palp (*magenta*) and Alexa-488 staining from the left palp (*green*). The thick fiber bundle from the left palp merges with the thin sub-bundle from the right palp (arrowhead). (The preparation is slightly overexposed.) ES, esophagus; VNC, ventral nerve cord; LbN, labial nerve; d, dorsal; v, ventral; l, lateral. Scale bars: 50 µm.

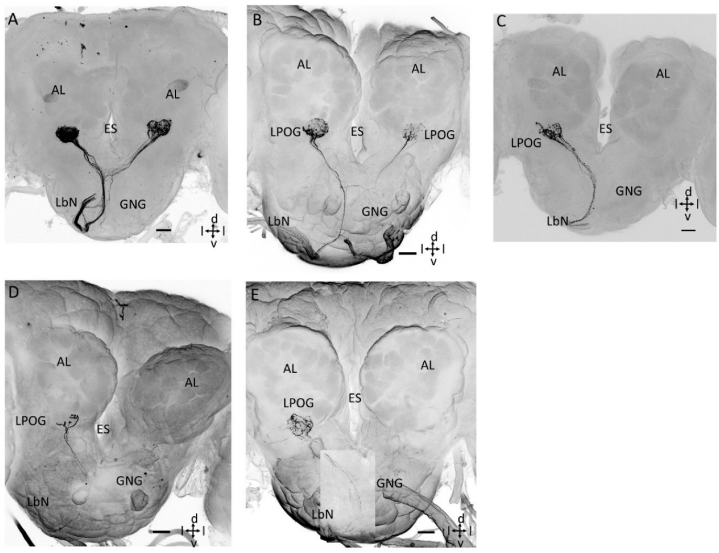

Fig. S2 Confocal images of five preparations, labelled via focused mass staining from the labial pit organ (LPO). **A-E**: All preparations showed a principally similar staining pattern including terminal branches in the LPO glomerulus (LPOG) exclusively. The labeling in the ipsilateral LPOG was generally stronger than in the contralateral LPOG. AL, antennal lobe; ES, esophagus; GNG, gnathal ganglion; LbN, labial nerve; d, dorsal; v, ventral; l, lateral. Scale bars: 50 µm.

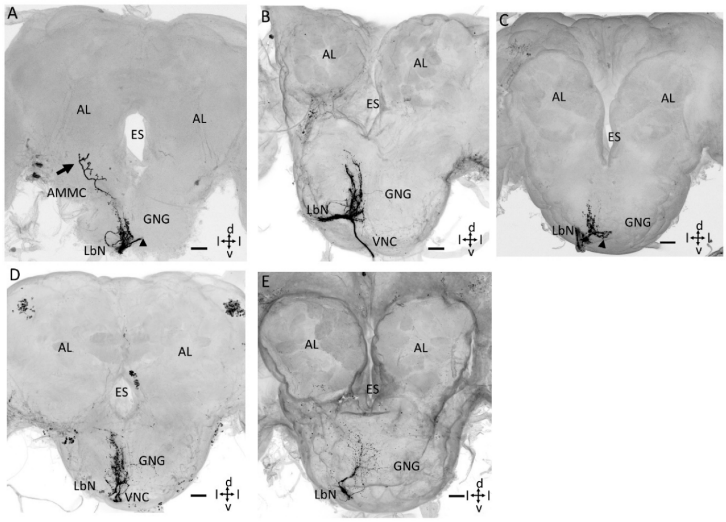

Fig. S3 Confocal images of five preparations, labelled via mass staining from the outer cuticle of the labial palp (longitudinal section). **A-E**: All preparations showed a principally similar staining pattern including terminal branches in the gnathal ganglion (GNG), the antennal mechanosensory and motor center (AMMC), and the ventral nerve cord (VNC). Generally, no labeling was visualized in the antennal lobe (AL). ES, esophagus; LbN, labial nerve; d, dorsal; v, ventral; l, lateral. Scale bars: 50 µm.

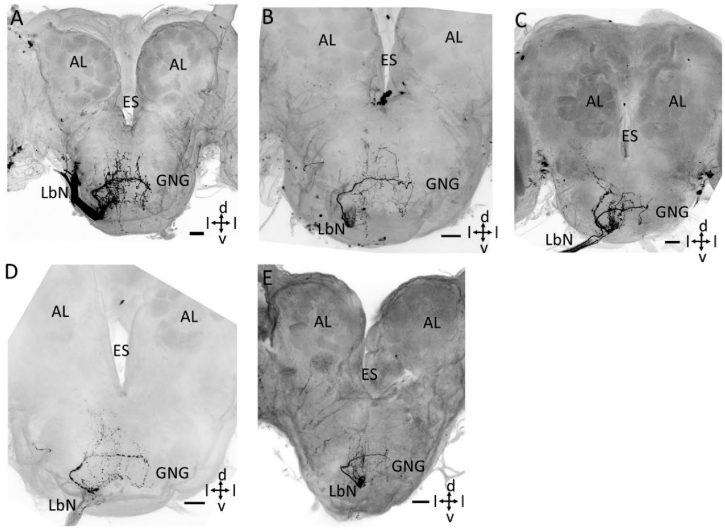

Fig. S4 Confocal images of five preparations, labelled via mass staining from the outer tip of the labial palp. **A-E**: All preparations showed a principally similar staining pattern including bilateral terminal branches in the gnathal ganglion (GNG). No labeling was visualized in the antennal lobe (AL). ES, esophagus; LbN, labial nerve; d, dorsal; v, ventral; l, lateral. Scale bars: 50 µm.

Paper II

www.nature.com/scientificreports

scientific reports

Check for updates

OPEN

Neuronal architecture of the second-order CO_2 pathway in the brain of a noctuid moth

X. Chu[1,4], P. KC[1,4], E. Ian[1], P. Kvello[2], Y. Liu[3], G. R. Wang[3] & B. G. Berg[1]✉

Many insects possess the ability to detect fine fluctuations in the environmental CO_2 concentration. In herbivorous species, plant-emitted CO_2, in combination with other sensory cues, affect many behaviors including foraging and oviposition. In contrast to the comprehensive knowledge obtained on the insect olfactory pathway in recent years, we still know little about the central CO_2 system. By utilizing intracellular labeling and mass staining, we report the neuroanatomy of projection neurons connected with the CO_2 sensitive antennal-lobe glomerulus, the labial pit organ glomerulus (LPOG), in the noctuid moth, *Helicoverpa armigera*. We identified 15 individual LPOG projection neurons passing along different tracts. Most of these uniglomerular neurons terminated in the lateral horn, a previously well-described target area of plant-odor projection neurons originating from the numerous ordinary antennal-lobe glomeruli. The other higher-order processing area for odor information, the calyces, on the other hand, was weakly innervated by the LPOG neurons. The overlapping LPOG terminals in the lateral horn, which is considered important for innate behavior in insects, suggests the biological importance of integrating the CO_2 input with plant odor information while the weak innervation of the calyces indicates the insignificance of this ubiquitous cue for learning mechanisms.

Insects navigate through a complex environment by using multisensory information. Herbivorous species detect variations in plant-emitted carbon dioxide (CO_2) concentration for the purpose of determining the host plant quality. Actually, small fluctuations of atmospheric CO_2 may affect many behaviors in insects, from foraging to oviposition, reviewed by Stange and Stowe[1], Guerenstein and Hildebrand[2], and Cummins et al.[3]. In the polyphagous, lepidopterous *Helicoverpa armigera,* for instance, CO_2 signals ensure that the larvae get access to the metabolically most active parts of the plant during feeding[4]. Furthermore, adult hawkmoths of the species *Manduca sexta* detect freshly opened and nutritious flowers of *Datura wrightii* based on their elevated CO_2 emission[5]. Another example is the female cactus moth, *Cactoblastis cactorum,* utilizing ambient CO_2 levels to locate the photosynthetically most active part of the host plant cactus, *Opuntia stricta,* for egg laying[6].

Previous studies on different lepidopteran species have shown that external CO_2 fluctuations are detected by sensory neurons housed in a specialized organ located on a section of the mouthparts called the labial palps[6–8]. In *H. armigera*, the labial pit organ (LPO) houses ca. 1200 CO_2 sensory neurons[9]. These LPO neurons express three types of gustatory receptor genes[10,11]. Previous mass staining experiments from the relevant segment of the labial palps have demonstrated sensory fibers targeting various sites including bilateral projections to one glomerulus in each antennal lobe (AL), called the LPO glomerulus (LPOG)[9,12]. A recent study reported that the LPO sensory projections which include bilateral, ipsilateral, and contralateral neurons, target the LPOG exclusively[13]. The remaining AL glomeruli, comprising three male-specific glomeruli (the macroglomerular complex, MGC) and ca. 75 ordinary glomeruli, receive input from antennal neurons tuned to pheromones and plant odors, respectively[14]. None of these sensory neurons, which form the antennal nerve, target the LPOG.

In the AL, all sensory neurons including those projecting both from the antenna and the LPO, make synapses with second-order neurons within the numerous glomeruli. There are two types of AL neurons, local interneurons (LNs) and projection neurons (PNs). The latter cells carry odor information to higher processing centers in the protocerebrum via several parallel antennal-lobe tracts (ALTs; Fig. 1). The most prominent tract, the medial ALT, is reported to connect the antennal lobe with the calyces of the mushroom bodies (Ca, center for associative learning)[15,16] and the lateral horn (LH, center for innate behavior)[17] in many moths, including

[1]Chemosensory Laboratory, Department of Psychology, Norwegian University of Science and Technology, NTNU, Trondheim, Norway. [2]Department of Teachers Education, Norwegian University of Science and Technology, NTNU, Trondheim, Norway. [3]State Key Laboratory for Biology of Plant Diseases and Insect Pests, Institute of Plant Protection, Chinese Academy of Agricultural Sciences, Beijing, China. [4]These authors contributed equally: X. Chu and P. KC. ✉email: bente.berg@ntnu.no

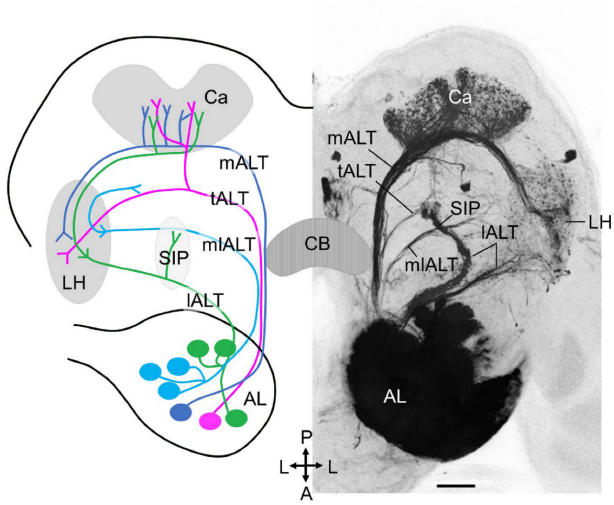

Figure 1. Overview of antennal-lobe tracts (ALTs) in moth. *Left*: Schematic drawing of the medial, transverse, mediolateral, and lateral ALT (mALT, tALT, mlALT, and lALT). *Right*: A corresponding confocal image obtained by mass filling the AL. Ca, Calyces of the mushroom body; LH, lateral horn; SIP, superior intermediate protocerebrum; CB, central body. A, anterior; L, lateral; P, posterior; Scale bar, 50 µm.

M. sexta [18], *Bombyx mori*[19,20], *Heliothis virescens* [21,22], *Helicoverpa zea*[23], *Helicoverpa assulta*[24], and *H. armigera*[25]. Two other well-described tracts are the lateral and mediolateral ALT, both of which target protocerebral regions mainly outside the Ca[18,26].

In moth, there are three minor tracts formed by relatively few neurons, two of which are the transverse ALT[27] and the dorsomedial ALT[18,27]. The transverse tract projects partly in parallel with the mediolateral tract. The mediolateral tract splits off from the medial tract at the anterior edge of the central body (CB), while the transverse tract splits off at the posterior edge of the CB (Fig. 1). The number of axons forming the transverse tract is slightly lower than that in the mediolateral tract (in *Drosophila melanogaster*, 60 axons in the transverse tract vs. 80–100 axons in mediolateral tract)[28]. The transverse tract was first described in *D. melanogaster*[28]. Lately, individual neurons confined to this tract have been described in various insect species, such as *H. virescens*[27,29], *H. armigera*[26], *Hieroglyphus banian*[30], and *D. melanogaster*[31,32]. The other minor tract, the dorsomedial tract, consisting of a few neurons only, was first reported in *M. sexta*[18]. So far, only two studies have described the complete morphology of individual neurons confined to this tract in the noctuid moth[21,26].

Generally, output neurons originating from the ordinary glomeruli and the MGC have been relatively well studied in moths, reviewed by Martin et al.[33]. Previous studies in several species have shown that the second-order circuits for pheromone and plant odor signals are mainly separated[18,25]. The projections of LPOG output neurons, on the other hand, have been poorly described. So far, only one study on this system has been carried out, reporting two types of CO_2-responding neurons originating from the LPOG in *M. sexta*[34]. Based on the previously well-described chemosensory pathway including (1) distinct AL glomeruli for input about pheromones, plant odors, and CO_2, respectively[9,13,14], and (2) a general separation of pheromone and plant odor signals at the subsequent synaptic level[18,25,35], it is particularly interesting to investigate how second-order neurons carrying signals from CO_2 are arranged. In the present study, we performed a series of intracellular staining and mass staining experiments enabling tracing of the PNs forming this pathway in *H. armigera*. Totally, five morphological LPOG neuron types passing along different ALTs were found. Their projection targets were mainly segregated from pheromone output regions but overlapped to a certain extent with terminals of plant odor neurons. Notably, most LPOG PNs were confined to other tracts than the prominent medial tract.

Results

Outline of protocerebral regions serving as targets for LPOG PNs. To provide a framework for describing the main target areas of the LPOG PNs, we reconstructed a selection of protocerebral regions from the confocal image stack previously utilized for creating the representative brain model[25]. In addition to the main neuropil structures originally included in this 3D brain atlas, we added an assembly of nine areas in order

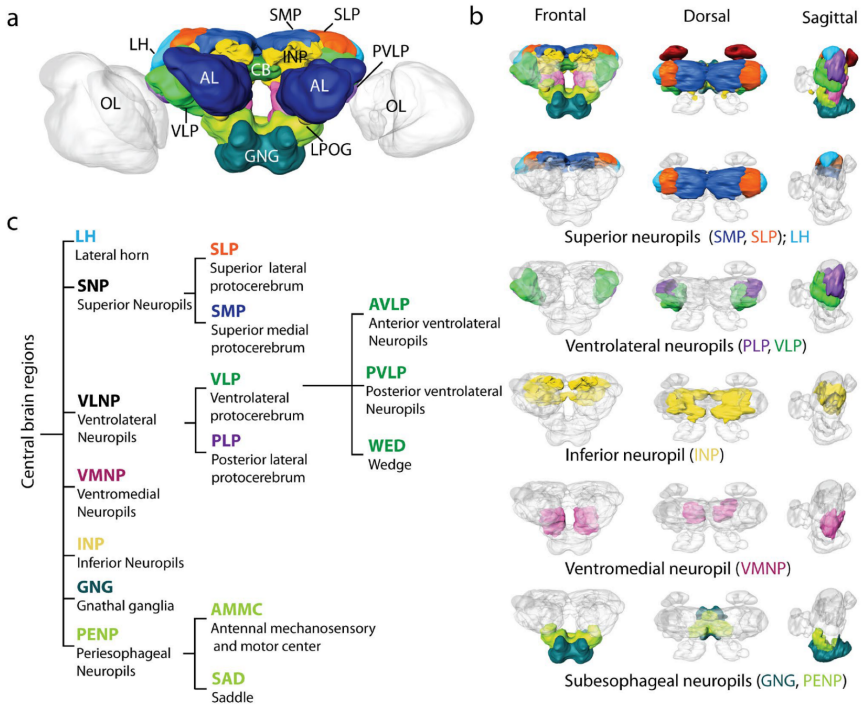

Figure 2. Layout of LPOG PN output regions. (**a**)Three-dimensional surface model of the representative brain of *Helicoverpa armigera*[25], in frontal view, including the relevant neuropils in. AL, antennal lobe; CB, central body; GNG, gnathal ganglion; INP, inferior neuropils; LH, lateral horn; OL, optical lobes; SMP: superior medial protocerebrum; SLP, superior lateral protocerebrum; VLP ventrolateral protocerebrum. Scale bar: 100 µm. (**b**) The main defined neuropils targeted by LPOG neurons, indicated by distinct colors. From top to bottom: All defined central brain neuropils (*colored*) shown together with the continuous mass of undefined regions (*gray*). Scale bar: 100 µm. (**c**) Hierarchical diagram showing the neuropils in (**b**) including sub-regions.

to determine the main output regions of the LPOG neurons identified here (Fig. 2a, b). All newly reconstructed regions are listed and presented in Fig. 2c.

The PN pathway carrying CO_2 input is distinct from the canonical olfactory PN pathway. In order to obtain an anatomical overview of the PN pathway carrying CO_2 information in the moth brain, a series of focused mass staining experiments from the LPOG was first performed. Confirmation about dye application into the LPOG, and the LPOG exclusively, was obtained by examining the presence of labeled sensory neurons in the LPO (see confocal scanning in Supplementary Fig. S1) and a lack of staining in the ventral AL glomeruli, located adjacent to the lateral cell body cluster (LC). As demonstrated in one of the preparations, including the highest number of simultaneously labeled LPOG PNs (Fig. 3a), the projection pattern demonstrated extensive labeling in the LH. This pattern originated from overlapping terminals of axons passing along three distinct ALTs, the transverse, medial, and lateral tract. The transverse-tract neurons were particularly prominent. The relatively uncommon transverse-tract neuron type is previously reported to carry information from a few AL glomeruli only[26], and our data show that the LPOG is one of them. In addition to targeting the LH, some LPOG output neurons also projected to the Ca, however, with substantially weaker innervations. In order to compare the projection patterns of the LPOG PNs and a typical medial-tract PN, we placed confocal images of the two PN categories next to each other (Fig. 3a, b). The considerably stronger staining of the Ca in the medial-tract PN is obvious. Furthermore, the mass stained preparation in Fig. 1, including AL output neurons originating

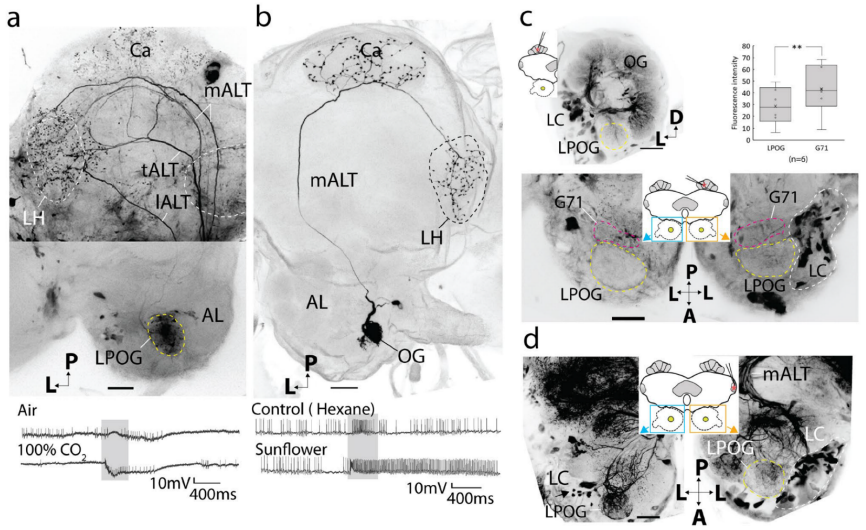

Figure 3. Comparison of LPOG PNs versus PNs connected with ordinary glomeruli. (**a**) Mass staining of LPOG-neurons via anterograde labeling from the LPOG. Labeled neurons confined to the transverse, medial, and lateral ALT (tALT, mALT, and lALT). Overlapping projection terminals occur in the lateral horn (LH) whereas the calyces (Ca) is weakly innervated. The tALT PNs bend off from the mALT at the posterior edge of the central body (dashed *white* line). Spiking activity of the mass stained LPOG neurons during application of fresh air and CO_2 is shown below. (**b**) Confocal image of a typical plant-odor sensitive mALT neuron with extensive innervations in the Ca. Spiking activity during stimulation with hexane and plant-odor is shown below. (**c**) Retrograde labeling from Ca. The upper confocal image shows substantially weaker labeling in the LPOG than in the ordinary glomeruli in the ipsilateral AL (frontal view). The box plot demonstrates the difference in fluorescence intensity between the LPOG and the neighboring glomerulus, G71. The additional confocal image below, including both ALs in dorsal view, demonstrates the location of the LPOG (*yellow* dashed circle) and G71 (*red* dashed circle). (**d**) Retrograde labeling from LH. Confocal image of the contralateral AL (*left*), showing extensive labeling in the LPOG. Nine stained somata (arrow) in the lateral cell body cluster (LC), connected with the LPOG, indicates at least nine bi- or contralateral LPOG neurons targeting the LH. Scale bars: 50 µm. A, anterior; L, lateral; P, posterior.

from seemingly all glomeruli, displays extensive innervations in the Ca as well. To quantify the characteristic difference in the terminal patterns of LPOG PNs versus PNs originating from ordinary glomeruli, we measured the fluorescence intensity within the Ca and the LH region in each of the three stained preparations referred to above. The Ca/LH-ratios were then calculated and found to be 0.42 for the LPOG PNs (Fig. 3a), 1.35 for the AL mass-stained preparation (Fig. 1), and 0.89 for the single medial-tract PN (Fig. 3b). Thus, we assumed that the LPOG PNs were relatively weakly connected to the Ca.

Next, to confirm the contrasting distribution of axon terminals in the LH vs. Ca of LPOG PNs, we carried out two types of retrograde mass staining experiments. We first injected fluorescent dye into the Ca, which resulted in extensive staining of all glomeruli in the ipsilateral AL except for one, the LPOG (Fig. 3c). By quantifying the mean fluorescent intensity in the ipsilateral LPOG and the neighboring glomerulus, G71 (Fig. 3c and Supplementary Fig. S2), we found that the LPOG was consistently weaker stained ($t(5) = 4.97$, $p = 0.004$). This confirmed our hypothesis of a relatively weak connection between the LPOG and the Ca. The second retrograde mass staining experiment involved application of dye into the lateral protocerebrum, including LH. This caused not only labeling of all glomeruli in the ipsilateral AL, including the LPOG, but also uncovered an assembly of stained axons linked to the LPOG in the contralateral AL (Fig. 3d). Here, nine labeled LC somata connected with the innervated glomerulus could be seen—indicating the presence of at least nine bilateral or contralateral LPOG PNs. Altogether, the results from the three kinds of mass staining experiments revealed that the LPOG, receiving input from the labial palp, has an output pathway differing substantially from that of PNs linked to the other AL glomeruli, receiving input from the antennae. The main characteristics of the LPOG pathway include: 1) a prominent involvement of the transverse ALT, 2) relatively weak terminal innervations of the Ca, and 3) a significant proportion of bilateral/contralateral PNs.

Tracts	Soma localization	Soma diameter (µm)	Dendritic arborisation (LPOG)	Ipsi-, contra-, or bilateral projections	Output regions	Number	Previous Reports LPOG PNs
tALT						*Total:10*	
$Pt\_a_{(LPOG)}$	LC	14.60 ± 0.70 (n = 3)	UG	Ipsilateral	Ca, LH, SLP, PLP, VLP	3	PIa(G)[34]
$Pt\_d_{(LPOG)}$	–	–	UG	Ipsilateral	SLP, SMP	1	**Novel**
$Pt\_e_{(LPOG)}$	MC	10.37 ± 0.62 (n = 3)	UG (LPOG[b])	Contralateral	LH[c], PLP[c]	3	Protocerebral neuron[34]
$Pt\_f_{(LPOG)}$	LC	8.58 (n = 1)*	UG	Bilateral	LH, VLP[b]	3	**Novel**
mALT						*Total :2*	
$Pm\_e_{(LPOG)}$	AC	18.10	UG	Ipsilateral	LH, SLP, INP, PLP	1	**Novel**
$Pm\_g_{(LPOG)}$	LC	9.98	UG	Contralateral	LH[c]	1	**Novel**
lALT							
$Pl\_g_{(LPOG)}$	LC	6.27	UG	Ipsilateral	LH, SLP, PLP	1	**Novel**
dmALT						*Total:1*	
$Pdm\_a_{(LPOG)}$	–	–	UG	Ipsilateral	SMP, INP, VMNP, AMMC, GNG	1	**Novel**
AST						*Total:1*	
$Past\_a_{(LPOG)}$	GNG	4.53	–	Ipsilateral	AMMC, VLP	1	**Novel**

Table 1. Overview of individual LPOG PNs confined to five different tracts. AC, anterior cell body cluster; ALT, antennal lobe tract; AMMC, antennal mechanosensory and motor center; AST, antennal subesophageal tract; [b]; bilateral; [c], contralateral; Ca, calyx; dmALT, dorsomedial ALT; GNG, gnathal ganglion; INP, inferior neuropil; lALT, lateral ALT; LC, lateral cell body cluster; LH, lateral horn; mALT, medial ALT; MC, medial cell body cluster; PNs, projection neurons; PLP, posterior lateral protocerebrum; SLP, superior lateral protocerebrum; SMP, superior medial protocerebrum; tALT, transverse ALT; UG, uniglomerular; VLP, ventrolateral protocerebrum; VMNP, ventromedial neuropil; *, the soma diameter of one of the three $Pt\_f_{(LPOG)}$ PN is stated, the two remaining somata were not visible.

LPOG neurons are uniglomerular PNs with rich morphological diversity. As the two PN pathways, devoted to CO_2 and ordinary odorants, respectively, display substantially different projection patterns at the neuron population level, we next aimed at investigating how these differences were expressed at the single-neuron level. We thus carried out intracellular dye injection into the thick dendrites of LPOG PNs. Fifteen LPOG neurons were morphologically identified, all having glomerular dendritic arborizations focused in the LPOG solely. These neurons were confined to five different tracts: ten to the transverse ALT, two to the medial ALT, one to the lateral ALT, one to the dorsomedial ALT, and one to the antenno-suboesophageal tract (AST). Naming of neuron types and subtypes is an adaptation of the system used in previous studies[18,26,27]. This implies that the five neuron types were named according to the tract they projected along (i.e., Pt, Pm, Pl, Pdm, and Past) whereas the neuron subtypes were classified according to their axonal projection patterns in the protocerebrum. For the name, $Pt\_a_{(LPOG)}$, "*P*" indicates the PN category, "*t*" applies to the transverse-tract type, "*a*" refers to the PN subtype, while "$_{(LPOG)}$" represents the uniglomerular dendritic arborization. An overview of the individually stained neurons and their corresponding output regions is shown in Table 1 and Fig. 4.

The main share of stained LPOG neurons passed along the transverse antennal-lobe tract. Even though relatively few projection neurons are reported to connect the AL to the protocerebrum via the transverse tract, the main proportion (more than 65%) of labeled neurons originating from the LPOG passed along this route. The transverse-tract neurons were morphologically diverse, including both uni- and bilateral neurons. They all left the AL together with the medial ALT and projected along its path until the posterior edge of the CB. Here, they bent off from the medial tract, passing along the pedunculus before projecting their wide-spread terminal branches in different areas of the ipsilateral and/or contralateral protocerebrum. The transverse-tract neurons comprised four subtypes, two unilateral and two bilateral (Fig. 5).

Unilateral transverse-tract neurons. Four of the ten labeled transverse-tract LPOG PNs were unilateral. Three of these unilateral neurons were morphologically similar forming one distinct subtype and the fourth constituted another subtype. The three first-mentioned neurons were the only ones innervating the Ca. In addition, these neurons projected to several regions in the lateral protocerebrum, including the LH, superior lateral protocerebrum (SLP), posterior lateral protocerebrum (PLP), and ventrolateral protocerebrum (VLP, Figs. 4d, 5a). This neuron subtype which was named $Pt\_a_{(LPOG)}$, is similar to an LPOG PN previously described in *M. sexta*[34]—by then, defined as a medial-tract PN. The fourth unilateral transverse-tract neuron, constituting a distinct subtype, bypassed the Ca anteriorly and targeted the lateral part of the SLP and superior medial protocerebrum (SMP, Figs. 4e, 5b). This neuron was categorized as $Pt\_d_{(LPOG)}$ subtype[18,26].

Bilateral transverse-tract neurons. The six other transverse-tract neurons were bilateral, forming two equally sized subtypes. One subtype, including three stained neurons, had dendritic arborizations in the LPOG of both ALs (Figs. 4f, 5c). This neuron subtype projecting to the contralateral PLP and LH, was previously reported in *M. sexta*[34]. We named it $Pt\_e_{(LPOG)}$. The second bilateral transverse-tract neuron subtype, comprising three neurons

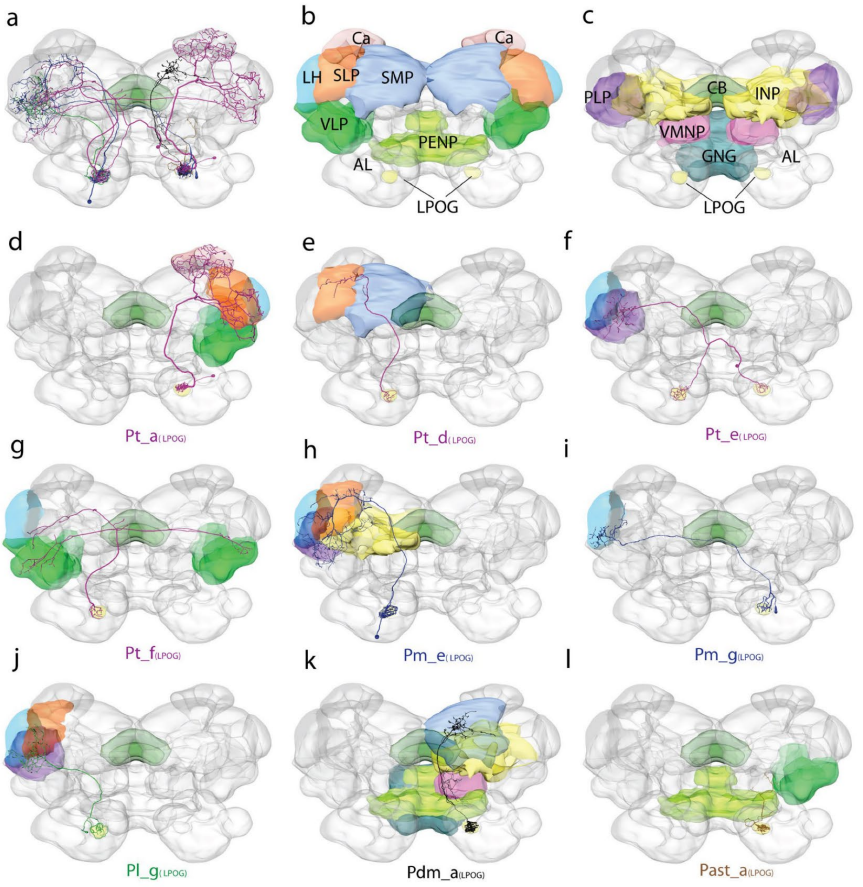

Figure 4. Overview of the anatomical architecture of the LPOG output neurons. (**a**) Summary diagram of the nine LPOG PN subtypes, color-coded according to the tract they are confined to: Transverse-tract neurons in *magenta*, medial-tract neurons in *blue*, lateral-tract neuron in *green*, dorsomedial tract neuron in *black*, and neuron in the antennal subesophageal tract in *orange*. Scale bar: 100 µm. (**b–c**) Summary diagram of the brain neuropils targeted by the LPOG PNs, color-coded in correspondence with all other figure panels. AL, antennal lobe; GNG, gnathal ganglion; INP, inferior neuropils; LH, lateral horn; PENP, periesophageal neuropils; PLP, posterior lateral protocerebrum; SMP, superior medial protocerebrum; SLP, superior lateral protocerebrum; VLP, ventrolateral protocerebrum; VMNP, ventromedial neuropils. (**d–l**) 3D reconstructions of the nine LPOG PN subtypes manually registered into the representative brain (dorsal view).

as well, originated in one LPOG only. The main axon passed ipsilaterally up to the ventrolateral edge of the CB. Here, it divided into two branches, one terminating in the LH and the VLP of the ipsilateral hemisphere and the other terminating in the VLP of the contralateral hemisphere (Figs. 4g, 5d). This neuron subtype, named Pt_f$_{(LPOG)}$, is previously not described.

LPOG neurons confined to the medial antennal-lobe tract bypass the calyces (Ca). One of the notable features of the mass-stained LPOG PNs was the weak innervation of the Ca—even when multi-

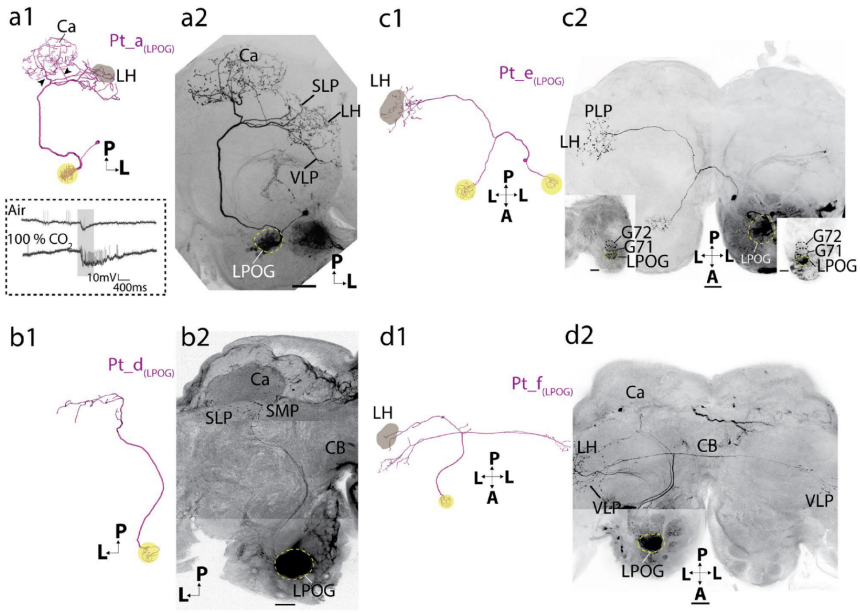

Figure 5. Four transverse-tract LPOG neurons, including two ipsilateral and two bilateral subtypes. (**a1, a2**) 3D reconstruction and confocal image of a Pt_a$_{(LPOG)}$ neuron subtype. The ipsilateral neuron projected to the calyces (Ca) via two axonal fibers (arrowheads) before terminating in the lateral horn (LH), superior lateral protocerebrum (SLP), and ventrolateral protocerebrum (VLP). The soma was in the lateral cell body cluster. (Spike activities during stimulation with fresh air and CO_2 is shown to exemplify how LPOG neurons were identified during the experiment.) (**b1, b2**) 3D reconstruction and confocal image of a Pt_d$_{(LPOG)}$ neuron subtype. The ipsilateral neuron originated in the LPOG and projected to the superior medial protocerebrum (SMP) and SLP without innervating the Ca. (**c1, c2**) 3D reconstruction and confocal image of a Pt_e$_{(LPOG)}$ neuron subtype. This bilateral neuron arborized in the LPOG of both ALs and terminated in the LH contralateral to the site of the cell body. The two LPOGs were connected via the antennal-lobe commissure. The soma was in the medial cell body cluster. The neuron was co-stained with a weakly labeled lateral-tract LPOG neuron. The two insets in **c2** are confocal images showing the dendritic arborizations in each AL. The LPOG is located adjacent to glomerulus G71. (**d1, d2**) 3D reconstruction and confocal image of a Pt_f$_{(LPOG)}$ neuron subtype. This bilateral LPOG neuron terminated in the ipsilateral LH and in the VLP of both hemispheres. The neuron was co-stained with a Pt_d$_{(LPOG)}$ neuron and a lateral-tract LPOG neuron. (The reconstruction of neuronal dendrites in **b1**, **c1**, and **d1** are shown for illustrative purposes only. Due to prestaining/mass staining of the LPOG, the detailed arborizations were not visible.) All images are in dorsal orientation. CB, central body; A, anterior; L, lateral; P, posterior; Scale bars: 50 µm.

ple medial-tract neurons were labeled (Fig. 3a). The single-neuron staining experiments affirmed this feature. The two medial-tract LPOG neurons individually stained here, formed two subtypes—both bypassing the Ca (Figs. 4h, i and 6a, b).

One unilateral medial-tract neuron originating in the LPOG bypassed the Ca but innervated various areas of the protocerebrum including the LH, SLP, PLP, and VLP (Figs. 4h, 6a). In addition, the axon extended a few side-branches into the inferior neuropil (INP). We classified this subtype as Pm_e$_{(LPOG)}$, in accordance with previously reported neurons displaying similar morphologies[27]. The other medial-tract neuron originating in the LPOG projected to the contralateral protocerebrum (Figs. 4i, 6b). The axon of this subtype passed along the initial part of the ipsilateral medial ALT, however, then it turned and passed along the posterior edge of the CB, crossing the brain midline and targeting the contralateral LH exclusively. This new subtype was named Pm_g$_{(LPOG)}$.

A lateral-tract neuron connecting the LPOG directly to the LH. One of the 15 labeled LPOG output neurons projected along the lateral ALT. This neuron targeted various regions in the ipsilateral protocer-

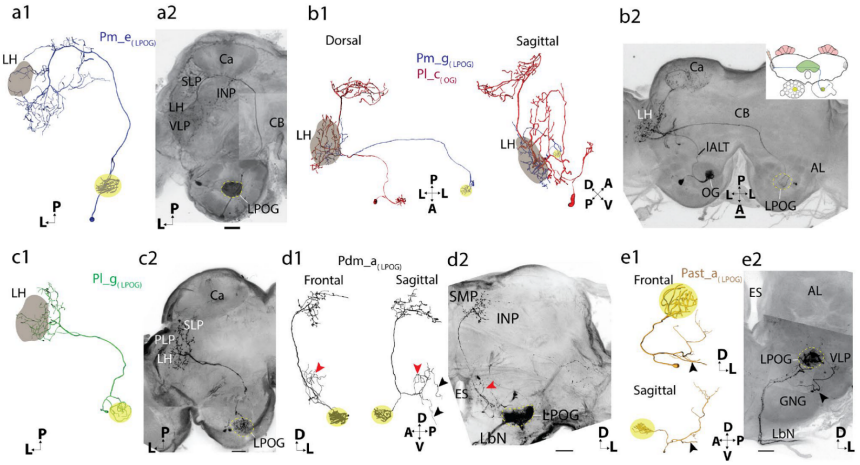

Figure 6. Morphologies of LPOG-neurons confined to the medial tract (**a-b**), lateral tract (**c**), dorsomedial tract (**d**) and antennal-subesophageal tract (**e**). (**a1, a2**) 3D reconstruction and confocal image of a medial-tract neuron of the Pm_e$_{(LPOG)}$ subtype. The wide-spread terminals of this unilateral neuron targeted the lateral horn (LH), superior lateral protocerebrum (SLP), inferior neuropil (INP), and superior lateral protocerebrum (SLP). The axon of the neuron bypassed the calyces (Ca) on its anterior border. (**b1, b2**) 3D reconstruction and confocal image of a medial-tract neuron of the Pm_g$_{(LPOG)}$ subtype (stained from the LH). The axon of this neuron followed the medial tract ipsilaterally before it turned, passed the brain midline, and terminated in the contralateral LH. This neuron was co-stained with a lateral-tract neuron from an ordinary glomerulus in the contralateral antennal lobe, showing the general overlap in the LH of output neurons from the LPOG and ordinary glomeruli. The schematic drawing in **b2** indicates the labeling site of the Pm_g$_{(LPOG)}$ neuron, i.e., the contralateral LH. (**c1, c2**) 3D reconstruction and confocal image of a lateral-tract neuron of the Pl_g$_{(LPOG)}$ subtype. This neuron projected to the lateral horn (LH) and superior lateral protocerebrum (SLP). Its cell body was localized in the lateral cell body cluster. **(d1, d2**) 3D reconstruction and confocal image of an LPOG neuron passing in the dorsomedial tract. Reconstruction of the Pdm_a$_{(LPOG)}$ neuron showed the axon of the neuron dividing into two main branches, one dorsally projecting branch terminating in the superior medial protocerebrum (SMP) and the inferior neuropil (INP), and one ventrally projecting branch innervating the ventro-medial neuropil (VMNP, *red* arrowhead). The neuron also projected to the antennal mechanosensory and motor center (AMMC, *black* arrowhead) and the gnathal ganglion (GNG). (**e1, e2**) 3D reconstruction and confocal image of an LPOG neuron confined to the antennal-subesophageal tract (AST). The neuron, named Past_a$_{(LPOG)}$, extended blebby terminals in the AMMC (*black* arrowhead). The cell body was localized in the GNG. Several fibers in the labial pit nerve (LbN), which project from the labial pit organ, were co-stained. (The reconstructions of dendrites in **a1, d1,** and **e1** are shown for illustrative purposes only. Due to prestaining of the LPOG, the detailed arborization pattern was not visible.) AL, antennal lobe; Ca, calyx; CB, central body. D, dorsal; V, ventral; P, posterior; L, lateral; A, anterior; VLP, ventrolateral protocerebrum; Scale bars: 50 µm.

ebrum including the LH, PLP, and a small part of the SLP (Figs. 4j, 6c). The lateral-tract LPOG neuron had dense dendritic arborization in the LPOG. This newly described neuron was classified as Pl_g$_{(LPOG)}$.

LPOG neurons confined to minor tracts. In addition to the three LPOG neuron types described above, including PNs confined to the transverse, medial, and lateral ALT, the single neuron labeling technique explored two rare types, which are not frequently stained. One of these LPOG neurons projected in the dorsomedial ALT (dmALT), which is a relatively thin fiber bundle passing more dorsally and medially than the prominent medial tract. Whereas previously described neurons confined to the dorsomedial tract are reported to project bilaterally[26], the neuron identified here projects unilaterally. From the LPOG, the main axon passed along the dmALT to the SMP, INP, and the ventro-medial neuropil (VMNP, Figs. 4k, 6d). In addition, a few fibers projected to the antennal mechanosensory and motor center (AMMC) and the gnathal ganglion (GNG). So far, no PN subtypes confined to the dmALT have been reported. This newly described neuron was therefore classified as Pdm_a$_{(LPOG)}$.

One LPOG output neuron projected in the antennal suboesophageal tract (AST; Figs. 4l, 6e). The small cell body of the neuron (approximately 4.5 µm in diameter) was localized outside the AL, in the dorsolateral cell-body rind in the ipsilateral GNG. The neuron projected ventrally, side by side with the sensory bundle from the

LPO. Then it turned laterally and sent terminal projections into the ventral area of the AMMC and VLP. This newly described neuron was classified as Past_a$_{(LPOG)}$.

Discussion

Here, we present new anatomical data on the central pathway processing CO_2 information in the noctuid moth, *H. armigera*. Totally, 15 individual AL PNs originating from the LPOG were stained. This morphologically heterogenous neuron assembly included nine subtypes, most of which were not previously described. A considerable amount of PNs, i.e. ten, passed along the up to now poorly described transverse ALT. The typical medial-tract neuron innervating the Ca before terminating in the LH, was not found. In order to estimate the real number of LPOG output neurons, we combined the results from the mass-staining and single-unit labeling experiments. The highest number of LPOG PNs observed in the anterogradely mass-stained preparations were five (Fig. 3a), including the three ipsilateral subtypes, Pt_a$_{(LPOG)}$, Pm_e$_{(LPOG)}$, and Pl_g$_{(LPOG)}$. From the retrograde staining performed from the lateral protocerebrum, including nine stained somata linked to the LPOG in the contralateral AL (Fig. 3d), we can conclude that at least nine bilateral/contralateral PNs originate from the LPOG (possibly making up Pt_e$_{(LPOG)}$, Pt_f$_{(LPOG)}$, and/or Pm_g$_{(LPOG)}$ subtypes). In addition, we stained three distinct PN subtypes not represented in any of the mass-stained preparations, i.e. Pt_d$_{(LPOG)}$, Pdm_a$_{(LPOG)}$, and Past_a$_{(LPOG)}$ (Fig. 4e, k, l). Taken together, we assume there are at least 17 PNs originating from the LPOG. This number is comparable with the amount of CO_2 output neurons from the V-glomerulus in *Drosophila*, in which 12 PNs were imaged by using the photoactivatable green fluorescent protein technique[36].

Notably, 12 of the 15 LPOG neurons presented here had overlapping projection terminals in the LH, which constitutes a main output target for PNs originating from the numerous ordinary glomeruli (see introduction). The comprehensive data on AL output neurons recently obtained from *H. armigera*—including both plant odor and pheromone neurons[25,26], constitutes an excellent base for exploring putative interactions between the CO_2 pathway and these two olfactory sub-systems.

The CO_2 pathway and the sub-systems devoted to plant-odors and pheromones. In Lepidoptera, CO_2 and plant odors are detected by sensory neurons localized on different organs. From here, the two categories of sensory neurons project to distinct sets of AL glomeruli, i.e., the LPOG and the ordinary glomeruli, respectively. As both stimulus inputs are relevant for detecting the quality of host plants (see introduction), it is likely that the two signal pathways interact in the central nervous system. Given that all LPOG PNs are uniglomerular, as those identified in this study, there seems to be a continuation of the segregated paths also at the second-order level, implying a system organized mainly according to a labeled-line principle[37]. On the other hand, the LPOG is not totally segregated from the other glomeruli but interconnected via numerous multiglomerular LNs innervating the AL globally. In a recent study of AL neurons in *H. armigera*, about 90% of the LNs were reported to arborize in the LPOG[26]. Even though a substantial proportion of these LNs had relatively weak innervations in the LPOG, this indicates that processing does occur across the glomerular categories. Like in other insects, the main proportion of LNs in heliothine moths is GABAergic[38]. Indeed, we can't rule out the possibility that LPOG PNs could be influenced by excitatory LNs[39–42] or by polysynaptic GABAergic inputs[43]. Anyway, considering the typical global pattern of LNs arborizing in the LPOG, we suggest that a modest degree of signal integration takes place across the sub-systems at this level.

The finding of *uniglomerular* LPOG neurons exclusively, forming a distinct output pathway for CO_2 information, as presented here, is in accordance with the labeled-line principle characterizing the two previously well-described olfactory sub-systems devoted to plant odors and pheromones, respectively[18,20,25,26,35]. Unlike the pheromone sub-system, having its distinct output area in the lateral protocerebrum, the CO_2 sub-system has axon terminals overlapping with the plant-odor PNs. As shown in Fig. 6b, reconstructions of two co-stained neurons, one from the LPOG and the other from an ordinary glomerulus, demonstrates the overlapping terminals in the LH. This overlap indicates that the LH is a significant region for integration of sensory inputs about plant odors and CO_2. One putative downstream site for receiving information processed in the LH is the SMP[44]. Interestingly, the SMP is also directly innervated by at least two LPOG neuron subtypes identified here (Pt_d$_{(LPOG)}$ and Pdm_a$_{(LPOG)}$). Thus, to record response-patterns of SMP-neurons during stimulation with plant-odors and CO_2 constitutes an exciting subject for future studies. Taken together, we suggest that the LH is an essential site for integrating CO_2 and plant odor signals.

In contrast to the substantial overlap with parts of the plant odor sub-system, the LPOG projections had weak innervations in the main target areas of the male-specific MGC neurons, including the SLP and the superior intermediate protocerebrum (SIP)[25]. Although some of the LPOG PNs stained here, i.e. four neuron subtypes (Pt_a$_{(LPOG)}$, Pt_d$_{(LPOG)}$, Pm_e$_{(LPOG)}$, and Pl_g$_{(LPOG)}$), had axonal terminals in the SLP, they targeted a distinct area localized more ventrally and lateral-posteriorly as compared to the MGC PNs[25,35,45].

The finding that PNs carrying CO_2 signals interact more intensively with plant odor PNs than with pheromone PNs fits well with previous studies in *Drosophila* demonstrating extensive synaptic interactions in the LH between cholinergic PNs[46]. These cholinergic PNs include neurons responding to CO_2[47,48]. In addition, a population of plant/food odor PNs also target the same region[49]. Overall, the results presented here take us one step further towards understanding the neuronal architecture underlying moths' ability to measure fine fluctuations in CO_2 for determining the nutritional quality of relevant host plants[5,50].

CO_2 signaling is modestly involved in sensory learning. The calyces of the mushroom bodies are a neuropil for sensory integration and memory, important for experience-dependent reactions[51–55]. In contrast to the main olfactory pathway, which innervates the Ca extensively (Fig. 1), the LPOG PNs had a rather restricted innervation of this neuropil. Both the mass-stained and single-unit stained preparations demonstrated consider-

ably less terminals in the Ca than in the LH (Figs. 3a, 5,6). Actually, only one of the nine LPOG neuron subtypes, Pt_a$_{(LPOG)}$, innervated the Ca. Its distributed and blebby terminals in the Ca correspond with the features of the typical uniglomerular plant-odor PNs and differ from the innervation pattern of pheromone PNs[18,25,35]. In the fruit fly, PNs tuned to CO_2, which are connected with the V-glomerulus, also innervate the Ca modestly; the only neuron type targeting this neuropil is a bilateral lateral-tract neuron[36]. The general projection pattern of LPOG neurons bypassing the Ca suggests that the CO_2 signaling system is minimally involved in sensory learning, particularly olfactory learning.

The apparent trivial role of CO_2 input for memory suits well with the fact that this gas is ubiquitous, serving as a minor compartment of the Earth's atmosphere. Like the CO_2 PNs, other AL output neurons tuned to universal cues, such as temperature and humidity, also display little or no connection with Ca. For instance, both in the fruit fly and cockroach, PNs carrying thermo- and hygro-sensory signals have modest or no innervation in the Ca[32,56].

Functional implications of CO_2 signaling in the other brain areas. In addition to targeting the LH, the CO_2 PNs identified here also projected to various other neuropils, such as VLP, PLP, and SMP (see Fig. 4 and Table 1). In fruit flies, output neurons from the V-glomerulus, which corresponds with the LPOG, are reported to terminate in similar neuropil regions[36]. One major difference between the CO_2 systems in moth and fruit fly is that seemingly all LPOG neurons in moth are uniglomerular whereas the majority of those connected with the V-glomerulus in the fly is multiglomerular. Whether this is related to the peripheral organization in flies including CO_2 sensory neurons co-located with olfactory neurons on the antenna, is an open question. Regardless of dendritic arrangement in the AL, however, the second-order pathways for CO_2 signaling in the two insect groups are rather comparable.

Given these similarities across two insect model species, it is encouraging to speculate about the functional roles of these neuropils. The VLP, which is one of the major innervation areas of olfactory PNs[27], is also targeted by neurons carrying information about vision[57], audition[58], and temperature and humidity[32]. We found that the VLP region is targeted by two transverse-tract LPOG subtype neurons, Pt_a$_{(LPOG)}$ and Pt_f$_{(LPOG)}$, and an antennal subesophageal tract neuron, Past_a$_{(LPOG)}$. Thus, the data presented here, coincides with the previous studies demonstrating the involvement of the VLP in integration of multimodal information. The PLP, which also constitutes an essential target area for olfactory neurons[27], is reported to receive visual information both in fruit flies[32,57] and in the silk moth[59]. In the data presented here, we found at least four LPOG neuron subtypes (Pt_a$_{(LPOG)}$, Pt_e$_{(LPOG)}$, Pm_e$_{(LPOG)}$, and Pl_g$_{(LPOG)}$) targeting the PLP region. Taken together, the previously considered integration areas for multimodal processing, the VLP and PLP, receive input about CO_2 as well.

Diverse transverse-tract neurons indicate their multifunctional roles. In *H. armigera*, the transverse-tract neurons originate frequently from glomeruli localized in the ventral and posterior part of the AL[26]. We noticed that the majority of stained LPOG neurons, i.e., 10 of 15, were confined to this ALT. They are further classified into four morphological subtypes. Two subtypes, Pt_a$_{(LPOG)}$ and Pt_e$_{(LPOG)}$, were previously described in *M. sexta*[34]—by then, they were classified as an inner-tract PIa(G) neuron and a protocerebral neuron, respectively. Unlike the classic ALTs (including the medial, lateral, and mediolateral ALT), the transverse ALT is known to be formed by a relatively restricted number of neurons displaying diverse morphologies[27,28]. This implies that the target areas of the transverse-tract neurons are less confined as compared to neurons in other tracts. A previous study on the fruit fly reported transverse-tract neurons originating from two posteriorly located glomeruli conveying information about temperature and humidity[32]. Notably, these non-odor responding neurons in the fly are morphologically comparable to some transverse-tract PNs found in *H. armigera*. Generally, the restricted number of neurons confined to the transverse ALT and their high degree of heterogeneity indicate that, in contrast to the main tracts, the tALT is formed by a few functionally unique PNs.

Conclusion

The anatomical data presented here, including visualization of individually labeled LPOG PNs forming the second-order pathway for CO_2 signals in the moth brain, contribute to improve our general understanding of parallel olfactory systems in insects. Besides, the high-resolution confocal data of individual neurons and neuron populations form the basis for future experiments exploring both anatomical and physiological characteristics of the central pathways involved in processing input about external fluctuations in CO_2.

Materials and methods

Insects and preparation. Male and female *Helicoverpa armigera* pupae (Lepidoptera; Noctuidae, Heliothinae), obtained from Keyun Bio-pesticides (Henan, China), were allowed to eclose in climate chambers (Refrigerm 200 and 6E, Struers-Kebolab, Albertsund, Denmark, or Binder KBF 720, Tuttlingen, Germany) at 24 °C and 70% air humidity on a 14:10 h light/dark cycle (lights on at 18:00). After emergence, the moths were supplied a 10% sucrose solution. The moths were 1–4 days old when the experiments were performed. According to Norwegian law of animal welfare, there are no restrictions regarding experimental use of Lepidoptera.

Preparation of the insect has been described in detail elsewhere[13,25]. Briefly, the moth was restrained inside a plastic tube with the head exposed and then immobilized with dental wax (Kerr Corporation, Romulus, MI, USA). The brain was exposed by opening the head capsule and removing the intracranial muscles and tracheas. The exposed brain was continuously supplied with Ringer's solution (in mM: 150 NaCl, 3 $CaCl_2$, 3 KCl, 25 sucrose, and 10 N-tris (hydroxymethyl)-methyl-2-amino-ethanesulfonic acid, pH 6.9).

Iontophoretic staining of individual PNs originating from the LPOG. The procedure of iontophoretic staining of AL PNs was performed as previously described[25,27,35]. Sharp electrodes were made by pulling quartz capillaries (OD: 1 mm, ID: 0.5 mm, with filament; Sutter instrument) on a horizontal puller (P-2000, Sutter instruments, CA, United States). The tip of the electrode was filled either with 4% biotinylated dextran-conjugated tetramethylrhodamine (3000 mw, micro-Ruby, Molecular Probes) in 0.2 M potassium acetate (KAc) or 4% Alexa Fluor 488 dextran (10,000 mw, Molecular Probes) in distilled water. A chloridized silver wire placed in the eye served as a reference electrode. The recording electrode having a resistance of 200–300 MΩ, was backfilled with 0.2 M KAc. Iontophoretic staining of single neurons was conducted in two ways. (i) We carefully inserted the electrode into the LPOG region from the dorsal AL area (n = 10) via a micromanipulator (Leica, Wetzlar, Germany). Contact with an LPOG-neuron was confirmed by a response when applying a CO_2 puff (Fig. 3a). (ii) We pre-stained the LPO sensory neurons with micro-Ruby 48 h prior to the iontophoretic staining of LPOG output neurons. With clear visualization of the LPOG under a Zeiss stereo discovery V12 microscope equipped with epifluorescence, we inserted the electrode into the LPOG from a frontal position (n = 5). Each neuron was stained by applying 200 ms depolarizing current pulses of 2–3 nA, at 1 Hz, for 10 min. After labeling, the insects were kept overnight at 4 °C in dark to allow anterograde axonal transportation of the dye. Then the brain was dissected from the head capsule and fixed in a paraformaldehyde solution (4% PFA in 0.1 M phosphate buffer, pH 6.9) for 2 h at room temperature or overnight at 4 °C before it was dehydrated in an ascending ethanol series (50%, 70%, 90%, 96%, and 2 × 100%; 10 min each), and finally cleared in methyl salicylate (Sigma- Aldrich, Germany).

Mass staining of output neurons originating from the LPOG. Mass staining of LPOG projection neurons was conducted in 8 male moths. Here, we applied the fluorescent dye into the relevant AL region via a sharp electrode with low resistance (~40 MΩ). Borosilicate capillaries (OD: 1 mm, ID: 0.5 mm, with filament 0.13 mm; Hilgenberg GmbH, Germany) were pulled on a horizontal puller (P-97, Sutter instruments, CA, United States). The tip of the glass electrode was filled with 4% micro-Ruby solution. The staining site was identified by testing the local field potentials during CO_2 stimulation (Fig. 3a). After that, the region was mass stained by applying a series of depolarizing current pulses of 50 nA at 1 Hz for 30 min. In addition to the anterograde mass staining, two types of retrograde labeling experiments were performed including application of dye crystals into the Ca and the LH, respectively. The dissection and dehydration were conducted as described above.

Stimulation delivery. During the electrophysiological recording, a pulse of CO_2 was delivered by a stimulation system including two parallel paths, one carrying a continuous airstream and the other the 400 ms CO_2 stimulus (100%, AGA AS, Oslo, Norway). A solenoid valve system (General Valve Corp.) regulated the application of the stimulus. To identify the neuron responses, application of the CO_2 stimulus and the control (fresh air) was repeated three times.

Confocal microscopy. Brains with successfully stained neurons were imaged using a confocal laser scanning microscope (LSM 800, Zeiss, Jena, Germany), equipped with C-Apochromat 10x/0.45 water objective, C-Apochromat 10x/0.3 air objective, and Plan-Neofluar 20x/0.5 air objective. Brains stained with micro-Ruby were scanned with a HeNe laser at 561 nm, and the emitted light was filtered through a 560–600 nm band pass filter. Preparations stained with Alexa Flour 488 were scanned with an Argon laser at 493 nm, including a 505–550 nm band pass filter. A synapsin-labeled preparation was carefully scanned utilizing two channels, in order to show that the neuropil structures visualized by the auto-fluorescent signal of endogenous fluorophores was in great agreement with the synapsin signal (Supplementary, Fig. S3). Thus, relevant structures in the brain containing the stained neurons were visualized by imaging the auto-fluorescence. Since many auto-fluorescent molecules in the tissue are excited at 493 nm, an Argon laser at 493 nm in combination with a 505–550 nm band pass filter was used. For all confocal scans, serial optical sections with a resolution of 1024 × 1024 pixels were obtained at 1.5–9 µm intervals through the entire depth of brain. The confocal images shown in this study were edited in ZEN 2.3 (blue edition, Carl Zeiss Microscopy GmbH, Jena, Germany). Brightness and contrast of the images were adjusted in Photoshop, version 21.

Reconstruction and registration of neurons into the representative brain. The 3D reconstruction of relevant neuropil structures was based on the previously conducted confocal stacks for the representative brain[25]. We used the nomenclature established by Ito, et al.[60] with the exceptions of the VLP. Our definition of the VLP, included the anterior and posterior VLP, along with the wedge. Furthermore, the superior intermediate protocerebrum (SIP) located adjacent to the SMP, was not specifically indicated in this study since none of the identified neurons projected to the SIP.

Individually labeled neurons and the surrounding brain neuropils were manually reconstructed from consecutive confocal sections by means of the visualization software AMIRA 5.3; the neurons were reconstructed by using the skeleton module of the software[61,62] and the brain structures by using the segmentation editor. Thus, each neuron was traced so that a surface model built by cylinders of distinct lengths and thicknesses was created. The relevant neuropils were reconstructed based on the autofluorescence signals, as described above. To compensate for the refraction indexes, the z-axis dimension of the neuron and brain structures was multiplied by a factor of 1.16 for the water lens objective and 1.54 for the dry lens. Manual registration of individual neurons into a representative brain from Chu et al.[25] followed the same procedure as described in Ian et al.[27].

To provide a framework for determining the target areas of the LPOG PNs, we reconstructed nine new protocerebral regions from the confocal image stack previously utilized for creating the representative brain model[25],

utilizing the segmentation editor of AMIRA. Unspecified neuropil regions have previously been characterized in the lepidopteran brain by Ian et al.[27] and Heinze and Reppert[63].

Image intensity processing and statistical analysis. As retrograded staining from the Ca labeled dendrites of all AL PNs linked with this neuropil, we could investigate putative differences in connection pattern between the LPOG and a typical ordinary glomerulus by measuring the glomerular fluorescence intensities. Here, we compared the fluorescence intensities in the LPOG and the neighboring glomerulus, G71, in six moths. We selected four confocal sections including all parts of each glomerulus. The fluorescence intensity within each of these two glomeruli was quantified by using Image J, respectively (https://imagej.net). Paired sample *t* test was performed to compare the mean intensities. All probabilities given are two-tailed. The Statistical package for the social sciences (SPSS), version 25, was used for statistical analysis.

Received: 6 August 2020; Accepted: 4 November 2020
Published online: 16 November 2020

References

1. Stange, G. & Stowe, S. Carbon dioxide sensing structures in terrestrial arthropods. *Microsc. Res. Tech.* **47**, 416–427. https://doi.org/10.1002/(SICI)1097-0029(19991215)47:6416::AID-JEMT53.0.CO;2-X (1999).
2. Guerenstein, P. G. & Hildebrand, J. G. Roles and effects of environmental carbon dioxide in insect life. *Annu. Rev. Entomol.* **53**, 161–178. https://doi.org/10.1146/annurev.ento.53.103106.093402 (2008).
3. Cummins, E. P., Selfridge, A. C., Sporn, P. H., Sznajder, J. I. & Taylor, C. T. Carbon dioxide-sensing in organisms and its implications for human disease. *Cell. Mol. Life. Sci.* **71**, 831–845. https://doi.org/10.1007/s00018-013-1470-6 (2014).
4. Rasch, C. & Rembold, H. Carbon-dioxide—highly attractive signal for larvae of *Helicoverpa armigera*. *Die Naturwissenschaften* **81**, 228–229. https://doi.org/10.1007/BF01138549 (1994).
5. Thom, C., Guerenstein, P. G., Mechaber, W. L. & Hildebrand, J. G. Floral CO_2 reveals flower profitability to moths. *J. Chem. Ecol.* **30**, 1285–1288. https://doi.org/10.1023/B:JOEC.0000030298.77377.7d (2004).
6. Stange, G., Monro, J., Stowe, S. & Osmond, C. B. The CO2 sense of the moth *Cactoblastis cactorum* and its probable role in the biological control of the CAM plant *Opuntia stricta*. *Oecologia* **102**, 341–352. https://doi.org/10.1007/bf00329801 (1995).
7. Bogner, F., Boppre, M., Ernst, K. D. & Boeckh, J. CO2 sensitive receptors on labial palps of *Rhodogastria moths* (Lepidoptera: Arctiidae): physiology, fine structure and central projection. *J. Comp. Physiol. A Sens. Neural Behav. Physiol.* **158**, 741–749 (1986).
8. Stange, G. High resolution measurement of atmospheric carbon dioxide concentration changes by the labial palp organ of the moth *Heliothis armigera* (Lepidoptera: Noctuidae). *J. Comp. Physiol. A* **171**, 317–324. https://doi.org/10.1007/BF00223962 (1992).
9. Zhao, X. C. *et al.* Fine structure and primary sensory projections of sensilla located in the labial-palp pit organ of *Helicoverpa armigera* (Insecta). *Cell. Tissue Res.* **353**, 399–408. https://doi.org/10.1007/s00441-013-1657-z (2013).
10. Ning, C., Yang, K., Xu, M., Huang, L. Q. & Wang, C. Z. Functional validation of the carbon dioxide receptor in labial palps of *Helicoverpa armigera* moths. *Insect. Biochem. Mol. Biol.* **73**, 12–19. https://doi.org/10.1016/j.ibmb.2016.04.002 (2016).
11. Xu, W. & Anderson, A. Carbon dioxide receptor genes in cotton bollworm *Helicoverpa armigera*. *Naturwissenschaften* **102**, 11. https://doi.org/10.1007/s00114-015-1260-0 (2015).
12. Kent, K. S., Harrow, I. D., Quartararo, P. & Hildebrand, J. G. An accessory olfactory pathway in Lepidoptera: the labial pit organ and its central projections in *Manduca sexta* and certain other sphinx moths and silk moths. *Cell. Tissue Res.* **245**, 237–245. https://doi.org/10.1007/bf00213927 (1986).
13. KC, P. *et al.* Revisiting the labial pit organ pathway in the noctuid moth *Helicoverpa armigera*. *Front. Physiol.* https://doi.org/10.3389/fphys.2020.00202 (2020).
14. Zhao, X. C. *et al.* Glomerular identification in the antennal lobe of the male moth *Helicoverpa armigera*. *J. Comp. Neurol.* **524**, 2993–3013. https://doi.org/10.1002/cne.24003 (2016).
15. Heisenberg, M., Borst, A., Wagner, S. & Byers, D. Drosophila mushroom body mutants are deficient in olfactory learning. *J. Neurogenet.* **2**, 1–30. https://doi.org/10.3109/01677068509100140 (1985).
16. McGuire, S. E., Le, P. T. & Davis, R. L. The role of Drosophila mushroom body signaling in olfactory memory. *Science* **293**, 1330–1333. https://doi.org/10.1126/science.1062622 (2001).
17. Schultzhaus, J. N., Saleem, S., Iftikhar, H. & Carney, G. E. The role of the Drosophila lateral horn in olfactory information processing and behavioral response. *J. Insect. Physiol.* **98**, 29–37. https://doi.org/10.1016/j.jinsphys.2016.11.007 (2017).
18. Homberg, U., Montague, R. A. & Hildebrand, J. G. Anatomy of antenno-cerebral pathways in the brain of the sphinx moth *Manduca sexta*. *Cell. Tissue. Res.* **254**, 255–281 (1988).
19. Seki, Y., Aonuma, H. & Kanzaki, R. Pheromone processing center in the protocerebrum of *Bombyx mori* revealed by nitric oxide-induced anti-cGMP immunocytochemistry. *J. Comp. Neurol.* **481**, 340–351. https://doi.org/10.1002/cne.20392 (2005).
20. Kanzaki, R., Soo, K., Seki, Y. & Wada, S. Projections to higher olfactory centers from subdivisions of the antennal lobe macroglomerular complex of the male silkmoth. *Chem. Senses* **28**, 113–130. https://doi.org/10.1093/chemse/28.2.113 (2003).
21. Rø, H., Müller, D. & Mustaparta, H. Anatomical organization of antennal lobe projection neurons in the moth *Heliothis virescens*. *J. Comp. Neurol.* **500**, 658–675. https://doi.org/10.1002/cne.21194 (2007).
22. Berg, B. G., Almaas, T. J., Bjaalie, J. G. & Mustaparta, H. The macroglomerular complex of the antennal lobe in the tobacco budworm moth *Heliothis virescens*: specified subdivision in four compartments according to information about biologically significant compounds. *J. Comp. Physiol. A.* **183**, 669–682. https://doi.org/10.1007/s003590050290 (1998).
23. Vickers, N. J., Christensen, T. A. & Hildebrand, J. G. Combinatorial odor discrimination in the brain: attractive and antagonist odor blends are represented in distinct combinations of uniquely identifiable glomeruli. *J. Comp. Neurol.* **400**, 35–56 (1998).
24. Zhao, X.-C. & Berg, B. G. Arrangement of output information from the 3 macroglomerular units in the heliothine moth *Helicoverpa assulta*: morphological and physiological features of male-specific projection neurons. *Chem. Senses* **35**, 511–521. https://doi.org/10.1093/chemse/bjq043 (2010).
25. Chu, X., Heinze, S., Ian, E. & Berg, B. G. A novel major output target for pheromone-sensitive projection neurons in male moths. *Front. Cell Neurosci.* https://doi.org/10.3389/fncel.2020.00147 (2020).
26. Kymre, J. H., Berge, C. N., Chu, X., Ian, E. & Berg, B. G. Antennal-lobe neurons in the moth *Helicoverpa armigera*—morphological features of projection neurons, local interneurons, and centrifugal neurons. *J. Comp. Neurol.* (2020). **(in press)**.
27. Ian, E., Zhao, X. C., Lande, A. & Berg, B. G. Individual neurons confined to distinct antennal-lobe tracts in the heliothine moth: morphological characteristics and global projection patterns. *Front. Neuroanat.* **10**, 101. https://doi.org/10.3389/fnana.2016.00101 (2016).

28. Tanaka, N. K., Suzuki, E., Dye, L., Ejima, A. & Stopfer, M. Dye fills reveal additional olfactory tracts in the protocerebrum of wild-type Drosophila. *J. Comp. Neurol.* **520**, 4131–4140. https://doi.org/10.1002/cne.23149 (2012).
29. Ian, E., Berg, A., Lillevoll, S. C. & Berg, B. G. Antennal-lobe tracts in the noctuid moth, *Heliothis virescens*: new anatomical findings. *Cell Tissue Res.* **366**, 23–35. https://doi.org/10.1007/s00441-016-2448-0 (2016).
30. Singh, S. & Joseph, J. Evolutionarily conserved anatomical and physiological properties of olfactory pathway through fourth-order neurons in a species of grasshopper (*Hieroglyphus banian*). *J. Comp. Physiol. A. Neuroethol. Sens. Neural. Behav. Physiol.* **205**, 813–838. https://doi.org/10.1007/s00359-019-01369-7 (2019).
31. Frank, D. D., Jouandet, G. C., Kearney, P. J., Macpherson, L. J. & Gallio, M. Temperature representation in the Drosophila brain. *Nature* **519**, 358–361. https://doi.org/10.1038/nature14284 (2015).
32. Marin, E. C. *et al.* Connectomics analysis reveals first-, second-, and third-order thermosensory and hygrosensory neurons in the adult Drosophila brain. *Curr. Biol.: CB* **30**, 3167-3182.e3164. https://doi.org/10.1016/j.cub.2020.06.028 (2020).
33. Martin, J. P. *et al.* The neurobiology of insect olfaction: sensory processing in a comparative context. *Prog. Neurobiol.* **95**, 427–447. https://doi.org/10.1016/j.pneurobio.2011.09.007 (2011).
34. Guerenstein, P. G., Christensen, T. A. & Hildebrand, J. G. Sensory processing of ambient CO_2 information in the brain of the moth *Manduca sexta*. *J. Comp. Physiol. A.* **190**, 707–725. https://doi.org/10.1007/s00359-004-0529-0 (2004).
35. Zhao, X.-C. *et al.* Representation of pheromones, interspecific signals, and plant odors in higher olfactory centers; mapping physiologically identified antennal-lobe projection neurons in the male heliothine moth. *Front. syst. Neurosci.* **8**, 186–186. https://doi.org/10.3389/fnsys.2014.00186 (2014).
36. Lin, H. H., Chu, L. A., Fu, T. F., Dickson, B. J. & Chiang, A. S. Parallel neural pathways mediate CO_2 avoidance responses in Drosophila. *Science* **340**, 1338–1341. https://doi.org/10.1126/science.1236693 (2013).
37. Galizia, C. G. & Rossler, W. Parallel olfactory systems in insects: anatomy and function. *Annu. Rev. Entomol.* **55**, 399–420. https://doi.org/10.1146/annurev-ento-112408-085442 (2010).
38. Berg, B. G., Schachtner, J. & Homberg, U. γ-aminobutyric acid immunostaining in the antennal lobe of the moth *Heliothis virescens* and its colocalization with neuropeptides. *Cell. Tissue. Res.* **335**, 593–605. https://doi.org/10.1007/s00441-008-0744-z (2009).
39. Assisi, C., Stopfer, M. & Bazhenov, M. Excitatory local interneurons enhance tuning of sensory information. *PLoS Comput. Biol.* **8**, e1002563. https://doi.org/10.1371/journal.pcbi.1002563 (2012).
40. Aungst, J. L. *et al.* Centre-surround inhibition among olfactory bulb glomeruli. *Nature* **426**, 623–629. https://doi.org/10.1038/nature02185 (2003).
41. Huang, J., Zhang, W., Qiao, W., Hu, A. & Wang, Z. Functional connectivity and selective odor responses of excitatory local interneurons in drosophila antennal lobe. *Neuron* **67**, 1021–1033. https://doi.org/10.1016/j.neuron.2010.08.025 (2010).
42. Yaksi, E. & Wilson, R. I. Electrical coupling between olfactory glomeruli. *Neuron* **67**, 1034–1047. https://doi.org/10.1016/j.neuron.2010.08.041 (2010).
43. Shao, Z., Puche, A. C., Kiyokage, E., Szabo, G. & Shipley, M. T. Two GABAergic intraglomerular circuits differentially regulate tonic and phasic presynaptic inhibition of olfactory nerve terminals. *J. Neurophysiol.* **101**, 1988–2001. https://doi.org/10.1152/jn.91116.2008 (2009).
44. Dolan, M.-J. *et al.* Neurogenetic dissection of the Drosophila lateral horn reveals major outputs, diverse behavioural functions, and interactions with the mushroom body. *eLife* **8**, e43079. https://doi.org/10.7554/eLife.43079 (2019).
45. Lee, S.-G., Celestino, C. F., Stagg, J., Kleineidam, C. & Vickers, N. J. Moth pheromone-selective projection neurons with cell bodies in the antennal lobe lateral cluster exhibit diverse morphological and neurophysiological characteristics. *J. Comp. Neurol.* **527**, 1443–1460. https://doi.org/10.1002/cne.24611 (2019).
46. Bates, A. S. *et al.* Complete connectomic reconstruction of olfactory projection neurons in the fly brain. *Curr. Biol.* **30**, 3183-3199. e3186. https://doi.org/10.1016/j.cub.2020.06.042 (2020).
47. Bräcker, L. B. *et al.* Essential role of the mushroom body in context-dependent CO2 avoidance in Drosophila. *Curr. Biol.* **23**, 1228–1234. https://doi.org/10.1016/j.cub.2013.05.029 (2013).
48. Varela, N., Gaspar, M., Dias, S. & Vasconcelos, M. L. Avoidance response to CO2 in the lateral horn. *PLoS Biol.* **17**, e2006749–e2006749. https://doi.org/10.1371/journal.pbio.2006749 (2019).
49. Jeanne, J. M., Fişek, M. & Wilson, R. I. The organization of projections from olfactory glomeruli onto higher-order neurons. *Neuron* **98**, 1198-1213.e1196. https://doi.org/10.1016/j.neuron.2018.05.011 (2018).
50. Stange, G. Effects of changes in atmospheric carbon dioxide on the location of hosts by the moth, *Cactoblastis cactorum*. *Oecologia* **110**, 539–545. https://doi.org/10.1007/s004420050192 (1997).
51. Schildberger, K. Multimodal interneurons in the cricket brain: properties of identified extrinsic mushroom body cells. *J. Comp. Physiol. A* **154**, 71–79 (1984).
52. Buehlmann, C. *et al.* Mushroom bodies are required for learned visual navigation, but not for innate visual behavior, in ants. *Curr. Biol.* https://doi.org/10.1016/j.cub.2020.07.013 (2020).
53. Li, Y. & Strausfeld, N. J. Multimodal efferent and recurrent neurons in the medial lobes of cockroach mushroom bodies. *J. Comp. Neurol.* **409**, 647–663. https://doi.org/10.1002/(sici)1096-9861(19990712)409:4%3c647::Aid-cne9%3e3.0.Co;2-3 (1999).
54. Namiki, S. & Kanzaki, R. Morphology and physiology of olfactory neurons in the lateral protocerebrum of the silkmoth *Bombyx-mori*. *Sci.Rep.* **9**, 16604. https://doi.org/10.1038/s41598-019-53318-8 (2019).
55. Joiner, W. J., Crocker, A., White, B. H. & Sehgal, A. Sleep in Drosophila is regulated by adult mushroom bodies. *Nature* **441**, 757–760 (2006).
56. Nishino, H. *et al.* Projection neurons originating from thermo- and hygrosensory glomeruli in the antennal lobe of the cockroach. *J. Comp. Neurol.* **455**, 40–55. https://doi.org/10.1002/cne.10450 (2003).
57. Otsuna, H. & Ito, K. Systematic analysis of the visual projection neurons of *Drosophila melanogaster*. I. Lobula-specific pathways. *J. Comp. Neurol.* **497**, 928–958. https://doi.org/10.1002/cne.21015 (2006).
58. Pfuhl, G., Zhao, X.-C., Ian, E., Surlykke, A. & Berg, B. G. Sound-sensitive neurons innervate the ventro-lateral protocerebrum of the heliothine moth brain. *Cell. Tissue. Res.* **355**, 289–302. https://doi.org/10.1007/s00441-013-1749-9 (2014).
59. Namiki, S., Wada, S. & Kanzaki, R. Descending neurons from the lateral accessory lobe and posterior slope in the brain of the silkmoth *Bombyx mori*. *Sci. Rep.* **8**, 9663. https://doi.org/10.1038/s41598-018-27954-5 (2018).
60. Ito, K. *et al.* A systematic nomenclature for the insect brain. *Neuron* **81**, 755–765. https://doi.org/10.1016/j.neuron.2013.12.017 (2014).
61. Evers, J. F., Schmitt, S., Sibila, M. & Duch, C. Progress in functional neuroanatomy: precise automatic geometric reconstruction of neuronal morphology from confocal image stacks. *J. Neurophysiol.* **93**, 2331–2342. https://doi.org/10.1152/jn.00761.2004 (2005).
62. Schmitt, S., Evers, J. F., Duch, C., Scholz, M. & Obermayer, K. New methods for the computer-assisted 3-D reconstruction of neurons from confocal image stacks. *NeuroImage* **23**, 1283–1298. https://doi.org/10.1016/j.neuroimage.2004.06.047 (2004).
63. Heinze, S. & Reppert, S. M. Anatomical basis of sun compass navigation I: the general layout of the monarch butterfly brain. *J. Comp. Neurol.* **520**, 1599–1628. https://doi.org/10.1002/cne.23054 (2012).

Acknowledgements

We are grateful to Jonas Hansen Kymre, Marte Schjetne, Sara Holm, Aleksander Berg, and Ida Camilla Kjos for contributing with the data collection.

Author contributions

X.C., P.KC, G.R.W., and B.G.B. designed the project; X.C. and P.KC performed the experiments and prepared the figures; X.C., P.KC, E.I. and B.G.B. analyzed the data; X.C., P.KC, and B.G.B. wrote the outline of the manuscript; X.C., P.KC, E.I., P.K., L.Y., G.R.W., and B.G.B. reviewed and finalized the manuscript.

Funding

This project was funded by the Norwegian Research Council, Project No. 287052, to BG Berg, and the National Natural Science Foundation of China, Project No. 31861133019, to GR Wang.

Competing interests

The authors declare no competing interests.

Additional information

Supplementary information is available for this paper at https://doi.org/10.1038/s41598-020-76918-1.

Correspondence and requests for materials should be addressed to B.G.B.

Reprints and permissions information is available at www.nature.com/reprints.

Publisher's note Springer Nature remains neutral with regard to jurisdictional claims in published maps and institutional affiliations.

Paper III

Elevated levels of CO_2 affect sex pheromone processing in the moth olfactory system

Pramod KC[1], Elena Ian[1], Xi Chu[1], Bente Gunnveig Berg[1]

[1]Chemosensory laboratory, Dept. of Psychology, Norwegian University of Science and Technology, NTNU, Trondheim, Norway

Number of pages: 28

Word count: (i) whole manuscript: 5915; (ii) abstract: 288

Number of figures: 5

Number of tables: 1

Keywords: carbon dioxide, pheromone, antennal-lobe projection neurons, calcium imaging, suppression

ISBN 978-82-326-6536-5 (printed ver.)
ISBN 978-82-326-6683-6 (electronic ver.)
ISSN 1503-8181 (printed ver.)
ISSN 2703-8084 (online ver.)

NTNU

Norwegian University of
Science and Technology